

Role of lung dendritic cells in acute pulmonary inflammation

Inaugural Dissertation
submitted to the
Faculty of Medicine
in partial fulfillment of the requirements
for the PhD-Degree
of the Faculties of Veterinary Medicine and Medicine
of the Justus Liebig University Giessen

by
Werner von Wulffen
of
Hannover
Giessen 2008

From the Department of Internal Medicine II
Director / Chairman: Prof. Dr. W. Seeger
of the Faculty of Medicine of the Justus Liebig University Giessen

First Supervisor and Committee Member: Prof. Dr. J. Lohmeyer, Giessen
Second Supervisor and Committee Member: Prof. Dr. Th. Tschernig, Hannover
Committee Members: Prof. Dr. H.-J. Thiel and PD Dr. K. Mayer, Giessen
Date of Doctoral Defense: August 6th, 2008

Table of Contents

Table of Contents	I
Abbreviations	IV
List of Figures.....	VI
List of Tables.....	VII
1 Introduction	1
1.1 Dendritic cells	1
1.2 Dendritic cells in the lung.....	6
1.3 Fms-like tyrosine kinase 3-ligand (Flt3L)	7
1.4 Pneumonia, acute lung injury (ALI), and adult respiratory distress syndrome (ARDS)	9
1.5 <i>Klebsiella pneumoniae</i>	11
1.6 Aims of the study	12
2 Materials and Methods	13
2.1 Mice	13
2.2 Reagents	13
2.3 Monoclonal antibodies	15
2.4 Treatment protocols.....	17
2.4.1 Treatment with Flt3L and <i>in vivo</i> application of mAb.....	17
2.4.2 Intratracheal instillation of LPS.....	17
2.4.3 Infection experiments with <i>Klebsiella pneumoniae</i>	18
2.4.4 <i>In vivo</i> depletion of circulating neutrophils.....	18
2.4.5 Peritoneal LPS injection	18
2.5 Analysis of mice.....	19
2.5.1 Recovery of blood, spleens, bronchoalveolar lavage fluid, and mediastinal lymph nodes.....	19
2.5.2 Isolation and identification of lung DC and lung M ϕ	20
2.5.3 Flow cytometry and cell sorting	21
2.5.4 Immunohistochemistry	22
2.5.5 ELISA and protein concentration measurement.....	22
2.5.6 SDS-PAGE of BAL fluid	23

2.5.7 FITC albumin leakage assay.....	23
2.6. Functional characterization of lung DC	24
2.6.1 Allogenic mixed lymphocyte reaction and MTT test	24
2.6.2 Sorting of DC and <i>in vitro</i> stimulation	25
2.6.3 RNA isolation, cDNA synthesis, and PCR.....	25
2.7 Statistics	29
3 Results	30
3.1 Identification and characterization of lung DC.....	30
3.1.1 Flow cytometric characteriziation	30
3.1.2 Morphology of flow-sorted lung DC and M ϕ	31
3.1.3 Stimulatory properties in an allogenic mixed lymphocyte reaction (MLR).....	32
3.2 Effect of systemic Flt3L application.....	32
3.2.1 Effect of Flt3L application on the accumulation of lung DC	32
3.2.2 Time course of Flt3L-elicited DC accumulation in peripheral blood, spleen, and mediastinal lymph nodes.....	35
3.3 Expression patterns of adhesion molecules	36
3.4. Blockade of Flt3L elicited DC recruitment to the lung by monoclonal antibodies against adhesion molecules.....	39
3.5 Effect of Flt3L induced lung DC accumulation on the lung inflammatory response to LPS.....	41
3.5.1 Cells in lung homogenate.....	41
3.5.2 Cells in BAL fluid	43
3.5.3 Proinflammatory cytokines in BAL fluid	44
3.5.4 Assessment of lung leakage	45
3.6 <i>Klebsiella pneumoniae</i> infection in Flt3L pretreated mice.....	47
3.7 LPS-induced peritonitis in Flt3L pretreated mice	50
3.8 Expression of proinflammatory cytokines by lung DC.....	51
3.8.1 <i>In vivo</i> expression of proinflammatory cytokines in lung DC after LPS instillation	51
3.8.2 Effect of Flt3L on LPS-induced cytokine gene expression in lung DC	52

4 Discussion	53
4.1 Identification and characterization of lung DC.....	54
4.2 Treatment with Flt3L	55
4.3 Adhesion molecules and recruitment of lung DC	56
4.4 Aggravated lung inflammation to LPS in Flt3L pretreated mice	60
4.5 <i>Klebsiella pneumoniae</i> infection in Flt3L pretreated mice	63
4.6 Conclusion and future perspectives.....	64
5 Summary	67
5.1 Summary	67
5.2 Zusammenfassung	69
6 References	71
7 Appendix	87
7.1 Publications	87
7.2 Declaration	88
7.3 Acknowledgments	89
7.4 Curriculum vitae.....	90

Abbreviations

A _{550/620}	Absorption at 550/620 nm
ALI	acute lung injury
APC	allophycocyanin
ARDS	adult respiratory distress syndrome
BAL	bronchoalveolar lavage
bp	base pairs
CD	cluster of differentiation
CFU	colony-forming units
DC	dendritic cell(s)
FCS	fetal calf serum
FITC	fluorescein-iso-thiocyanate
Flt3L	Fms-like tyrosine kinase-3 ligand
FSC	forward scatter
HBSS	Hank's balanced salt solution
HEPES	2-(4-(2-Hydroxyethyl)- 1-piperaciny)-ethansulfonic acid
HSA	human serum albumin
ICAM-1	intercellular adhesion molecule-1
IgG	immunoglobulin G
IL-12	Interleukin-12
JAM-c	junctional adhesion molecule-c
LPS	lipopolysaccharide
M ϕ	macrophage(s)
mAb	monoclonal antibody
MHC	major histocompatibility complex
MIP-2	macrophage inflammatory protein-2
MLR	mixed lymphocyte reaction
MTT	3-(4,5-Dimethylthiazol-2-yl)-2,5 diphenyltetrazoliumbromide
rAM	resident alveolar macrophage
SSC	side scatter

SD	standard deviation
TLR	Toll-like receptor
TNF- α	Tumor necrosis factor- α
PAMP	pathogen-associated molecular pattern
PBS ^{-/-}	phosphate-buffered saline without Ca ²⁺ and Mg ²⁺
PCR	polymerase chain reaction
PE	phycoerythrin
PFA	paraform aldehyde
PMN	polymorphnuclear granulocyte
PRR	pattern recognition receptor
PSGL-1	P-selectin glycoprotein ligand-1
qRT-PCR	quantitative reverse transcriptase-polymerase chain reaction
RT-PCR	reverse transcriptase-polymerase chain reaction
VCAM-1	vascular cell adhesion molecule-1
VLA-4/-5	very late antigen 4/5

List of Figures

- Fig. 1.1: The life cycle of dendritic cells
- Fig. 1.2: Model of dendritic cell effector function
- Fig. 3.1: Flow cytometric identification of lung DC and lung M ϕ
- Fig. 3.2: Flow cytometric characterization of lung DC and lung M ϕ
- Fig. 3.3: Morphology of flow-sorted lung DC and lung M ϕ
- Fig. 3.4: Mixed lymphocyte reaction
- Fig. 3.5: Identification of lung DC and lung M ϕ in lung homogenates from Flt3L- and vehicle-treated mice
- Fig. 3.6: Time course of DC Flt3L-elicited lung DC accumulation
- Fig. 3.7: Time course of Flt3L-elicited accumulation of PMN in mouse lungs
- Fig. 3.8: Phenotypic characterization of DC and M ϕ obtained from lungs of vehicle- and Flt3L treated mice
- Fig. 3.9: Percentage of monocytes in peripheral blood after systemic Flt3L treatment
- Fig. 3.10: DC in spleens after Flt3L treatment
- Fig. 3.11: DC in mediastinal lymph nodes after Flt3L treatment
- Fig 3.12: Expression profiles of adhesion molecules
- Fig. 3.13: Analysis of the adhesion molecules mediating Flt3L elicited accumulation of lung DC
- Fig. 3.14: Effect of β 2 integrin blockade on the accumulation of CD11c-positive cells in the lungs of Flt3L treated mice.
- Fig. 3.15: DC in spleens and mediastinal lymph nodes in mice treated with Flt3L \pm function-blocking mAb
- Fig. 3.16: Numbers of DC and PMN in lungs in response to intratracheal LPS application
- Fig. 3.17: Total BAL cells in response to intratracheal LPS application
- Fig. 3.18: Differential cell counts in BAL fluid
- Fig. 3.19: Proinflammatory cytokines in BAL fluid
- Fig. 3.20: Total protein content in BAL fluid
- Fig. 3.21: SDS-PAGE of BAL fluids

- Fig. 3.22: FITC albumin leakage after intratracheal LPS instillation
- Fig. 3.23: BAL fluid cells after *K. pneumoniae* infection
- Fig. 3.24: Proinflammatory cytokines in BAL fluid after *K. pneumoniae* infection
- Fig. 3.25: Total protein in BAL fluid and FITC albumin leakage after *K. pneumoniae* infection
- Fig. 3.26: Survival after intratracheal infection with *K. pneumoniae*
- Fig. 3.27: Cells in peritoneal lavage after Flt3L and/or LPS injection
- Fig. 3.28: Expression of TNF- α and MIP-2 mRNA in lung DC and lung M ϕ after intratracheal LPS instillation
- Fig. 3.29: Induction of proinflammatory cytokine expression in DC from Flt3 and vehicle-treated mice
- Fig. 4.1: Schematic outline of the major findings and the possible future perspectives presented in this thesis

List of Tables

- Table 2.1: List of monoclonal antibodies
- Table 2.2: cDNA synthesis
- Table 2.3: List of PCR primers
- Table 2.4: RT-PCR reactions
- Table 2.5: qRT-PCR reactions

1 Introduction

1.1 Dendritic cells

Dendritic cells (DC) are specialized leukocytes that are present in virtually all organs of mammalian bodies. Their key function is the sampling and processing of antigens, which they then present in major histocompatibility complex (MHC) II molecules to cells of the adaptive immune system, mainly effector CD4-positive T cells. A couple of decades ago, macrophages were believed to be the main antigen-presenting cells [1]. In the last years, it has been established that indeed DC are mainly responsible for fulfilling this role in mammalian organisms [2-6], although other cells of the immune system, such as macrophages, monocytes, and B cells, are also capable of presenting antigens to a lesser degree. Furthermore, in recent years, other possible antigen-presenting cells have emerged, such as hepate stellate cells and myofibroblasts [7, 8]. However, the role of these cells and their potential participation in mounting a specific immune response has to be further defined.

The life cycle of DC is depicted in Fig. 1.1 (adapted from [3]). DC in the various organs most probably arise from blood-borne precursor cells. The nature of these precursor cells has long been a matter of debate. For human peripheral blood monocytes it has been established for many years that they can be differentiated *in vitro* to functional DC by adding appropriate cytokines such as GM-CSF and IL-4 [9-12]. This *in vitro* differentiation of human monocytes into DC can also be achieved by transendothelial migration; in this model, the migrated monocytes gained a DC phenotype, whereas the non-migrating monocytes differentiated into macrophages [13]. When examined in an *in vivo* mouse model, murine monocytes have been shown to be able to differentiate into functional DC, too [14]. Peripheral blood monocytes in both humans and mice have been shown to comprise several subsets with putative different functions [15, 16]. Recently, Fogg et al. have identified a circulating bone marrow-derived cell population in mice that is the progenitor cell for macrophages and DC [17]. However, the exact origin of DC in peripheral organs has not been delineated completely, since all of the putative precursor cells show a high *in vivo* plasticity [18]. Furthermore, monocytes also have the

potential to differentiate into specialized macrophages at various sites of the body [15, 19-21].

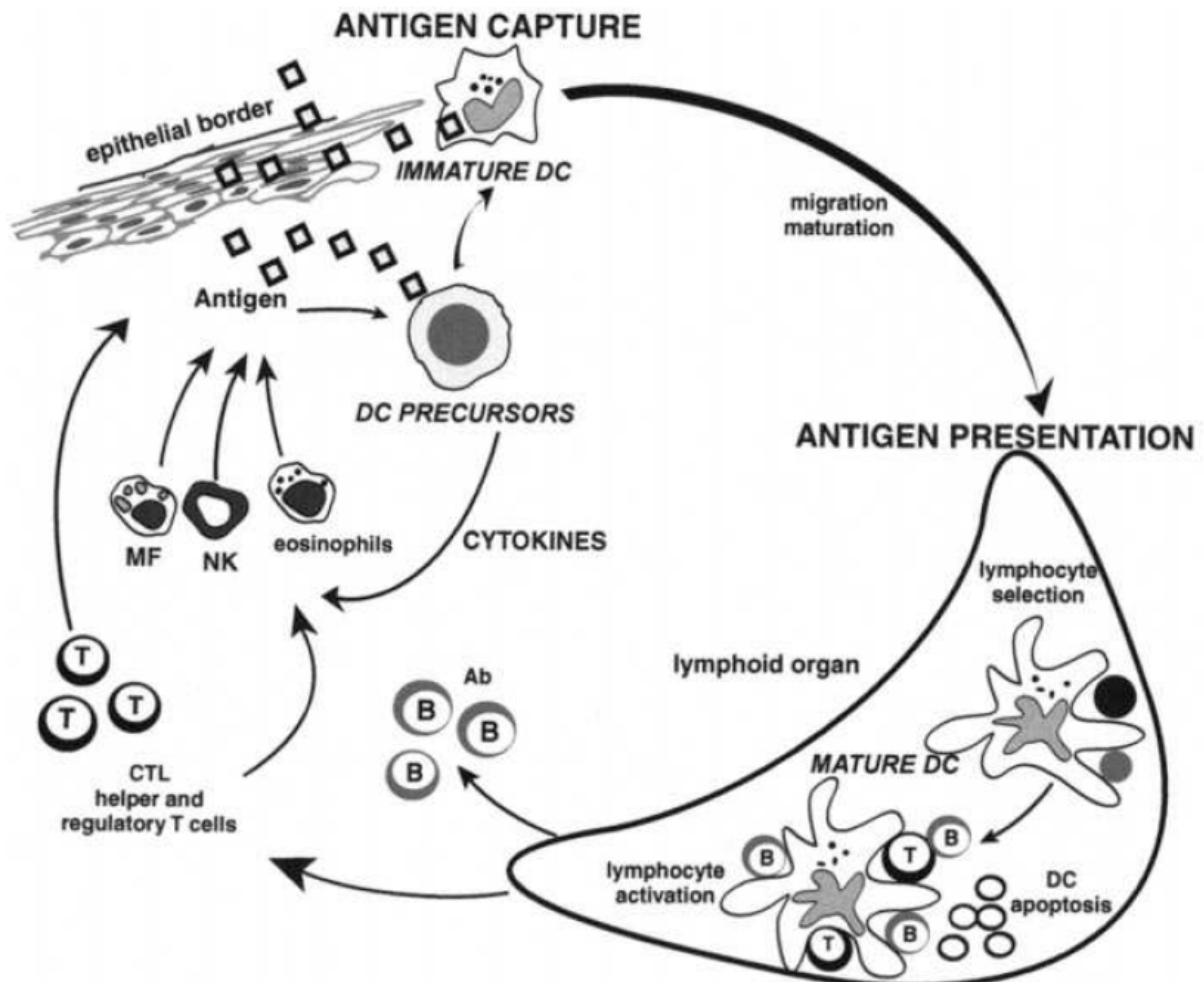


Fig. 1.1: The life cycle of dendritic cells

Circulating DC precursor cells enter tissues as immature DC. They can also directly encounter pathogens (e.g. viruses) that induce secretion of cytokines (e.g. $\text{IFN-}\alpha$), which in turn can activate eosinophils, macrophages (MF), and natural killer (NK) cells. After antigen capture, immature DCs migrate to lymphoid organs where, after maturation, they display peptide-major histocompatibility complexes, which allow selection of rare circulating antigen-specific lymphocytes. These activated T cells help DC in terminal maturation, which allows lymphocyte expansion and differentiation. Activated T lymphocytes migrate and can reach the injured tissue, because they can traverse inflamed epithelia. Helper T cells secrete cytokines, which permit activation of macrophages, NK cells, and eosinophils. Cytotoxic T cells eventually lyse the infected cells. B cells become activated after contact with T cells and DC and then migrate into various areas where they mature into plasma cells, which produce antibodies that neutralize the initial pathogen. It is believed that, after interaction with lymphocytes, DC die by apoptosis. Figure and legend were adapted from Banchereau et al. [3].

In peripheral organs, DC encounter many different antigens, which they sample and process for antigen presentation. In this stage, they have a high phagocytic activity, but express low levels of MHC II and costimulatory molecules that are necessary for initiating a T cell response, such as B7-1 (CD80), B7-2 (CD86), and CD40. Consequently, at this stage DC exhibit a weak stimulatory activity towards T cells. After ingestion of the antigen, DC process the antigens and present them in MHC II molecules. Simultaneously, DC undergo maturation, thereby losing their phagocytic activity and upregulating the expression of costimulatory molecules for a highly efficient antigen presentation to T cells. The maturation process is accompanied by a migration to the regional lymph nodes, where the antigen presentation and T cell proliferation takes place.

In addition to initiating an immune response, DC are also capable of suppressing the clonal expansion of T cells specific for the presented antigen. DC that suppress specific T cell proliferation have also been termed "tolerogenic DC" [22]. For this, DC produce and secrete a wide variety of cytokines and chemokines of both immunostimulatory (e.g., TNF- α , IL-12) or immunosuppressive action (e.g., IL-10, TGF- β) [3, 16]. Among many other ways, the *in vivo* generation of immunosuppressive DC can be initiated by the phagocytosis of apoptotic cells via a suppression of IL-12 production [23, 24] and by an upregulation of TGF- β production [25]. Independent of IL-10 or TGF- β secretion, the hepatocyte growth factor (HGF) is able to suppress vital DC functions like antigen presentation, thereby blocking the development of asthma in a mouse model [26]. Furthermore, DC are targets for classical immunosuppressive agents, such as rapamycin, and are depleted by the use of immunosuppressive drugs such as prednisolone, e.g., in patients after kidney transplantation [27-31].

By this, DC have been shown to be critical players in deciding whether the immune system mounts an effective immune response or rather dampens a response that might be detrimental for the organism. For many years it had been assumed that a mature DC phenotype is necessarily linked to the stimulation of antigen-specific T cells, thus mounting a specific immune response. However, in the last years it could be shown by many authors that DC that are phenotypically mature are capable of acting as tolerogenic DC

rather than stimulating an immune response against the presented antigen. Thus, this view on the term 'maturation' has been questioned recently, and it has been proposed to use it merely descriptively for DC that express high levels of MHC II, CD80, CD86, and CD40 molecules [32]. In the following, this terminology will be used throughout as a phenotypic rather than functional description of DC. Figure 1.2 depicts the current view on the different ways in which DC can shape the immune response to a respective antigen (adapted from [32]).

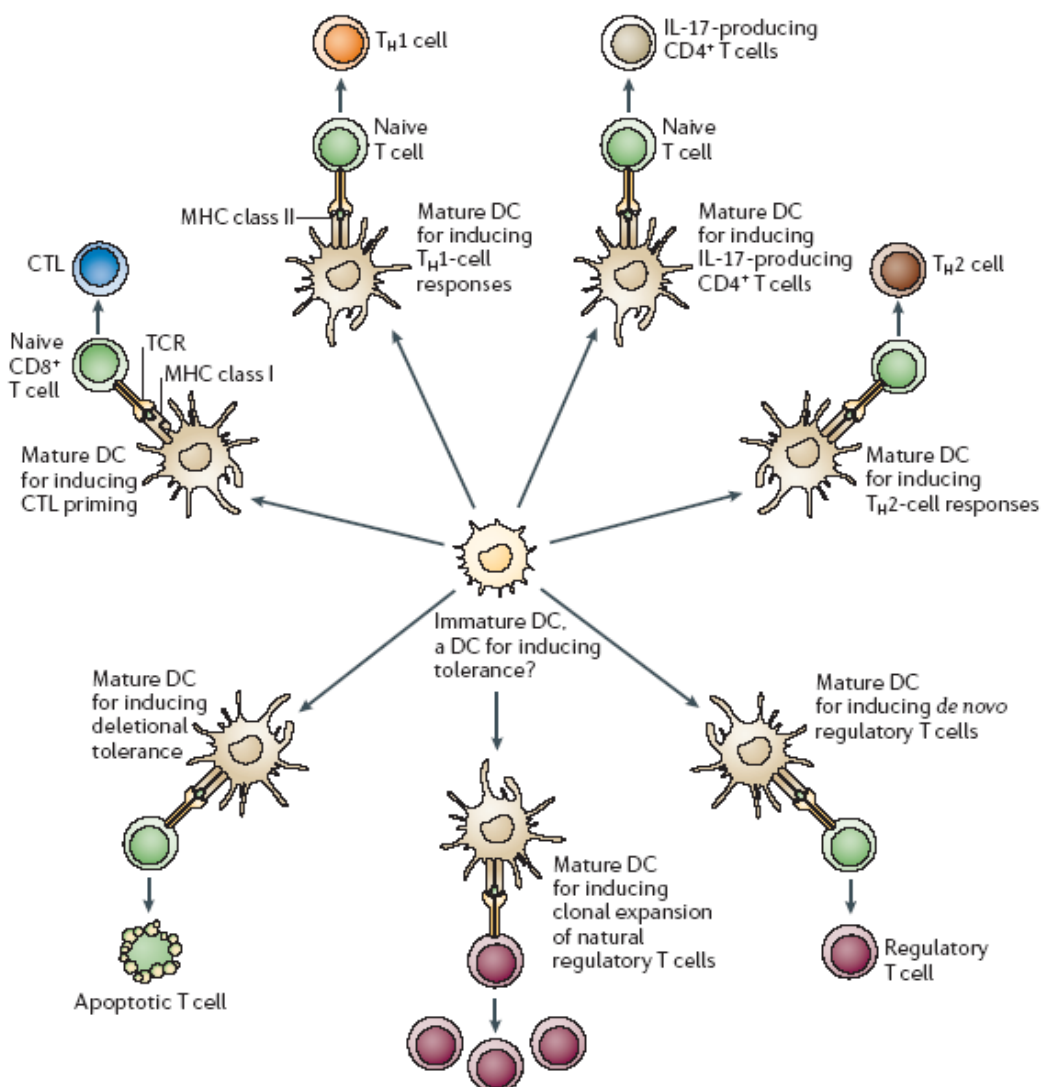


Fig. 1.2: Model of dendritic cell effector function

This view of DC function supposes that immature DC can give rise to multiple types of 'effector' DC that instruct distinct T-cell fates, including immunity, tolerance and immune deviation. Maturation refers to the changes that accompany immature DC transition to a given effector state in response to environmental signals of exogenous (for example, microbial) or endogenous (for example, cytokines, hormones and dying cells) origin. CTL, cytotoxic T lymphocyte; IL-17, interleukin-17; TCR, T-cell receptor; T_H , T helper. Figure and legend were adapted from Reis e Sousa [32].

The DC pool in mice and humans consists of several subsets, which have been intensively investigated in the past years [33-35]. The “classical” DC subsets express high levels of α_x integrin (CD11c) and MHC II as well as costimulatory molecules, as outlined above. Most prominent constituents of the “classical” DC pool in mice are the myeloid subset, characterized by the expression of the α_M integrin (CD11b), and the lymphoid subset (CD11b^{negative} CD8 α ^{positive}). Distinct from these, recently the plasmacytoid DC subset has been described, which expresses only intermediate levels of CD11c, but high levels of the B cell marker B220 (CD45R). Most importantly, these plasmacytoid DC are the major producers of type 1 interferons (Interferon-A and -B) and are therefore also termed interferon-producing cells (IPC). A special DC subset, the Langerhans cells, is located to the skin. The various DC subsets can be further differentiated, e.g. by expression of CD4 and DEC-205 (CD205), and are found in different phenotypic compositions in the various organs [33, 34]. Recently, functional differences in regard to antigen presentation and the stimulation between the DC subsets have been described. However, the exact role of the interplay of DC subsets remains to be further delineated [35, 36].

Apart from the molecules needed for antigen capture, uptake, processing and presentation, DC also express many receptors of the innate immune system, namely virtually all Toll-like receptors (TLR). The TLR belong to the expanding group of pattern recognition receptors (PRR); these germline-encoded receptors recognize conserved motifs of pathogens, such as lipopolysaccharide (LPS) and other compounds of bacterial cell walls, single-stranded RNA, and unmethylated CpG DNA [37]. These conserved pathogen motifs are usually referred to as pathogen-associated molecular patterns (PAMPs). The recognition of PAMPs via PRR represents one of the phylogenetically oldest immune pathways and is of crucial importance for the proper function of the immune system [37]. The expression of TLR by DC has been intensively investigated over the past years. In general, DC express virtually all known TLR, but their expression differs between DC subsets and anatomical locations [38]. Activation of DC via TLR stimulation is critical for the induction of DC maturation and the initiation of an effective immune response. Furthermore, DC

can produce various proinflammatory cytokines such as TNF- α , IL-6, IL-12, and IL-8 or the murine homologues, KC and MIP-2, respectively. Thereby, DC are indispensably integrated into both the innate and the adaptive immune system and are the main cells to bridge these two crucial parts of the immune system [38, 39]. However, the role of DC for the initiation and the course of acute inflammatory reactions remains poorly understood, while the role of DC in inflammations dominated by the adaptive immune system has been extensively addressed. The putative importance of DC also in both compartmentalized and systemic acute inflammations is underlined by the fact that, in addition to their well established role in organ-specific inflammatory responses, recent studies indicated an important role for DC in sepsis. In humans who died of severe sepsis, the number of DC in the spleen is dramatically reduced [40]. *In vivo* depletion of DC aggravates the course of sepsis in a mouse model [41], and survival can be improved in mouse models by adoptive transfer of DC or by *in vivo* transfection of DC and overexpression of IL-10 [41-43]. These findings support a concept of a DC-based intervention strategy to treat and circumvent a severe immunosuppression during sepsis, a condition that is correlated with a high mortality (reviewed in [44]).

1.2 Dendritic cells in the lung

DC of the lung are ideally situated in close proximity to alveolar epithelium and resident alveolar macrophages to sample and process inhaled antigens, thus rendering these cells critical to the initiation or suppression of adaptive immune responses of the lung. In both the conducting airways and the alveoli, they form interdigitating networks with their typical processi [45-48]. In the small intestine, DC have been shown to form balloon-like processi into the lumen that are important for antigen sampling [49, 50]. These DC processi also exist in the lungs of mice (H.-C. Reinecker, personal communication); their role for lung immunity, however, has not been delineated yet. Under steady-state conditions, DC in the lung display a high motility and volatility with an approximate turnover time of ≤ 2 days [45]. In case of inflammation, DC are rapidly recruited to the lung and the conducting airways in response to a broad spectrum of stimuli, including live and heat-killed bacteria, viruses, and ovalbumin [51-55]. Their

transporting of antigen to the regional lymph nodes is a critical step in mounting an immune response against the respective antigen. This transportation and antigen presentation is performed by special migratory DC [56]. DC are critical players in initiating and maintaining an effective immune response, e.g., in tuberculosis [57] and *Aspergillus fumigatus* infection [58]. However, most of the studies on lung DC have been performed in asthma models (reviewed in [48]). In contrast, little is known about the role of DC in acute lung inflammation in response to inhaled PAMPs like LPS or in the early phase of bacterial pneumonia.

One major obstacle in studying DC function in the lung is that at present there is no system for selective depletion of DC without depleting other cell populations. Approaches to deplete DC from the lung have been undertaken using thymidine kinase-transgenic mice, where DC are depleted after ganciclovir application [59]. Another approach [60] used mice that carry a transgenic receptor for diphtheria toxin under the control of the CD11c promoter [61]. The major disadvantage of these systems, at least when studying early inflammatory responses in the lung, is that other immune cells, namely alveolar macrophages, are also depleted. Therefore, for analyzing DC function in acute lung inflammation, a different system had to be established.

1.3 Fms-like tyrosine kinase 3-ligand (Flt3L)

Fms-like tyrosine kinase 3-ligand (Flt3L), also termed fetal liver kinase-2 (flk-2), is a hematopoietic growth factor that displays an important impact on proliferation and mobilization of multiple leukocyte types and their precursor cells, including B cell progenitor and myeloid precursor cells, NK cells, and DC [62]. After cloning of the gene encoding the human and murine Flt3L [63-65], it could be shown that the repeated systemic administration of recombinant human Flt3L into mice evokes a rapid and high mobilization of hematopoietic precursor cells and an increase in neutrophils, monocytoïd cells and lymphocytes in the peripheral blood and in multiple organs, including the spleen [66]. Furthermore, Maraskovsky et al. demonstrated that the administration of recombinant human Flt3L elicits a dramatic increase in numbers functional DC in mice. This increase takes place in multiple organs, including the lung [67].

The DC accumulating in the lung of Flt3L-treated mice belong mainly to the myeloid subset and display a more, although not complete, mature phenotype [68]. In rats, also a single intratracheal dose of Flt3L has been shown to increase the DC numbers [69].

Flt3L has been shown to synergize with a variety of other cytokines and growth factors in the generation of DC [70]. In marked contrast to the *in vitro* differentiation of DC from bone marrow, where granulocyte macrophage-colony stimulating factor (GM-CSF) is of crucial importance [71], in the *in vivo* situation, Flt3L in combination with granulocyte-colony stimulating factor (G-CSF) and other cytokines seems to be the most important growth factor for DC differentiation [70, 72].

Like in mice, the systemic administration of Flt3L to humans results in a drastic increase in circulating numbers of DC [73, 74]. These findings open the perspective of using Flt3L as an immunomodulatory agent in diseases like cancer. Indeed, in several mouse studies, the administration of Flt3L has been shown to exert a beneficial effect of inflammatory diseases such as asthma [75], infections with the intracellular pathogen *Listeria monocytogenes* [76, 77], viruses like herpes simplex virus [77], and *Pseudomonas aeruginosa* sepsis [78]. The combination of irradiation and systemic Flt3L application also improved the survival in a mouse model of metastatic lung cancer [79]. Furthermore, Flt3L treatment can revert an endotoxin tolerance-related immune paralysis [80]. However, in some instances, Flt3L application also leads to adverse effects, like in a murine tuberculosis model [81].

In the lung, until now the administration of Flt3L has only be addressed in the context of chronic inflammation and infection, like asthma and tuberculosis [76, 81]. Little is known about the lung DC pathobiology in mice in response to treatment with bacterial toxins or with bacteria typically causing an acute pneumonia. Likewise, the effect of systemic Flt3L application on the lung's inflammatory phenotype in acute pneumonia situation has not been delineated.

1.4 Pneumonia, acute lung injury (ALI), and adult respiratory distress syndrome (ARDS)

Pneumonia is one of the clinically most important infections and one of the leading causes of mortality worldwide. In western industrial countries the incidence is estimated as 1-11/1000 people per year. Although most patients can be sufficiently treated outside the hospital, a significant percentage of the pneumonia patients requires hospitalization [82-84]. A growing problem in treatment of pneumonia is the increasing prevalence of bacteria which are resistant to standard antibiotics [83, 84]. Therefore, the need for non-antibiotic based treatment options is emerging. This is underlined by the observation in the USA that after antibiotic treatment became available, mortality dropped from ca. 100/100.000 people per year in 1920 to approximately 40/100.000 people per year in 1950; however, since then mortality due to pneumonia has not changed significantly despite the introduction of a wide variety of new antibiotics and substantial improvement of supportive medical treatment [85]. On a worldwide scale, lung infections are the leading cause of mortality [86, 87].

Pneumonia can be caused by a variety of pathogens, including bacteria, viruses, fungi, and parasites. The prevalence of the different pathogens depends on many factors, e.g., age, immunosuppression, and concomitant diseases. The majority of pneumonia cases, however, is caused by bacteria [82, 84].

Acute bacterial pneumonia is characterized by an early production of proinflammatory cytokines, such as TNF- α and IL-6, and chemokines which attract immune cells, namely polymorphnuclear granulocytes (PMN) and, to a lesser extent, monocytes [88, 89]. In later phases, the infiltrating leukocytes have to be cleared from the lung parenchyma. At all stages, the delicate organ structure has to be conserved to maintain lung function for ventilation and gas exchange. This has to be achieved by balancing effective host defense and clearing of pathogens on one hand and maintainance of the lung structural integrity on the other hand [87].

The acute lung injury (ALI) and its severe form, the adult respiratory distress syndrome (ARDS), were initially described in 1967 [90]. It presents as a severe failure of the lung organ function and is characterized by a loss of the

pulmonary barrier function, resulting in pulmonary edema formation, the destruction of the fragile lung structure and subsequent severe hypoxemia [91-93]. ARDS can arise from both intrapulmonary conditions, such as pneumonia or aspiration, and extrapulmonary causes, e.g., trauma, major surgery, or sepsis of different origins [92, 93].

Pathophysiologically, ARDS is characterized by an excessive production of proinflammatory cytokines and recruitment of leukocytes to the alveolar space [94]. An important and early recognized feature of ARDS is also a severe dysregulation in the surfactant system, an observation that has prompted many trials analyzing the possible replacement of surfactant components in ARDS patients [93, 95-98]. A central role in the development of ARDS is often assigned to the uncontrolled influx and action of PMN [99]. However, it is a common clinical observation that full-blown ARDS also can develop in neutropenic patients [100, 101]. Although many efforts have been undertaken in the past decades to characterize the molecular and cellular events leading to ARDS, and many details have been elucidated, there are still many open questions. Most importantly, the overall mortality in ARDS has decreased since its initial description 30 years ago from 50-70% to 35-40%, but this decrease is probably mainly due to improved supportive care leading to less extrapulmonary complications rather than to a causal treatment of the lung disorder [93]. Although various therapeutic approaches have been tested in clinical trials, including surfactant replacement, corticosteroids, inhibition of neutrophil elastase and others, a specific treatment for this lung disorder could not be established yet, and therapeutic regimens for ARDS are based on treatment of the underlying reasons of lung failure and an optimized supportive care [93, 102, 103]. Therefore, a better understanding of the complex molecular and cellular events in the pathogenesis of ARDS is crucial for the development of new, causal treatment approaches of this severe disease.

Animal models are a well established tool in pneumonia and ARDS research. Among the model animals, mice are by far the most used species, and are used for many aspects of research, e.g., in pathogenesis, therapeutic interventions, and drug delivery [104-106]. The use of mice as model animals offers many advantages, e.g. their well characterized immune system with a uniquely vast

array of experimental tools available; the availability of inbred strains minimizing the influence of genetic variations on the course of infections; and the wide pool of genetically modified mice [104].

1.5 *Klebsiella pneumoniae*

The gram-negative bacterium *Klebsiella pneumoniae* belongs to the family of *Enterobacteriaceae*, and is the clinically most important species of the genus *Klebsiella*. It is found both in the environment, e.g., in water or soil, and as a colonizing bacterium of the mucosa of many mammalian organisms, including humans [107]. It is well known for causing severe pneumonia, especially in alcoholics and immunocompromized patients, and other infections such as urinary tract infections. Among the community-acquired pneumonia cases, it accounts for a minor but significant part of cases with often severe clinical course and high mortality [108, 109].

Furthermore, it is a major agent of hospital-acquired infections including ventilation-associated pneumonia and sepsis [107, 108] and seems to be spread easily from patient to patient despite strict fulfillment of standard hygiene procedures [110]. This becomes increasingly important since a growing part of the clinical isolates expresses extended-spectrum beta-lactamases (ESBLs), a virulence factor rendering these bacteria resistant to all beta-lactame antibiotics [111].

1.6 Aims of the study

In marked contrast to their well characterized role in chronic lung inflammations like asthma or tuberculosis, little is known about the lung DC pathobiology in acute lung inflammation. It is generally assumed that resident alveolar macrophages are central in the initiation and propagation of lung inflammation that develops in response to bacterial toxins and infections. However, some essential features of lung DC make these cells a highly attractive target population in acute lung inflammation: Their anatomical location with close proximity to epithelia, vessels, and alveolar macrophages; their unique equipment with TLR and other sensing molecules of the innate immune system; their capability of producing large amounts of proinflammatory cytokines; and their central position at the interface of innate and adaptive immune system. Up to now, the *in vivo* contribution of lung DC under acute inflammatory conditions has not been examined.

Since there is no satisfying model for selective depletion of lung DC, an overexpression model using the systemic application of Flt3L was used to enrich lung DC numbers. With this, the following questions were addressed in the present study to define the contribution of DC to lung acute inflammation:

1. What adhesion molecules do lung DC use in the setting of Flt3L elicited recruitment?
2. What is the role of Flt3L elicited lung DC in the early phase of the lung inflammatory response to a prototypic inhaled PAMP, lipopolysaccharide (LPS)?
3. What is the role of Flt3L elicited lung DC in the early phase of a bacterial pneumonia?

To answer these questions, at first a model of Flt3L elicited lung DC accumulation was established and characterized. Then, the adhesion molecules that mediate lung DC accumulation were analyzed by the use of monoclonal antibodies, and a selective inhibition of Flt3L elicited DC accumulation was achieved. Using this model, the role of Flt3L elicited lung DC in acute lung inflammation in response to lipopolysaccharide (LPS) and intratracheal infection with *Klebsiella pneumoniae* was analyzed.

2 Materials and Methods

2.1 Mice

Wild-type C57BL/6 mice (18-22 g) were purchased from Charles River (Sulzfeld, Germany) and were kept under conventional conditions with free access to food and water in the central animal facility of the Justus-Liebig-Universität Gießen (Zentrales Tierlabor). C3H/HEJ mice as donors for spleen lymphocytes were bred under conventional conditions in the central animal facility. All animal experiments were approved by and in accordance with the guidelines of the local government authority (Regierungspräsidium Gießen).

2.2 Reagents

Flt3L (Fms-like tyrosine kinase-3 ligand) was a kind gift from Amgen Inc. (Thousand Oaks, CA, USA). Lyophilized Flt3L was reconstituted in sterile water to a stock concentration of 1 mg/ml and stored at -80°C . For *in vivo* application, stocks were diluted with PBS-/- + 0.1% HSA to a final concentration of 100 $\mu\text{g/ml}$.

The other reagents used for the experiment are listed in the following:

Amphotericin B for cell culture	Gibco. Paisly, UK
Aqua dest., sterile	Braun, Melsungen, Germany
β -Mercaptoethanol 50 mM (for cell culture)	Gibco. Paisly, UK
β -Mercaptoethanol (for RNA isolation)	Sigma, Taufkirchen, Germany
<i>Escherichia coli</i> O111:B4 lipopolysaccharide (LPS), ultrapure	Calbiochem, La Jolla, CA, USA
Ethanol (70% and 100%)	Riedel de Haën, Seelze, Germany
Ethidium bromide solution (10 mg/ml)	Carl Roth (Karlsruhe, Germany)
FITC-labeled bovine albumin	Sigma (Taufkirchen, Germany)
Giemsa's azur eosin methylenblue	Merck, Darmstadt, Germany
Hank's balanced salt solution (HBSS)	PAA Laboratories, Pasching, Austria
HEPES (2-(4-(2-Hydroxyethyl)- 1-piperaciny)-ethansulfonic acid)	Gibco. Paisly, UK

Human serum albumine (HSA)	Sigma, Taufkirchen, Germany
Isofluran (1-chloro-2,2,2-trifluoroethyl-difluoromethyl ether)	Abbot, Wiesbaden, Germany
Ketavet® (Ketamine hydrochloride)	Pharmacia & Upjohn, Erlangen, Germany
Mouse serum, inactivated for 30 min at 56°C	Sigma, Taufkirchen, Germany
May-Grünwald's eosin methylen blue	Merck, Darmstadt, Germany
MTT (3-(4,5-Dimethylthiazol-2-yl)-2,5-diphenyltetrazoliumbromide)	Sigma, Taufkirchen, Germany
NaCl 0,9%, sterile	Braun, Melsungen, Germany
Na-Pyruvate for cell culture	Gibco. Paisly, UK
Non-essential amino acids 100x	Gibco, Paisly, UK
Octagam® (human immunoglobulin G)	Octapharma, Langenfeld, Germany
PBS ^{-/-} (without Ca ²⁺ and Mg ²⁺) 10x	PAA Laboratories, Pasching, Austria
Penicillin-streptomycin for cell culture	Gibco, Paisly, UK
EDTA (Versen) 1% in PBS ^{-/-}	Biochrom, Berlin, Germany
Fetal calf serum (FCS), inactivated for 30 min at 56°C	Gibco. Paisly, UK
RPMI-1640	PAA Laboratories, Pasching, Austria
Rompun® (Xylazine hydrochloride)	Bayer, Leverkusen, Germany
Softasept® N	Braun, Melsungen, Germany
TissueTek OTC	Sakura Finetek, Zoeterwoude, The Netherlands
Todd-Hewitt broth	Becton Dickinson, Franklin Lakes, NJ, USA
Tris-HCl	Carl Roth, Karlsruhe, Germany
Trypan blue solution 0.4%	Gibco, Paisly, UK
Tween 20 (Polyoxyethylene(20)-sorbitan-monolaurate)	Sigma, Taufkirchen, Germany

2.3 Monoclonal antibodies

The panel of anti-mouse monoclonal antibodies (mAbs) used for flow cytometric analyses, function-blocking experiments, and *in vivo* depletion of circulating neutrophils are listed in Table 2.1. All isotype controls were purchased from BD Biosciences (San Jose, CA, USA). For *in vivo* applications, only azide-free mAb preparations with a LPS content of < 0.01 ng/μg protein were used.

Specificity	Clone	Isotype	Label	Source
CD4	RM4-4	rat IgG2b	FITC	BD Biosciences
CD8 α	53-6.7	rat IgG2a	biotinylated	BD Biosciences
CD11a	M17/4	rat IgG2a	purified	Hybridoma (ATCC) [112]
CD11a	M17/4	rat IgG2a	PE	BD Biosciences
CD11b	M1/70	rat IgG2b	purified	Hybridoma (ATCC) [113]
CD11b	M1/70	rat IgG2b	APC	BD Biosciences
CD11c	N418	hamster	PE-Cy5.5	Caltag
CD11c	HL3	hamster	biotinylated	BD Biosciences
CD18	2E6	hamster	purified	Hybridoma (ATCC) [114]
CD18	C71/16	rat IgG	PE	BD Biosciences
CD19	1D3	rat IgG	PE	BD Biosciences
CD45	30-F11	rat IgG2b	FITC	BD Biosciences
CD45R/B220	RA3-6B2	rat IgG2a	PE	BD Biosciences
CD49d	PS/2	rat IgG2a	purified	Hybridoma (ATCC) [115]
CD49d	R1-2	rat IgG2b	PE	BD Biosciences
CD49e	5H10-27	rat IgG2a	PE	BD Biosciences
CD54/ICAM-1	YN1.1	rat IgG2a	purified	Hybridoma (ATCC)
CD62L	MEL-14	rat IgG2a	PE	BD Biosciences
CD86	GL1	rat IgG2a	PE	BD Biosciences
CD106/VCAM-1	M/K-2.7	rat IgG2a	purified	Hybridoma (ATCC) [115]
CD162/PSGL-1	2PH1	rat IgG1	PE	BD Biosciences
CD205	NLDC-145	rat IgG2a	Alexa647	Serotec (Oxford, UK)
F4/80	Cl:A3-1	rat IgG2b	FITC	Serotec (Oxford, UK)
F4/80	Cl:A3-1	rat IgG2b	Alexa647	Serotec (Oxford, UK)
GR-1	RB6-8C5	rat IgG2b	PE	BD Biosciences
GR-1	RB6-8C5	rat IgG2b	purified	BD Biosciences
I-AI-E (MHC II)	2G9	rat IgG2a	biotinylated	BD Biosciences
JAM-C	CRAM-18	rat IgG2a	purified	Serotec (Oxford, UK)
NK1.1	PK136	rat IgG2a	APC	BD Biosciences

Table 2.1: List of monoclonal antibodies

Hybridoma cell lines were obtained from the American Type Culture Collection (ATCC, Manassas, VA, USA) and were grown in 75 ml tissue culture flasks in RPMI-1640+20% FCS+glutamin+100 U/ml penicillin/streptomycin/amphotericin B. In the first passage, mouse peritoneal M ϕ were added as feeder cells. Supernatants were harvested, centrifuged to remove cell debris, and sterile-filtered through 0.2 μ m pore filters. IgG was isolated using HyTrap 1 ml Protein G columns (Amersham). The eluted IgG solution was then dialyzed against PBS⁻ over night. Protein content was assessed using a Bradford protein Kit (BioRad). Purity was checked by running samples of the antibody preparations on a standard PAGE electrophoresis. Activity was confirmed by flow cytometric analysis of mouse cells (leukocytes or alveolar epithelial cells) stained with the isolated antibody and a matching secondary antibody (anti-rat or anti-hamster-PE, STAR-73 or STAR-79, respectively, both from Serotec, Oxford, UK), and compared to the staining with a primary-labeled mAb of the same specificity (see Table 2.1). LPS content in antibody preparations was < 0.01 ng/ μ g protein, as determined by chromogenic limulus ameobocyte lysate test (BioWhittaker, Walkersville, MD, USA).

2.4 Treatment protocols

2.4.1 Treatment with Flt3L and *in vivo* application of mAb

Mice were treated systemically with Flt3L (10µg in 100 µl PBS/0.1% HSA) by daily subcutaneous injections into the hind leg using sterile single use injection syringes (Omnican 50, Braun, Melsungen, Germany). For this, mice were shortly anaesthetized by isofluran inhalation, and the hind leg was disinfected with Softasept®. Control mice received a daily injection of vehicle, i.e. 100 µl PBS/0.1% HSA.

Additionally, in some experiments, mice simultaneously received intraperitoneal injections of function-blocking mAbs with specificity to various adhesion molecules or their receptors (100µg/mouse diluted in 100 µl sterile saline) at days 1, 3, 5, 7 and 9 of Flt3L application. Control mice received injections of matching isotype control antibodies.

2.4.2 Intratracheal instillation of LPS

To evaluate the role of lung DC in LPS-induced lung inflammation, mice were pretreated for nine days with subcutaneous injections of Flt3L or vehicle and concomitantly received function-blocking antibodies with specificity to various adhesion molecules or their receptors. On day 9, mice were anaesthetized by intramuscular application of tetrazoline hydrochloride (2,5 mg/kg; Rompun®, Bayer) and ketamine (50 mg/kg; Ketavet®, Pharmacia Upjohn) and subsequently challenged intratracheally with LPS (1 µg ultrapure LPS/mouse) for 24h. For this, the anaesthetized but breathing mice were placed on the back, and the ventral neck region was shaved. After disinfection with Softasept®, a longitudinal skin incision was made, and the trachea was carefully exposed by blunt preparation. A 26 gauge Abbocath catheter (Hospira, Donegal Town, Ireland) was inserted, and 1 µg of ultrapure LPS in 70 µl sterile saline per mouse was slowly injected. After removing the Abbocath catheter, the skin incision was closed with 6x0 vicryl sutures (Ethicon, Norderstedt, Germany). After the instillation, mice were set back to the cages with free access to food and water.

2.4.3 Infection experiments with *Klebsiella pneumoniae*

The *Klebsiella pneumoniae* serotype 2 strain was purchased from ATCC (No 43816). *K. pneumoniae* were grown in Todd-Hewitt broth (BD Biosciences) for 18-24 h. Determination of colony-forming units (CFU) was done by plating ten-fold serial dilutions of bacterial suspensions on blood agar plates followed by incubation of the plates at 37°C for 18 hours and enumeration of the CFU. Bacteria were then diluted with PBS to the desired concentration (10^4 CFU/70 μ l per mouse) that were used for intratracheal infection experiments on day 9 of Flt3L treatment. The procedure was in analogy to the intratracheal application of LPS (see 2.4.2) Subsequently, mice were killed, lungs were subjected to bronchoalveolar lavage, and lungs were removed for further analysis as described in the following (see 2.5). Cell-free BAL supernatants were stored at -20°C for cytokine measurements. BAL fluid cellular constituents were counted using a Neubauer hemocytometer and cell differentials were determined on Pappenheim-stained cytospin preparations (see 2.5).

2.4.4 *In vivo* depletion of circulating neutrophils

In selected experiments, both Flt3L- and vehicle-pretreated mice were made transiently neutropenic by intraperitoneal injections of anti-GR-1 mAb (5 μ g/mouse diluted in 100 μ l saline) 24h prior to and at the time of intratracheal LPS instillation. This dose has previously been demonstrated to efficiently deplete circulating PMN, but not the GR-1-positive subset of circulating monocytes [116].

2.4.5 Peritoneal LPS injection

For induction of peritoneal inflammation, mice received an intraperitoneal injection of 20 μ g ultrapure LPS in a total volume of 100 μ l sterile saline, or saline alone. 24 h later, mice were killed and subjected to peritoneal lavage using PBS/2 mM EDTA. Peritoneal lavage fluid was analyzed for cell numbers, differential cell counts, TNF- α and IL-12 levels, and subjected to flow cytometry, as described for the BAL fluid (see 2.5.1).

2.5 Analysis of mice

2.5.1 Recovery of blood, spleens, bronchoalveolar lavage fluid, and mediastinal lymph nodes

At the indicated time points, mice were killed by overdosed isofluran inhalation in an exsiccator (Schott, Mainz, Germany). After soaking the fur with 70% ethanol, the abdominal cavity was opened, blood was drawn from the Vena cava inferior and transferred to small EDTA-containing blood collection tubes (Sarstedt, Nümbrecht, Germany) to prevent blood clotting. Blood smears were prepared using one drop of blood. The rest of the blood was subjected to erythrolysis using 0.8% ammonium chloride solution. Erythrolysis was stopped by adding RPMI-1640/10% FCS. After centrifugation (10 min, 300 x g, 4°C), erythrolysis was repeated. Cells were again centrifuged, washed twice in RPMI-1640, counted and then stained for flow cytometric analysis (see 2.5.3). All cell countings were performed using a standard Neubauer chamber. Cell viability in the various preparations was routinely > 97%, as assessed by trypan blue exclusion test.

Spleens were removed, transferred to a Petri dish containing 5 ml of RPMI-1640, cut into small pieces and homogenized with a syringe. After filtering through a 40 µm cell strainer (BD Falcon), cells were centrifuged (10 min, 300 x g, 4°C) and subjected to erythrolysis as described above. After washing, cells were counted and stained for flow cytometric analysis.

For bronchoalveolar lavage (BAL), skin and tissue of the ventral neck were carefully removed, and the trachea was exposed. A 20 gauge cannula was inserted, and the lungs were lavaged with a total of 6 ml of PBS⁻/2 mM EDTA. The first 1.5 ml were put in a separate 15 ml Falcon tube. Samples were centrifuged (10 min, 400 x g, 4°C). The supernatant of the first 1.5 ml was stored at -20°C for subsequent analysis of proinflammatory cytokines and BAL fluid protein content. The rest of the supernatant was discarded, cells were resuspended in RPMI-1640, and counted. After preparation of cytopspins using a cytocentrifuge (Cytospin 3, Shandon, Runcorn, UK), cells were stained for flow cytometric analysis.

After recovery of the BAL fluid, the chest cavity was opened. Mediastinal lymph nodes were carefully harvested and transferred to 1.5 ml Eppendorf tubes containing 200 μ l of RPMI-1640 + 0.7 mg/ml Collagenase A (Roche, Mannheim, Germany) and 50 μ g/ml DNase I (Serva, Heidelberg, Germany). After incubation at 37°C, 5% CO₂ for 60 min, lymph nodes were homogenized with a pipette and washed twice with RPMI-1640 (10 min, 300 x g, 4°C). After cell counting, cells were stained for flow cytometric analysis.

Blood smears and cytopins were stained with Pappenheim (May-Grünwald-Giemsa) stain and analyzed using a standard bright field microscope (Leica, Wetzlar, Germany). For differential cell counts, routinely 100 cells were counted.

2.5.2 Isolation and identification of lung DC and lung M ϕ

Isolation and identification of lung DC was performed as described in detail previously [56, 117], with some modifications. Lungs were lavaged with PBS^{-/-}/2 mM EDTA as described above. Then, a small incision was made into the left atrium, and lungs were perfused with 20 ml HBSS via the right ventricle using a 21 gauge injection cannula (Ecoflo Dispomed, Gelnhausen, Germany) until lungs were visually free of blood. After this, lungs were removed, transferred to sterile Petri dishes containing RPMI-1640 + 0.7 mg/ml Collagenase A (Roche, Mannheim, Germany) and 50 μ g/ml DNase I (Serva, Heidelberg, Germany), cut into small pieces and incubated for 90 min at 37°C, 5% CO₂ with gentle shaking. Subsequently, the digested lung tissue was suspended with a syringe and filtered through a 200 μ m and a 40 μ m cell strainer (BD Biosciences), followed by two washing steps of the resultant single cell suspensions in HBSS and PBS/2mM EDTA/0.5% FCS. Subsequently, lung homogenate cells were resuspended in PBS/2mM EDTA/0.5% FCS, and incubated with an excess concentration of unspecific IgG (Octagam) to reduce non-specific antibody binding, and then stained with magnetic bead-conjugated anti-CD11c antibodies (Miltenyi Biotec, Bergisch Gladbach, Germany), followed by magnetic separation according to the manufacturer's instructions. After washing in PBS/2mM EDTA/0.5% FCS, the resultant two major cell populations of lung

macrophages and lung DC were subjected to a detailed FACS analysis of cell surface antigen expression profiles (see 2.5.3).

Identification of alveolar DC in BAL fluid specimen of Flt3L pretreated mice in the absence or presence of LPS was done by flow cytometry. Most of the cells with a monocytic morphology contained in BAL fluids of Flt3L or Flt3L plus LPS pretreated mice were found to be CD11c^{hi}, CD11b^{hi}, MHCII^{mid-high} and CD86^{pos}, thus representing alveolar accumulating monocyte-derived myeloid dendritic cells.

2.5.3 Flow cytometry and cell sorting

All staining procedures were performed on flexible 96 well plates (BD Falcon) at 4°C in the dark. Cells ($1-5 \times 10^5$ /ml) were washed in cold PBS/5% mouse serum. Unspecific antibody binding was blocked with CD16/CD32 (Fc-block, BD Pharmingen) or by adding an excess concentration of unspecific IgG (Octagam®, Octapharma GmbH, Germany). Cells were stained with fluorochrome-labeled primary antibodies diluted to working concentrations in PBS/10% inactivated mouse serum for 20 min and washed twice in cold PBS/5% mouse serum. Biotinylated primary antibodies were further incubated for 5 min with APC-Cy7-conjugated streptavidin, followed by washing twice in cold PBS/5% mouse serum. Flow cytometric analysis was performed using a FACSCanto flow cytometer (BD Biosciences). Cell sorting was performed with a FACSVantage SE flow cytometer equipped with a DiVA sort option and an argon-ion laser operating at 488 nm excitation wavelength and a HeNe laser operating at 633 nm excitation wavelength. The BD FACSDiVa software package was used for data analysis (BD Biosciences). For further analysis and preparations of figures of flow cytometric experiments, the WinMDI 2.8 software was used.

2.5.4 Immunohistochemistry

Lungs were perfused with 20 ml HBSS until they were visually free of blood, inflated via the trachea with a 1:1 mixture of TissueTek OCT and PBS^{-/-}, then removed en bloc, transferred to TissueTek OCT, and snap-frozen in liquid nitrogen and stored at -80°C until further processing. Lung tissue cryosections (7 μm) were prepared using a cryotom (Leica Instruments, Wetzlar, Germany), mounted on glass slides and dried overnight at room temperature. After fixing in ice-cold acetone (10 min), the slides were washed in TBS/0.1% Tween 20, and endogenous biotin was blocked with a biotin blocking system (DAKOCytomation, Hamburg, Germany). Hamster-anti-mouse CD11c mAb (HL3), rat-anti-mouse CD11b (M1/70, both BD Biosciences), rat-anti-mouse F4/80 (Cl:A3-1, Serotec) and the respective isotype control Abs were appropriately diluted in background-reducing antibody diluent (DAKOCytomation), then pipetted to the tissue slides and incubated overnight at 4°C in a humidified atmosphere. After washing with TBS/0.1% Tween 20, slides were incubated for 45 min at room temperature with biotinylated mouse-anti-hamster IgG (BD Biosciences), or biotinylated goat-anti-rat IgG (DAKO), respectively, followed by washing and a further incubation with alkaline phosphatase-conjugated streptavidin (DAKO). Immunohistochemical staining was developed using the Fast Red Kit (DAKO), and lung tissue sections counterstained with filtered hemalaun (Fluka, Taufkirchen, Germany) were mounted using Ultramount medium (DAKO). Slides were examined using a microscope equipped with a digital imaging unit (Leica, Wetzlar, Germany).

2.5.5 ELISA and protein concentration measurement

Cytokine concentrations in BAL fluids were determined using DuoSet ELISA plates (R&D Systems, Minneapolis, MN, USA), according to the manufacturer's instructions. Total protein concentration in BALF was measured using the Bradford reagent kit (BioRad, Hercules, CA, USA). Measurements were performed using an UVmax ELISA reader, and data were analyzed using the KC software package (both Molecular Devices, Sunnyvale, CA, USA).

2.5.6 SDS-PAGE of BAL fluid

SDS polyacrylamide gel electrophoresis of total protein contained in BAL fluid was performed using 12% Criterion XT Bis-Tris gels (Bio-Rad, Hercules, CA, USA) at a constant voltage of 200 V for 1h. Gels were stained with Coomassie blue (Bio-Rad) for 1h. After destaining with water (3 x 15 min), densitometric analysis of the albumin band was performed using a GS-800TM Calibrated Densitometer and the 1-D analysis software Quantity One (both Bio-Rad). Relative densities were calculated in comparison to untreated control mice.

2.5.7 FITC albumin leakage assay

For the determination of lung leakage, in selected experiments mice received an injection of 1 mg FITC-labeled albumin in 100 μ l of sterile saline via lateral tail veins. One hour later, mice were sacrificed, and cell-free BAL fluid supernatants were collected as described above. Serum was recovered after centrifugation (15 min at 1000 x g) from coagulated blood. FITC fluorescence (absorbance wavelength of 488 nm and emission wavelength of 520 ± 20 nm) was measured in undiluted BAL fluid and serum samples (diluted 1:100 in PBS) using a fluorescence spectrometer (FLx 800; Bio-Tek Instruments, Winooski, VT, USA). The lung permeability index is defined as the ratio of fluorescence signals of undiluted BAL fluid samples to fluorescence signals of 1:100 diluted serum samples [118].

2.6. Functional characterization of lung DC

2.6.1 Allogenic mixed lymphocyte reaction and MTT test

Untouched CD4-positive T cells for stimulation experiments were isolated from spleens of C3H/HEJ mice. Mice were killed by overdosed isoflurane inhalation, and spleens were harvested aseptically and transferred to sterile petri dishes into RPMI-1640 + 10% FCS. After mechanical disruption, spleens were homogenized using a sterile syringe and filtered over a 100 μm and a 40 μm cell strainer. Erythrocytes were lysed using a sterile-filtered 0.8% ammonium chloride solution. Spleen cells were washed twice in RPMI-1640 + 10% FCS (10 min, 300 x g, 4°C), transferred to a sterile 75 ml cell culture flask and incubated for 3 h at 37°C, 5% CO₂. After the incubation, non-adherent cells were harvested, transferred to a 50 ml Falcon tube, washed twice in PBS/2mM EDTA/0.5% FCS (10 min, 300 x g, 4°C), and counted using a Neubauer chamber. Viability was assessed using trypan blue exclusion and was routinely > 97%. 1×10^8 cells were magnetically labeled using the Untouched CD4 Cell Isolation MACS Kit (Miltenyi Biotec, Bergisch Gladbach, Germany) according to the manufacturer's instructions. CD4 cells were separated using MACS LS columns. Purity was routinely >90% as confirmed by flow cytometric analysis using CD4-FITC antibodies (see Table 1).

Lung DC, lung M ϕ and lung PMN from C57BL/6 mice were flow-sorted as described in 2.5.3. Isolated CD4-positive T cells and sorted DC, lung M ϕ and PMN were resuspended in complete RPMI (RPMI-1640 + 10% FCS + 1 mM sodium pyruvate + 1x non-essential amino acids + 10 mM HEPES + 50 μM β -mercapto-ethanol + 100 U/ml penicillin-streptomycin). T cells (200.000 cells/well in a total volume of 200/ μl) were pipetted to a 96-well flat bottom plate. Sorted DCs, AM, or PMN (20.000 cells/well) were added to the wells as indicated. Cells were incubated at 37°C and 5% CO₂ for 3 days.

MTT (tetrazolium bromide) was stored as a 5 mg/ml stock solution in PBS^{-/-} at -20°C. For working dilutions, MTT was diluted to a final concentration of 0,175 mg/ml in complete RPMI. For assessment and quantification of viable cells, 96-well plates were centrifuged (3 min at 300 x g, 4°C). Medium was discarded, cells were resuspended in 200 μl of complete RPMI + MTT, and incubated for

90 min at 37°C, 5% CO₂. After this, cells were pelleted (3 min at 300 x g, 4°C), the supernatant was discarded, and cells were fixed for 30 min with PBS^{-/-} + 4% PFA at room temperature with continuous protection from light. After centrifugation of the cells (3 min at 300 x g, 4°C) and discarding of the supernatant, cells were dried for 15 min at room temperature under a fume hood. Tetrazolium crystals were solved in 200 µl/well isopropanol, and MTT absorption was assessed at $\lambda=550$ nm using a reference wave length of $\lambda=620$ nm in an ELISA reader (see 2.5.5). Wells with 200 µl isopropanol only served as blank controls. MTT specific absorption ($A_{550/620}$) of samples was calculated as $\text{Sample } A_{550/620} / \text{mean } A_{550/620}$ of blank controls.

2.6.2 Sorting of DC and *in vitro* stimulation

To assess the potential of lung DC and lung M ϕ to produce proinflammatory cytokines in response to LPS challenge *in vivo* and *in vitro*, lung DC and M ϕ were sorted according to their scatter and autofluorescence characteristics and CD11c expression profile, as described above. Sorted cells were pelleted and recovered in lysis buffer (Qiagen, Hilden, Germany). In other experiments, sorted DC (1×10^5 cells/250 µl in RPMI/10% FCS) were incubated in 48 well polystyrene plates in the absence or presence of ultrapure LPS (100 ng/ml, 6h, 37°C/5% CO₂). Subsequently, cells lysates were prepared and stored at -80°C for further gene expression analysis.

2.6.3 RNA isolation, cDNA synthesis, and PCR

RNA from sorted DC and lung M ϕ as well as from lung homogenates was isolated using the RNeasy Micro Kit (Qiagen, Hilden, Germany) according to the manufacturer's instructions. RNA content of the preparations was measured with a NanoDrop spectrophotometer (NanoDrop Technologies, Wilmington, DE, USA). RNA was stored at -80°C until further processing.

Primers used for conventional RT-PCR as well as quantitative RT-PCR (qRT-PCR) were designed as intron-spanning primers. Primers were synthesized by Metabion (Martinsried, Germany) and are listed in Table 2.3. Synthesis of cDNA and RT-PCR were done using GeneAmp 2400 PCR machines (Perkin Elmer,

Waltham, MA, USA). All chemicals for PCR reaction were purchased from Invitrogen (Carlsbad, CA, USA), unless mentioned otherwise.

The composition of the reaction for cDNA synthesis and the conditions for reaction are listed in Table 2.2. Each cDNA synthesis was done in a final sample volume of 25 μ l (5 ng/ μ l final cDNA concentration). Before addition of the MMLV-RT, samples were denatured for 5 min at 70°C and then immediately stored on ice. For further PCR reactions, cDNA was diluted 1:5 (1 ng/ μ l final cDNA concentration). Stocks and working dilutions of cDNA were stored at – 20°C.

Total RNA	125 ng
Random hexamers	10 pmol
dNTPs	10 mM
5x first strand buffer	5 μ l
DTT	250 mM
RNAse inhibitor	20 U
MMLV reverse transcriptase	200 U
H ₂ O (molecular biology grade)	to a final volume of 25 μ l
Conditions for cDNA synthesis: 50 min at 37°C, followed by 5 min at 96°C, then 4°C.	

Table 2.2: cDNA synthesis

<p>β-actin (amplicon size 104 bp) forward 5'-ACC CTA AGG CCA ACC GTG A-3' reverse 5'-CAG AGG CAT ACA GGG ACA GCA-3',</p>
<p>Flt3L (amplicon size 133) forward 5'-ACA GTC CCA TCT CCT CCA AC-3' reverse 5'-TAG GAA GAG GCT CCA CAA GG-3'</p>
<p>IL-12 p35 (amplicon size 94 bp) forward 5'-AGA CCA CAG ATG ACA TGG TGA-3' reverse 5'-GTC CCG TGT GAT GTC TTC AT-3'</p>
<p>MIP-2 (amplicon size 89 bp) forward 5'-ATC CAG AGC TTG AGT GTG ACG C-3' reverse 5'-AAG GCA AAC TTT TTG ACC GCC-3'</p>
<p>PBGD (amplicon size 138 bp) forward 5'-GGT ACA AGG CTT TCA GCA TCG-3' reverse 5'-ATG TCC GGT AAC GGC GGC-3'</p>
<p>TNF-α (amplicon size 174 bp) forward 5'-CAT CTT CTC AAA ATT CGA GTG ACA A-3' reverse 5'-TGG GAG TAG ACA AGG TAC AAC CC-3'</p>

Table 2.3: List of PCR primers

Conventional RT-PCR for semiquantitative analysis of gene expression was prepared and run as listed in Table 2.4. Aliquots of 10 μ l for gel electrophoresis were taken after 28 and 30 cycles to ensure an analysis in the dynamic phase of the PCR reaction before reaching the plateau phase. Gels for electrophoresis were prepared with 1x TAE buffer and 1% Agarose (Gibco, Paisly, UK) + 0.5 mg/ml ethidium bromide. TAE buffer was prepared as a 50x TAE stock (pH 8.0; for 1000 ml solution 242 g Tris base + 75.1 ml Glacial acetic acid + 37.2 g Na₂EDTA + H₂O to 1000 ml). Electrophoresis was run at a constant voltage of 100 V for 60 min. PCR products were visualized under UV light and documented using a gel documentation system (PeqLab, Erlangen, Germany). The GeneRuler low range marker (Fermentas, Burlington, Ontario, Canada) served as marker for PCR product size.

Real-time RT-PCR for relative quantification of mRNA used PBGD (HMBS) and β -actin as the reference genes. Reactions were performed in an ABI 7700 Sequence Detection System (Applied Biosystems, Foster City, CA). The composition of the reaction samples and the PCR conditions are listed in Table 2.5. Additionally, agarose-gel analysis was performed to confirm the primary formation of a single specific PCR product. Fold-change in expression was determined ($2^{-\Delta\Delta Ct}$ method) as described in [119].

Total RNA	125 ng
10x PCR buffer	2,5 μ l
dNTPs	10 mM
MgCl ₂ 50 mM	2 mM
Forward primer	5 pM
Reverse primer	5 pM
Taq polymerase	2 U
H ₂ O (molecular biology grade)	to a final volume of 25 μ l
6min at 96°C, then 5 sec 95°C → 5 sec 60°C → 10sec 72°C for 30 cycles, then 4°C	

Table 2.4: RT-PCR reactions

cDNA template (1 ng/ μ l)	5 ng
Platinum [®] SYBR [®] Green qPCR SuperMix	10 μ l
MgCl ₂ 50 mM	2 mM
ROX Reference Dye 50x	0,5 μ l
Forward primer	45 pmol
Reverse primer	45 pmol
H ₂ O (molecular biology grade)	to a final volume of 25 μ l
6min at 96°C, then 5 sec 95°C → 5 sec 60°C → 10sec 72°C for 40 cycles, then 4°C	

Table 2.5: qRT-PCR reactions

2.7 Statistics

Data analysis and statistics were performed using Microsoft Excel Version 2000 and SPSS Version 12.0. All data are displayed as mean values \pm SD, unless otherwise noted. Statistical differences between treatment groups were estimated by Kruskal-Wallis test. If there were significant differences between the treatment groups ($p < 0.05$), further comparison of the groups was performed by Mann-Whitney U test. Differences were considered statistically significant when p values were < 0.05 .

3 Results

3.1 Identification and characterization of lung DC

3.1.1 Flow cytometric characterization

In normal mouse lung parenchymal tissue, two major populations of CD11c-positive cells have been reported, including lung dendritic cells and lung macrophages. Using flow cytometry, these two populations can be distinguished by their autofluorescence properties in the FL1 channel, with lung DC displaying a low autofluorescence and lung M ϕ a high autofluorescence [117]. Figure 3.1 shows a representative result of a lung preparation from an untreated mouse.

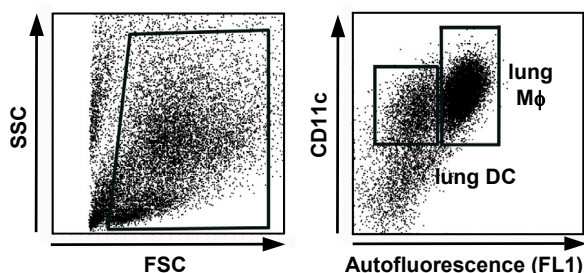


Fig. 3.1: Flow cytometric identification of lung DC and lung M ϕ

CD11c-positive cells were isolated from lung homogenates using magnetic beads and analyzed by flow cytometry for their CD11c expression and their autofluorescence properties.

As shown by others before, among the lung DC, two major subpopulations have been identified, including myeloid DC and plasmacytoid DC, of which the myeloid DC subset is the by far predominating DC population (>95%, [117]). Myeloid DC are characterized by their low autofluorescence and CD11b^{high}, CD11c^{high}, MHCII^{high} and CD86^{mid-high} and CD205^{low} cell surface antigen expression profile. In contrast, plasmacytoid DC are CD11c^{low-mid}, B220^{high} but CD11b^{negative}. As opposed to lung DC, CD11c-positive lung macrophages have been shown to be highly autofluorescent, and to be MHCII^{low-mid}, CD11b^{negative}, and CD86^{negative} [56, 117].

Adopting these protocols, and to further characterize the two CD11c-positive populations in mouse lungs in the current study, CD11c-positive cells purified from lung homogenate of untreated mice were stained with a panel of monoclonal antibodies (Fig. 3.2). By this, CD11c-positive cells with low autofluorescent properties were identified to be mostly MHCII^{high}, CD205^{low},

CD11b^{high} and CD86^{mid}, thus representing myeloid dendritic cells with a mostly immature phenotype. Only a minor part of the lung DC showed a plasmacytoid phenotype. In untreated or vehicle-treated mice, the third DC population described in mice, the lymphoid DC subset (CD11c^{high}, CD11b^{negative}, CD8α^{high}, B220^{negative}), was not or only in very limited numbers detected in lung homogenates. FACS analysis of the highly autofluorescent CD11c-positive cells collected from lung homogenates revealed a CD11c^{high}, MHCII^{low}, CD205^{negative-low}, CD11b^{negative}, CD86^{negative}, F4/80^{positive} immunophenotype, thus representing “classical” lung macrophages (Fig. 3.2). The monocyte-macrophage marker, F4/80, was expressed by both lung DC and lung Mφ.

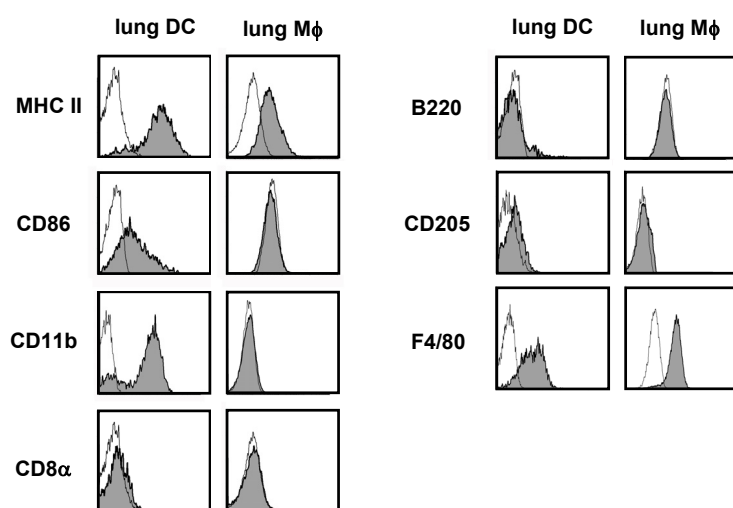


Fig. 3.2: Flow cytometric characterization of lung DC and lung Mφ

CD11c-positive cells from lung homogenates were stained for CD11c and the indicated antigens. Gates for identification of DC and Mφ were set as displayed in Fig. 3.1. Shaded histograms show the specific fluorescence for the indicated antigens; open histograms represent the respective unstained control. The data are representative of five independent experiments.

3.1.2 Morphology of flow-sorted lung DC and Mφ

Cytospin preparations of flow-sorted lung DC and lung Mφ were Pappenheim-stained and examined by light microscopy. As depicted in figure 3.3 and in accordance to the literature [68, 117], lung DC displayed a monocytic phenotype, while lung Mφ displayed the typical morphology of alveolar Mφ.

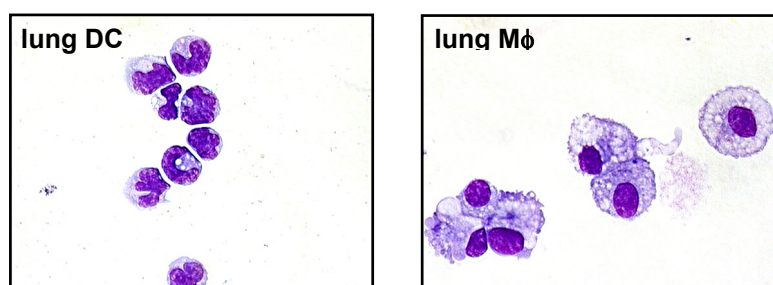


Fig. 3.3: Morphology of flow-sorted lung DC and lung Mφ

Pappenheim-stained cytopins of flow-sorted lung DC and lung Mφ. Original magnification, x 40.

3.1.3 Stimulatory properties in an allogenic mixed lymphocyte reaction (MLR)

To assess the role of lung DC to serve as antigen-presenting cells to naïve CD4-positive T cells in an allogenic MLR, flow-sorted lung DC, lung M ϕ and lung PMN from C57BL/6 mice were incubated for 3 days with spleen CD4-positive T cells from C3H/HEJ mice. After this, the number of viable cells in each well was assessed using a MTT test as outlined in 2.6.1. Although freshly isolated lung DC are mostly immature, thus displaying only a weak stimulatory potential in a MLR [68], they exhibited a stronger potential to induce T cell proliferation than lung M ϕ and lung PMN (Figure 3.4).

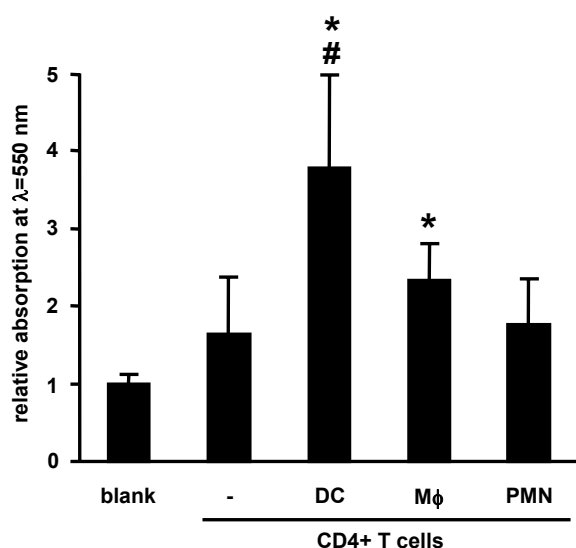


Fig. 3.4: Mixed lymphocyte reaction

Flow-sorted lung DC, lung M ϕ or lung PMN (20,000 cells per well) were co-incubated for 3 days with 200,000 CD4-positive T cells. After 3 days, the number of living cells was assessed using the MTT test as described in Materials and Methods section. Background MTT absorption in blank wells was used as standard. MTT absorption in wells with DC, M ϕ , or PMN was statistically compared to wells containing T cells only. * signifies $p < 0.05$ compared to T cells only. # signifies $p < 0.05$ of DC compared to M ϕ and PMN.

3.2 Effect of systemic Flt3L application

3.2.1 Effect of Flt3L application on the accumulation of lung DC

Although systemic Flt3L application has been shown to expand the DC pool in various organs, including the lung, a time course of the Flt3L elicited lung DC accumulation has so far not been reported. Therefore, a time course analysis was undertaken. The identification of lung DC and lung M ϕ was performed as described above. Figure 3.5 shows a representative direct comparison of the flow cytometric analysis of CD11c-positive cells from lung homogenates of a mouse treated systemically with Flt3L for nine consecutive days and a vehicle treated mouse that received PBS + 0.1% HAS only.

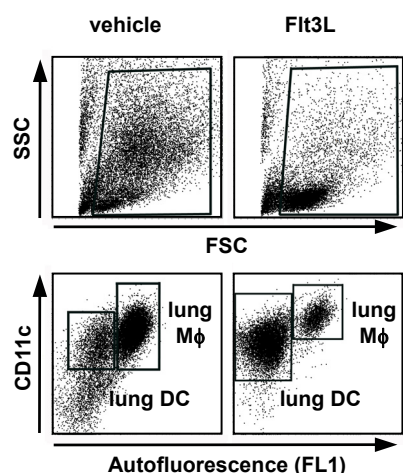


Fig. 3.5: Identification of lung DC and lung Mφ in lung homogenates from Flt3L- and vehicle-treated mice
Identification of DC and Mφ in lung homogenates were performed as described in 3.1 (see also Fig. 3.1).

As shown in Fig. 3.6, a significant increase in Flt3L-induced DC accumulation was noted in lung parenchymal tissue by day 5, with further increases observed on days 7 and 9 post-treatment. At day 9 of Flt3L treatment, numbers of lung DC were increased by a factor of ~12 compared to controls, while numbers of lung Mφ were not altered in response to Flt3L treatment (Fig. 3.6). Of note, Flt3L application in mice also increased the numbers of neutrophils accumulating in lung parenchymal tissue with a peak observed by day 9 post-treatment (Fig. 3.7).

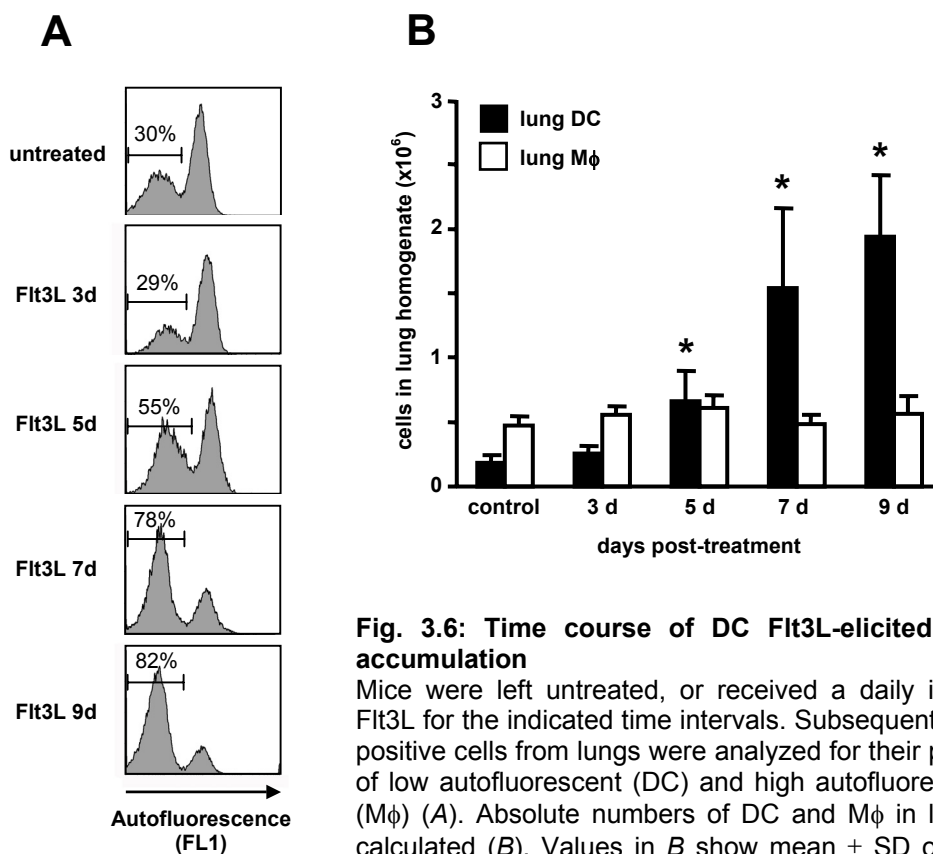


Fig. 3.6: Time course of DC Flt3L-elicited lung DC accumulation

Mice were left untreated, or received a daily injection of Flt3L for the indicated time intervals. Subsequently, CD11c-positive cells from lungs were analyzed for their proportions of low autofluorescent (DC) and high autofluorescent cells (Mφ) (A). Absolute numbers of DC and Mφ in lungs were calculated (B). Values in B show mean \pm SD of 3-5 mice per time point. * signifies $p < 0.05$ compared with control.

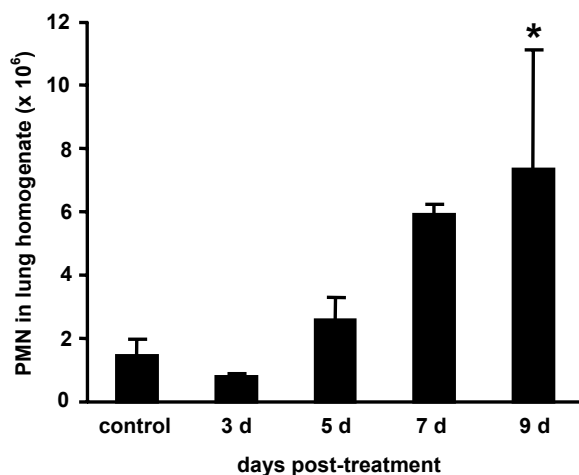


Fig. 3.7: Time course of Flt3L-elicited accumulation of PMN in mouse lungs

In lungs obtained from mice treated systemically with Flt3L for the indicated time points, the percentage of PMN was analyzed by flow cytometry (high SSC, CD45^{high}, GR-1^{high} cells). Absolute PMN numbers in lung homogenates were calculated accordingly. Data are presented as mean \pm SD of 3-5 mice per time point. * signifies $p < 0.05$ compared with control.

Furthermore, the DC and M ϕ obtained from lungs of Flt3L-treated mice were analyzed for their antigen expression profile as compared to the DC and M ϕ from the lungs of vehicle-treated mice (Fig. 3.8, see *also* Fig. 3.2). Like for the total numbers in mouse lungs, Flt3L had no impact on the antigen expression of lung M ϕ . In lung DC, the expression of MHC II and CD86 were comparable in both treatment groups, indicating that in both groups lung DC display an immature phenotype, which is in line with reports by others [68]. However, in response to Flt3L treatment, in addition to the myeloid DC subset which is dominating the lung DC pool in untreated and vehicle-treated mice, a small but detectable number of plasmacytoid DC (CD11c^{low-mid}, CD11b^{neg}, CD8 α ^{neg}, B220^{pos}) and lymphoid DC (CD11c^{pos}, CD11b^{neg}, CD8 α ^{pos}, B220^{neg}) was detected in lung homogenates.

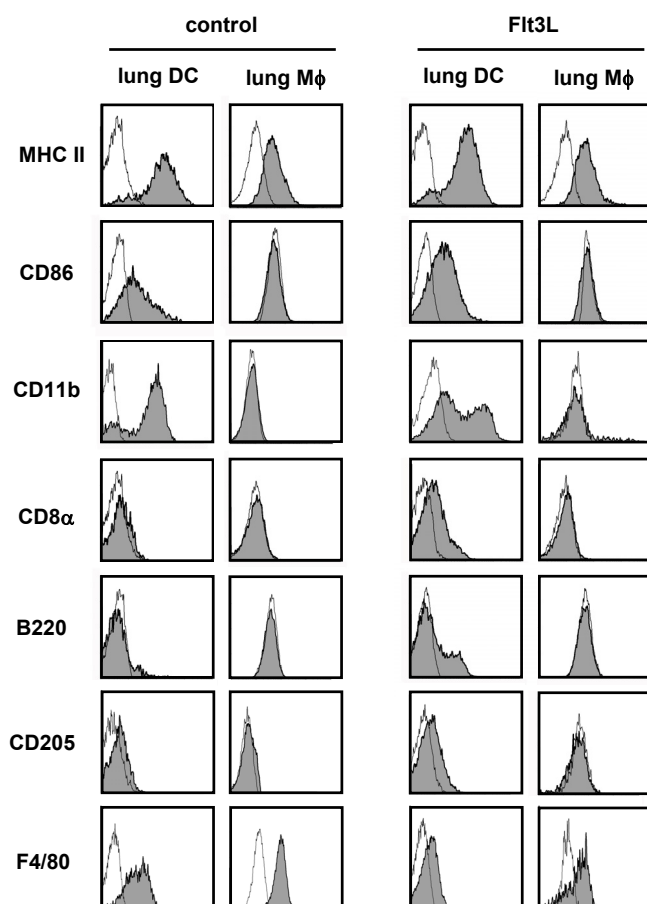


Fig. 3.8: Phenotypic characterization of DC and M ϕ obtained from lungs of vehicle- and Flt3L treated mice

Lung DC and M ϕ were identified as described and analyzed for the expression of the indicated antigens (see also legend to figure 3.2). Shaded histograms represent the specific antigen expression, open histograms display control. The data are representative of five independent experiments.

3.2.2 Time course of Flt3L-elicited DC accumulation in peripheral blood, spleen, and mediastinal lymph nodes

As described by several others before [67, 70, 72, 78], also in the present study the subcutaneous application of Flt3L led to increased numbers of circulating blood monocytes starting already on day 3, thus preceding the lung DC accumulation by approximately two days (Figure 3.9). In addition, DC accumulated in lung draining lymph nodes and the spleen with a similar time course as observed for the lung (Figure 3.10 and 3.11).

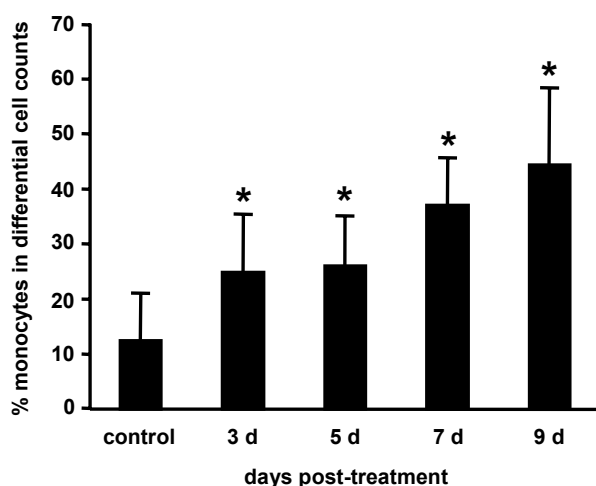


Fig. 3.9: Percentage of monocytes in peripheral blood after systemic Flt3L treatment

Mice were treated with a daily injection of 10 μ g Flt3L. At the indicated time points, mice were killed, and blood smears were prepared. Differential cell counts were done on Pappenheim-stained blood smears by counting 100 cells per mouse. Data are displayed of mean \pm SD of 3-5 mice per time point. * signifies $p < 0.05$ compared with control.

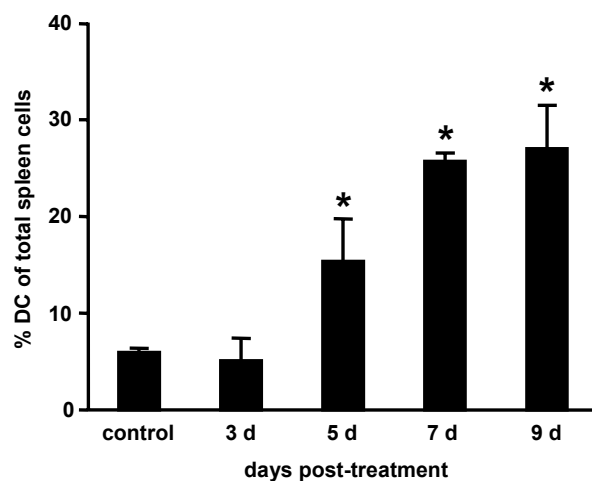


Fig. 3.10: DC in spleens after Flt3L treatment

At the indicated time points of systemic Flt3L treatment, spleen homogenates were prepared and analyzed by flow cytometry. Spleen DC were identified as CD11c^{positive} MHC II^{high} cells.

* signifies $p < 0.05$ compared with control.

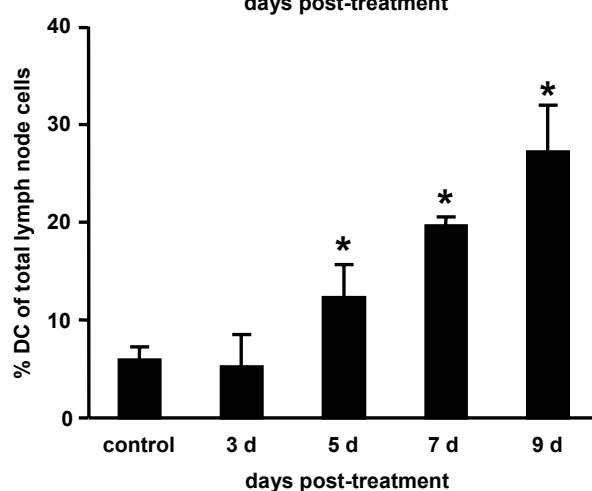


Fig. 3.11: DC in mediastinal lymph nodes after Flt3L treatment

At the indicated time points of systemic Flt3L treatment, homogenates of mediastinal lymph nodes were prepared and analyzed by flow cytometry. Lymph node DC were identified as CD11c^{positive} MHC II^{high} cells. * signifies $p < 0.05$ compared with control.

3.3 Expression patterns of adhesion molecules

The fact that systemic Flt3L treatment elicits both DC and PMN accumulation in the lung raises the necessity to differentiate between the role of Flt3L elicited lung DC versus co-recruited PMN during the acute inflammatory responses of the lung. In other words, the role of Flt3L elicited lung DC has to be carefully elaborated from the global impact of Flt3L treatment on acute lung inflammation.

A possible approach to discriminate between these two overlapping effects of Flt3L is the selective inhibition of Flt3L elicited DC recruitment to the lung by the use of function-blocking mAbs to cellular adhesion molecules. As a first step to this and to identify possible target molecules in Flt3L treated mice, a panel of mAbs was used to characterize the expression of different adhesion molecules on circulating peripheral blood monocytes (PBMo), circulating DC and PMN in

peripheral blood, lung DC, and lung M ϕ . The panel of mAbs comprised: Two of the α integrins that dimerize with the β_1 integrin chain and have been demonstrated to be the most important for the recruitment of monocytoïd cells in the mouse, α_4 integrin/VLA-4 and α_5 integrin/VLA-5 (CD49d and CD49e, respectively) [120, 121]; the β_2 integrin (CD18) and its dimerization partners α_L integrin (CD11a) and α_M integrin (CD11b); and the selectins primarily involved in monocyte recruitment in the mouse, L-selectin (CD62L) and the receptor for P-selectin, PSGL-1 (CD162).

As shown in Fig. 3.12, monocytes, circulating DC and PMN in mouse blood expressed all β_2 integrins, while the expression of β_1 integrins was restricted to monocytes and DC. Expression of CD62L was restricted to a subset of both PBMo and DC, but could not be attributed to a specific subset, like the GR-1-positive or -negative PBMo or the CD11b-positive or -negative DC.

After recruitment to the lung, DC did not change the expression of the analyzed antigens. Lung M ϕ , however, showed a different expression profile, as compared to circulating monocytes, with the absence of CD11b, CD49d, CD62L, and CD162.

Data presented in Fig. 3.12 represent adhesion molecule expression patterns after nine days of systemic Flt3L treatment. This expression profile was not different from the expression profile in vehicle-treated or untreated mice (data not shown).

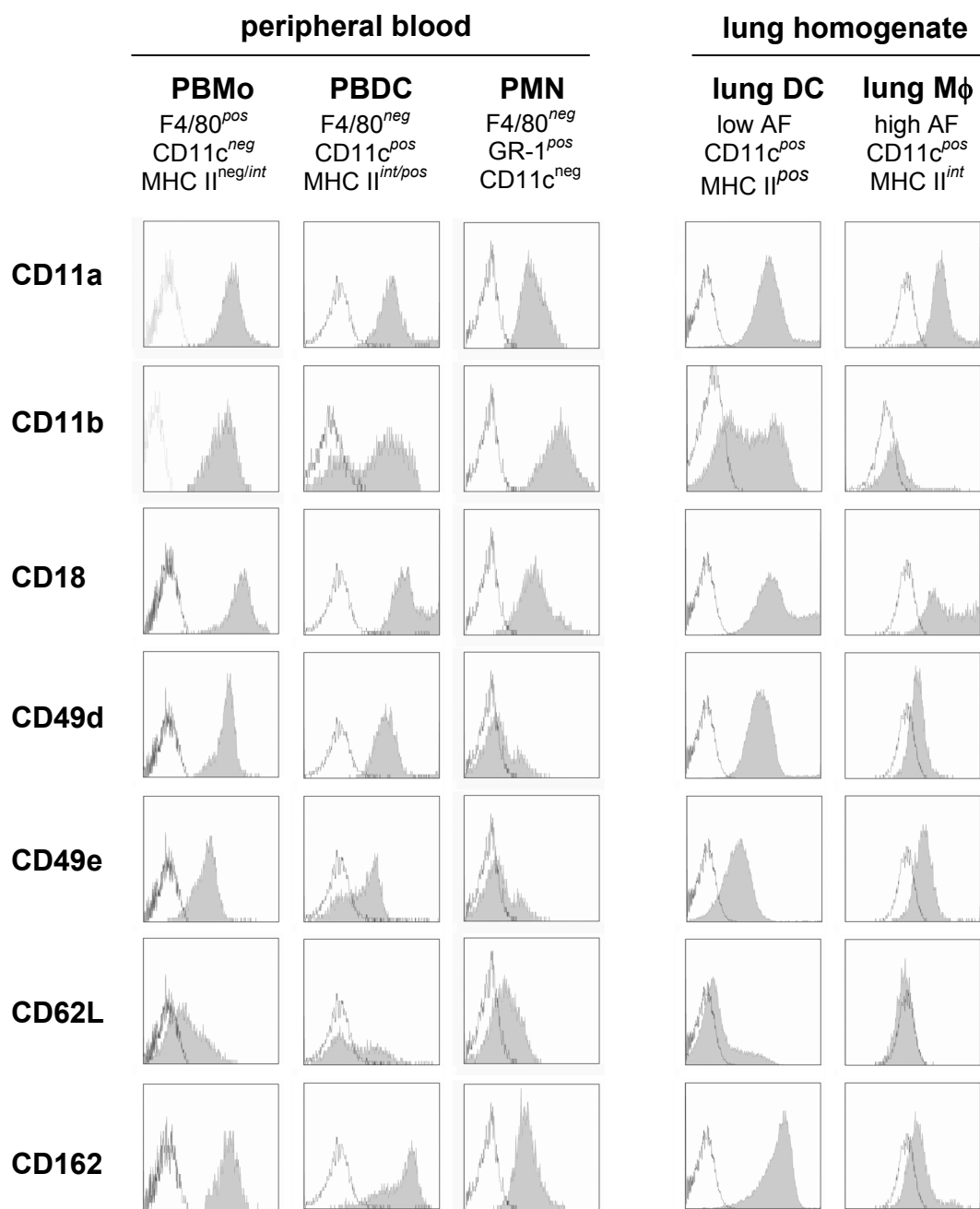


Fig 3.12: Expression profiles of adhesion molecules

Mice were treated for nine consecutive days with Flt3L, and peripheral blood monocytes (PBMo), peripheral blood DC (PBDC), blood neutrophils (PMN), lung DC, and alveolar macrophages (lung Mφ) were analyzed for the expression of the indicated adhesion molecules. Cell populations were identified by appropriate gating as indicated. Open histograms indicate the unstained cells, shaded histograms show the specific fluorescence. Results are representative of five independent experiments.

3.4. Blockade of Flt3L elicited DC recruitment to the lung by monoclonal antibodies against adhesion molecules

The next step in identifying possible target adhesion molecules was the application of function-blocking mAb in order to analyze the molecular pathways mediating the Flt3L elicited lung DC but not PMN accumulation, thus establishing a system to differentiate the role of Flt3L elicited lung DC versus co-recruited neutrophils in the lung's inflammatory response to bacterial LPS.

Therefore, mice were treated for nine consecutive days with Flt3L. Additionally, mice received intraperitoneal injections of function-blocking mAb or matching isotype control antibodies on days 1, 3, 5, 7, and 9 of Flt3L treatment. On day 10, mice were sacrificed and subjected to analysis.

As shown in Fig. 3.13, application of function-blocking mAb with specificity for the β_2 integrins CD11a, CD11b or the common β_2 chain CD18 significantly blocked the Flt3L elicited lung DC accumulation by >70% compared to controls. In marked contrast, blockade of the β_1 integrin CD49d (VLA-4) or its receptor CD106 (VCAM-1) did not reduce the Flt3L elicited lung DC accumulation. Also, blockade of the β_2 integrin receptor CD54 (ICAM-1) only slightly reduced numbers of lung DC in the lung parenchyma of Flt3L treated mice, implying that lung DC accumulation in response to Flt3L utilizes alternative adhesion pathways independent of ICAM-1. In addition, blockade of JAM-c, a junctional adhesion molecule localized at lung endothelial and epithelial tight junctions [122] slightly but non-significantly blocked the Flt3L-elicited lung DC accumulation. These data show that Flt3L elicited lung DC accumulation largely depends on engagement of β_2 but not β_1 integrins or JAM-c.

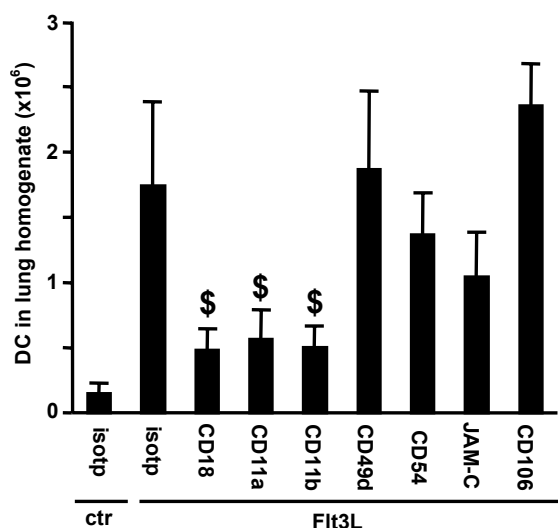


Fig. 3.13: Analysis of the adhesion molecules mediating Flt3L elicited accumulation of lung DC

Mice were treated for 9 consecutive days with Flt3L and function-blocking mAb to the indicated adhesion molecules. On day 10, number of lung DC was analyzed as outlined above. Values are presented as mean \pm SD of 3-5 mice per treatment group. \$ signifies $p < 0.05$ as compared with Flt3L-treated isotype control group. isotp, isotype control IgG.

This conclusion is also supported by an immunohistochemistry analysis as presented in Fig. 3.14, showing that the Flt3L induced accumulation of CD11c^{positive}/CD11b^{positive} lung DC within the lung interstitial compartment was nearly completely blocked in Flt3L-treated mice co-treated with anti-CD11a mAb. At the same time, numbers of resident alveolar macrophages located within the alveolar air space (CD11c^{positive}, F4/80^{positive}, CD11b^{negative}) remained unaffected.

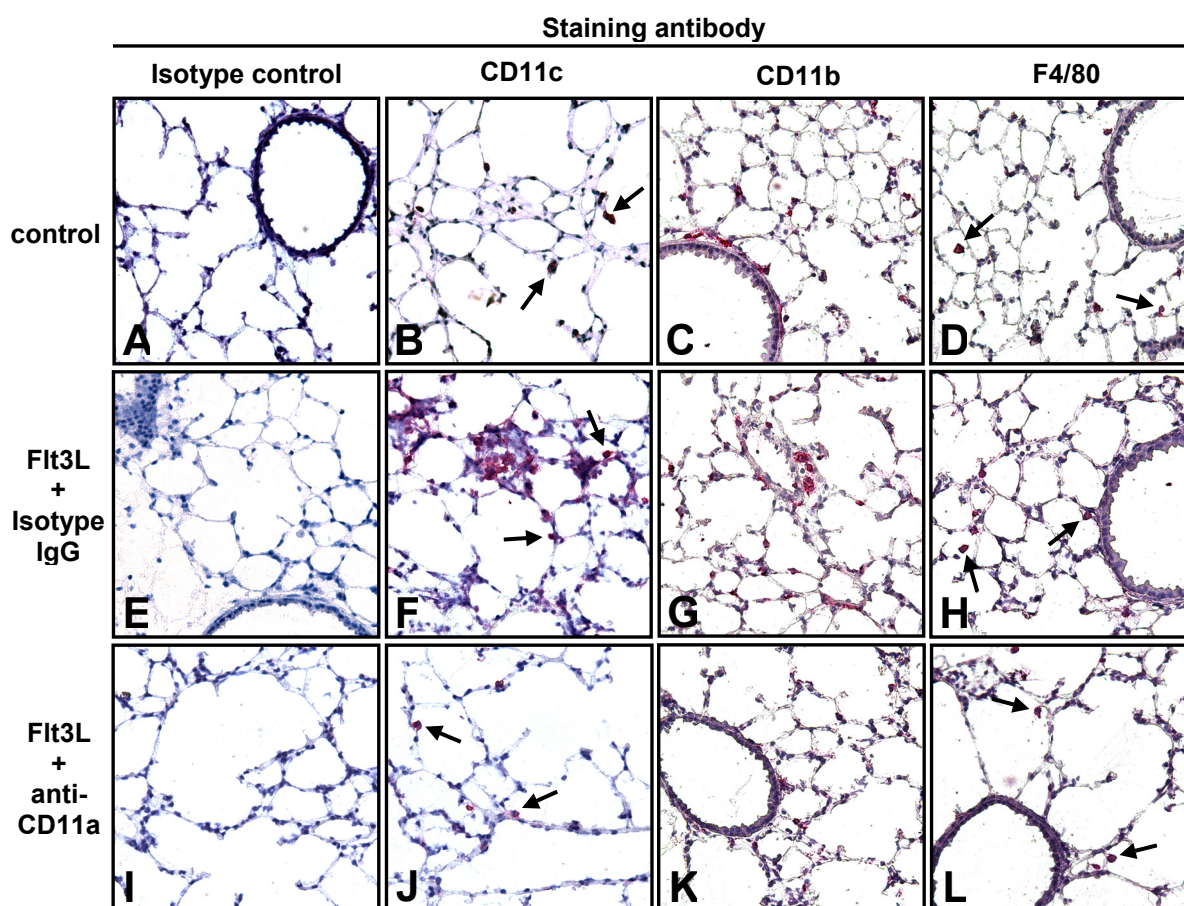


Fig. 3.14: Effect of $\beta 2$ integrin blockade on the accumulation of CD11c-positive cells in the lungs of Flt3L treated mice.

Mice were either injected with vehicle (A-D) or Flt3L for nine days (10 $\mu\text{g}/\text{mouse}/\text{day}$) (E-L) in the presence of either isotype control (A-H) or function-blocking anti-CD11a mAb (I-L). Subsequently, mice were killed and immunohistochemistry was performed on lung cryosections stained with anti-CD11c mAb (B,F,J), anti-CD11b mAb (C,G,K), anti-F4/80 mAb (D,H,L), or control Ab (A,E,I), as indicated. Note that in anti-CD11a mAb pretreated mice, numbers of intra-alveolar CD11c-/F4/80-positive, CD11b-negative cells representing alveolar macrophages (arrows) remained unchanged, while Flt3L elicited CD11c-/CD11b-positive cells accumulating in the lung interstitial compartment (lung DC) were strongly reduced. Original magnification, x20.

The analysis of DC in spleens and mediastinal lymph nodes of the mice co-treated with Flt3L and function-blocking antibodies showed that, in marked contrast to the findings in lung DC recruitment, Flt3L-elicited DC recruitment to these organs was not blocked by any of the function-blocking mAb applied in this study (Fig. 3.15). This indicates that the blocking effect of anti- β_2 integrin mAb on lung DC accumulation is due to a specific blockade of DC migration to the lung as opposed to a possibly occurring antibody-mediated depletion of precursor cells in peripheral blood. Also, proportions of myeloid, lymphoid and plasmacytoid DC subsets were not significantly affected in lungs, mediastinal lymph nodes or spleens in mice pretreated with Flt3L in the absence or presence of blocking antibodies (data not shown).

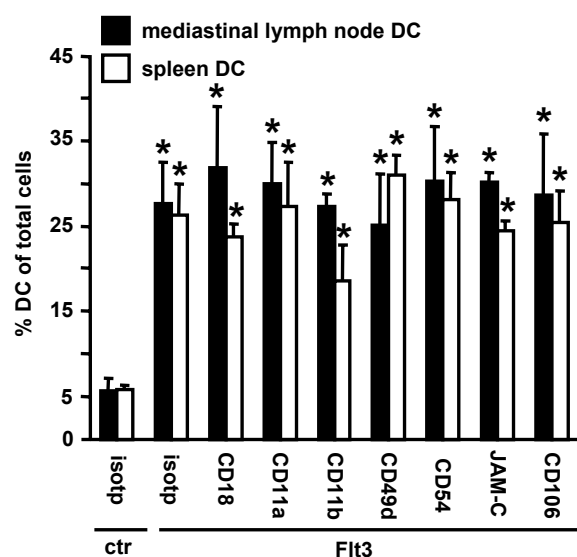


Fig. 3.15: DC in spleens and mediastinal lymph nodes in mice treated with Flt3L \pm function-blocking mAb

Mice were treated as described in Fig. 3.13. On day 10, spleens and mediastinal lymph nodes were harvested, and percentages of DC (CD11c^{positive}, MHC II^{high}) were analyzed by flow cytometry. Values are presented as mean \pm SD of 3-5 mice per treatment group. * signifies $p < 0.05$ compared with vehicle-treated mice. isotp, isotype control IgG.

3.5 Effect of Flt3L induced lung DC accumulation on the lung inflammatory response to LPS

3.5.1 Cells in lung homogenate

To evaluate the role of lung DC in LPS-induced lung inflammation, mice were either left untreated or were pretreated with LPS for 24h or were pretreated with Flt3L for nine days to increase numbers of lung DC within the lung parenchymal tissue followed by intratracheal application of LPS for 24h. As shown in Fig. 3.16, LPS application in the absence of Flt3L pretreatment only slightly

increased numbers of lung DC in lung parenchymal tissue, whereas Flt3L application alone significantly increased numbers of lung DC. However, application of LPS into the lungs of Flt3L pretreated mice further increased numbers of DC in lung parenchymal tissue approximately four-fold over lung DC numbers observed in the lungs of Flt3L only treated mice. This indicates that Flt3L plus LPS treatment of mice synergistically enhanced the lung DC accumulation compared to either treatment regimen alone. This synergistic action of Flt3L and LPS to elicit a drastic increase in lung DC numbers was strongly and significantly reduced in the presence of anti-CD11a but not anti-CD49d blocking antibodies, again demonstrating that acute inflammatory lung DC accumulation in response to Flt3L plus LPS was critically dependent on engagement of β_2 integrins but not β_1 integrins (Fig. 3.16). In addition, the observed co-recruitment of neutrophils into the lung parenchymal tissue of Flt3L treated mice was also further increased in mice challenged with Flt3L plus LPS (Fig. 3.16). In striking contrast to the inflammatory lung DC accumulation, neutrophil recruitment did not depend on engagement of CD11a or CD49d, corresponding to previously published results [121]. Collectively, these data show that both the lung DC and neutrophil accumulation is strongly increased in mice co-treated with Flt3L in the presence of intratracheal LPS, and blockade of CD11a selectively and significantly attenuates the inflammatory lung DC but not lung neutrophil recruitment. Thus, anti-CD11a blocking antibody application is an effective tool to dissect the effects of Flt3L elicited lung DC versus lung neutrophils on the lung inflammatory response to endotoxin challenge.

To further differentiate the contribution of Flt3L elicited lung DC versus neutrophils on LPS induced lung inflammation, both Flt3L- and vehicle-pretreated mice were concomitantly depleted of circulating neutrophils via systemic application of anti-GR-1 mAb. This treatment regimen has been shown recently to deplete circulating neutrophils but not Gr-1 positive monocyte subsets in peripheral blood [116]. Importantly, transient neutropenia induced in Flt3L plus LPS and LPS only treated mice efficiently depleted lung neutrophils without affecting numbers of lung DC (Fig. 3.16).

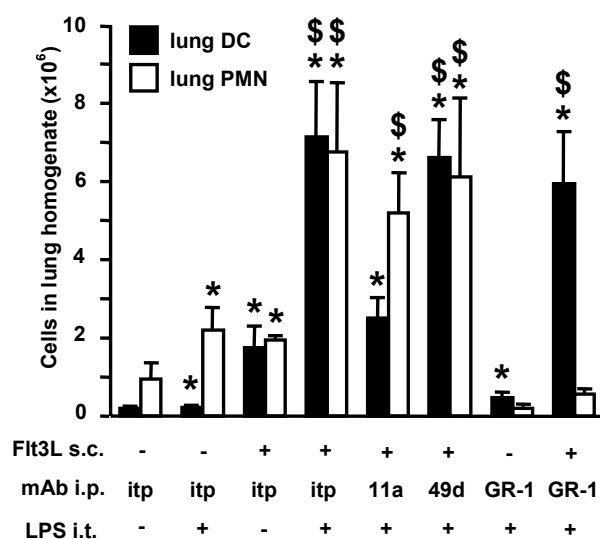


Fig. 3.16: Numbers of DC and PMN in lungs in response to intratracheal LPS application

Mice were treated as described above, and numbers of DC and PMN in lungs were analyzed by flow cytometry as described. Values are presented as mean \pm SD of 4 mice per group.

* signifies $p < 0.05$ compared to vehicle-treated mice; \$ signifies $p < 0.05$ compared to Flt3L only treated mice. # signifies $p < 0.05$ compared to LPS only treated mice. itp, isotype control IgG

3.5.2 Cells in BAL fluid

The analysis of BAL fluid cellular constituents from mice of the various treatment groups showed that LPS treatment alone elicited a ~5 fold increase in total BAL cell numbers (Fig. 3.17), attributable to a moderate neutrophilic alveolitis with low numbers of co-recruited alveolar DC in the absence of lymphocytes (Fig. 3.18 A and B), which is in line with previously published results [118, 123, 124]. Of note, Flt3L treatment alone did neither induce an increase in total BAL cells nor an alveolar accumulation of neutrophils or an alveolar DC or lymphocyte recruitment (Fig. 3.17, 3.18 A and B). In striking contrast, Flt3L-pretreated mice challenged with LPS for 24h developed a significantly increased neutrophilic alveolitis compared to mice challenged with LPS alone and recruited significantly more DC into the alveolar air space (200-300 fold above control) than induced by either treatment regimen alone (Fig. 3.18 A and B). Anti-CD11a mAb but not anti-CD49d mAb application in Flt3L pretreated mice significantly attenuated the alveolar DC recruitment in response to LPS and also reduced the numbers of alveolar recruited neutrophils (Fig. 3.17 A), which was not observed for the lung interstitial compartment (Fig. 3.16), implying that the β_2 integrin CD11a is critical to lung parenchymal and alveolar recruitment of both lung and alveolar DC, whereas CD11a appears to be more relevant for the neutrophil recruitment across the alveolar epithelial as opposed to the capillary endothelial barrier.

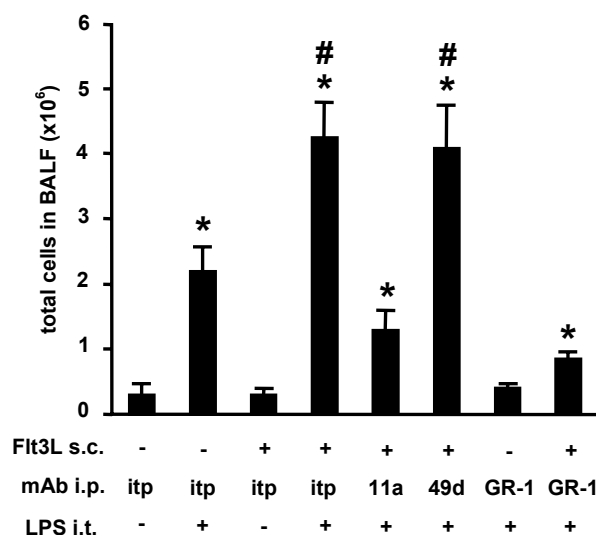


Fig. 3.17: Total BAL cells in response to intratracheal LPS application

Mice were treated as described above, and lungs were lavaged on day 10 (= 24h after intratracheal LPS application). Cells in BAL fluid were counted with a Neubauer chamber. Values are presented as mean \pm SD of 4 mice per group.

* signifies $p < 0.05$ compared to vehicle-treated mice; # signifies $p < 0.05$ compared to LPS only treated mice. itp, isotype control IgG

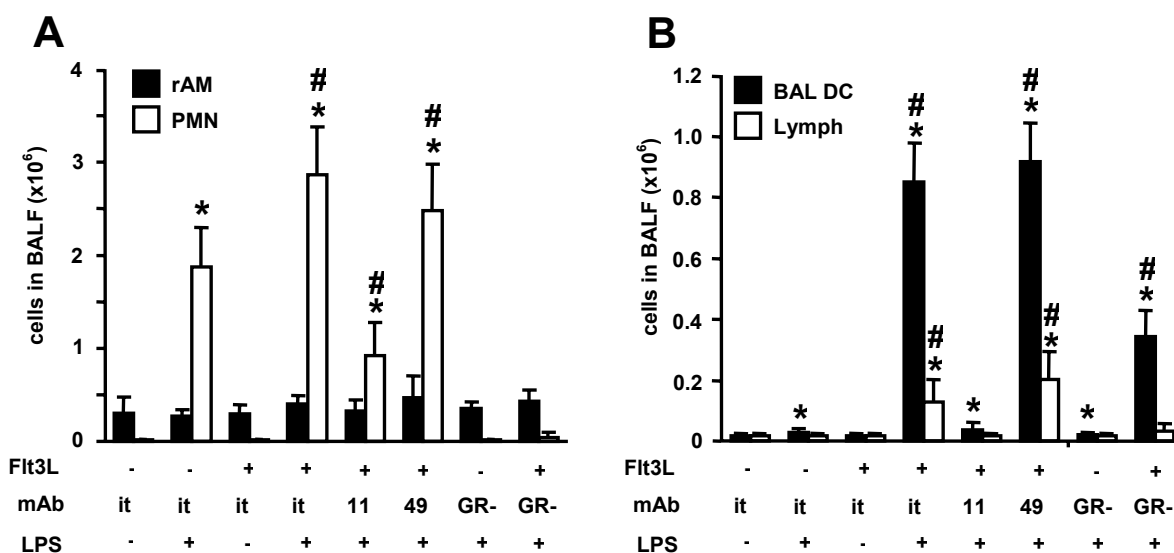


Fig. 3.18: Differential cell counts in BAL fluid

Cells in BAL were differentiated by differential cell counts on Pappenheim-stained cytopins as well as by flow cytometry into rAM and PMN (A) and DC and Lymphocytes (B), respectively. Note that the number of resident alveolar macrophages (rAM) did not change significantly by any treatment. Values are presented as mean \pm SD of 4 mice per group.

* signifies $p < 0.05$ compared to vehicle-treated mice; # signifies $p < 0.05$ compared to LPS only treated mice. itp, isotype control IgG. Lymph, lymphocyte.

3.5.3 Proinflammatory cytokines in BAL fluid

The proinflammatory mediator release and lung barrier dysfunction in mice of the various treatment groups was also assessed. LPS challenge but not Flt3L pre-treatment of mice elicited a weak alveolar liberation of TNF- α and IL-12 (Fig. 3.19). In contrast, Flt3L pretreated and LPS challenged mice responded with strongly increased BAL fluid TNF- α levels (Fig. 3.19 A) and excessive IL-12

levels in BAL fluid (Fig. 3.19 B). This effect could be nearly completely abrogated by pre-treatment of the mice with anti-CD11a but not anti-CD49d blocking antibodies. In contrast, induction of transient neutropenia in mice pretreated with Flt3L plus LPS only weakly attenuated BAL fluid TNF- α and IL-12 levels.

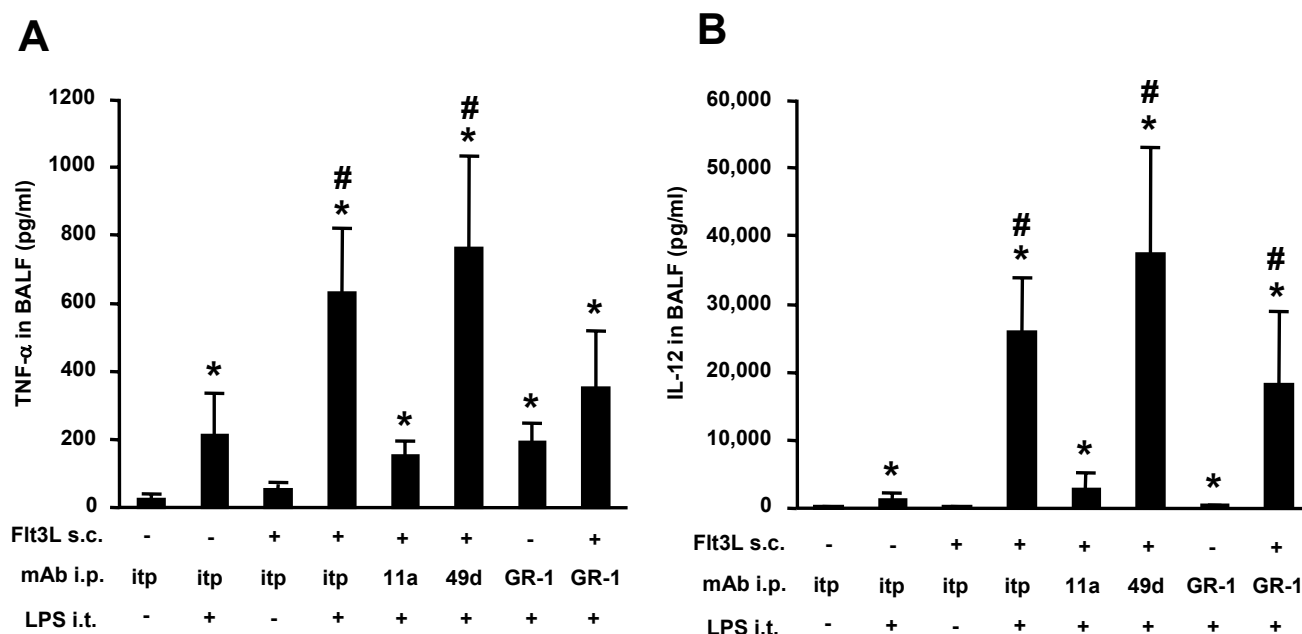


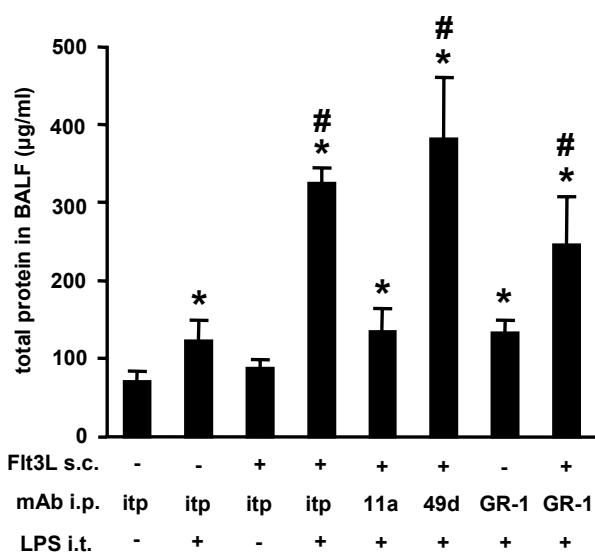
Fig. 3.19: Proinflammatory cytokines in BAL fluid

BAL fluid concentrations of TNF- α (A) and IL-12 (B) were measured by ELISA. Values are presented as mean \pm SD of 4 mice per group. * signifies $p < 0.05$ compared to vehicle-treated mice; # signifies $p < 0.05$ compared to LPS only treated mice. itp, isotype control IgG.

3.5.4 Assessment of lung leakage

Furthermore, in order to characterize the inflammatory phenotype upon intratracheal LPS application, the function of the lung barrier was assessed by different approaches to measure an increased leakage to the alveolar space. Firstly, total protein in BAL fluid was measured using a Bradford assay (Fig. 3.20). Secondly, BAL fluid from the various treatment groups was subjected to gel electrophoresis, and the intensity of the 66 kDa band representing mouse serum albumine was quantified and compared to the vehicle-treated, non-inflamed control (Fig. 3.21 A and B). Finally, the lung leakage after intratracheal LPS instillation was assessed using the leakage of intravenously administered FITC-labeled albumin into the alveolar space (Fig. 3.22).

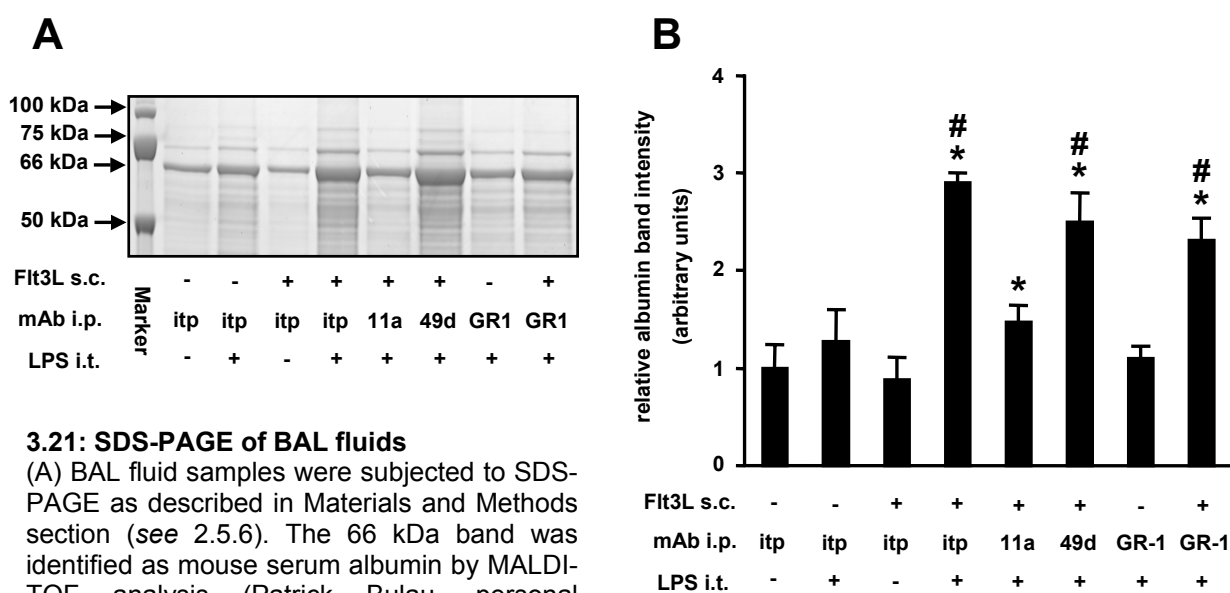
As shown in Figures 3.20-3.22, intratracheal LPS challenge but not Flt3L pretreatment of mice elicited a moderate increase in lung permeability. However, the intratracheal instillation of LPS to mice that had been pretreated with Flt3L resulted in a strongly and significantly increased lung permeability. As for the proinflammatory cytokines in BAL fluid, the induction of transient neutropenia in mice pretreated with Flt3L plus LPS had no effect on the lung permeability in these mice.



3.20: Total protein content in BAL fluid

Total protein in BAL fluid was measured by Bradford protein assay. Values are presented as mean \pm SD of 4 mice per group.

* signifies $p < 0.05$ compared to vehicle-treated mice; # signifies $p < 0.05$ compared to LPS only treated mice. itp, isotype control IgG.



3.21: SDS-PAGE of BAL fluids

(A) BAL fluid samples were subjected to SDS-PAGE as described in Materials and Methods section (see 2.5.6). The 66 kDa band was identified as mouse serum albumin by MALDI-TOF analysis (Patrick Bulau, personal communication).

(B) The intensity of the albumin band was quantified densitometrically. Relative densities were calculated compared with the vehicle-treated, not LPS-challenged treatment group. Values are presented as mean \pm SD of 4 mice per group. * signifies $p < 0.05$ compared to vehicle-treated mice; # signifies $p < 0.05$ compared to LPS only treated mice. itp, isotype control IgG.

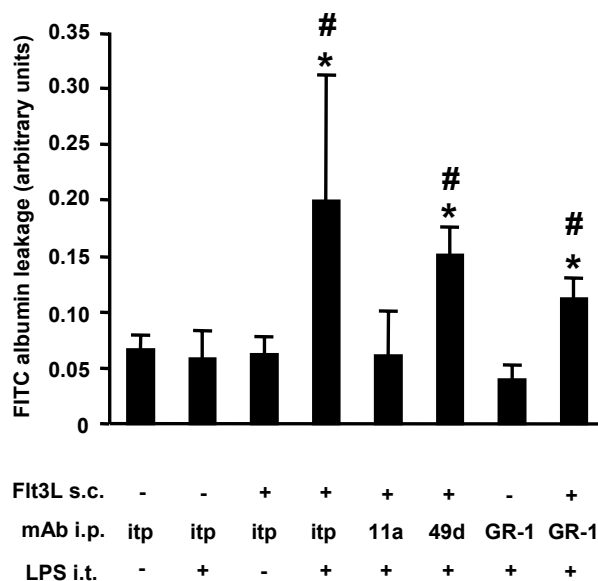


Fig. 3.22: FITC albumin leakage after intratracheal LPS instillation

For assessment of lung leakage, mice were injected intravenously with 1 mg of FITC-labeled albumin one hour before analysis. FITC fluorescence in serum and BAL fluid was measured, and ratios were calculated (see also 2.5.7). Values are presented as mean \pm SD of 4 mice per group. * signifies $p < 0.05$ compared to vehicle-treated mice; # signifies $p < 0.05$ compared to LPS only treated mice. itp, isotype control IgG.

Collectively, these data show that LPS challenge of Flt3L pretreated mice significantly aggravates the lung inflammatory response, as reflected by strongly increased lung parenchymal and alveolar DC and neutrophil numbers, as well as in significantly increased BAL fluid TNF- α , IL-12, and serum protein levels. Importantly, selective inhibition of Flt3L elicited lung parenchymal and alveolar DC accumulation significantly attenuated both the LPS induced cytokine release and lung permeability changes, whereas transient neutropenia did not significantly attenuate the increased lung permeability observed in Flt3L pretreated plus LPS challenged mice.

3.6 *Klebsiella pneumoniae* infection in Flt3L pretreated mice

To investigate whether the Flt3L-mediated amplification of the inflammatory response to LPS also occurred in a model of Gram-negative pneumonia, mice were pretreated for nine days with Flt3L or vehicle, followed by intratracheal instillation of 10^4 CFU *K. pneumoniae* as described in Materials and Methods section (see 2.4.3). At 24 h, 48 h, and 96 h post-infection, mice were analyzed of the developing lung inflammatory response, as described for the analysis of mice after intratracheal LPS instillation. Infection of vehicle-treated mice with 10^4 CFU *K. pneumoniae* caused a marked inflammation comparable to the changes observed in mice in response to LPS instillation. Similar to the findings made in LPS-challenged mice, Flt3L pretreated mice were found to exhibit

increased total BAL fluid cell numbers compared to vehicle-treated mice, attributable to a modest increase in PMN numbers and a strong increase in BAL DC numbers (Fig. 3.23 A-C). This was accompanied by a slight, but not significant increase in BAL TNF- α levels (Fig. 3.24 A) and a strong increase in BAL fluid IL-12 levels (Fig. 3.24 B). Similar to the LPS model, Flt3L pre-treatment also led to an increased lung permeability as assessed by total BAL protein content and i.v. FITC albumin leakage into the alveolar air space (Fig. 3.25). Moreover, and most importantly, Flt3L pre-treatment of mice also led to an increased mortality upon infection of the mice with *K. pneumoniae*, whereas *K. pneumoniae*-infected vehicle-treated mice were able to control the infection (Fig 3.26).

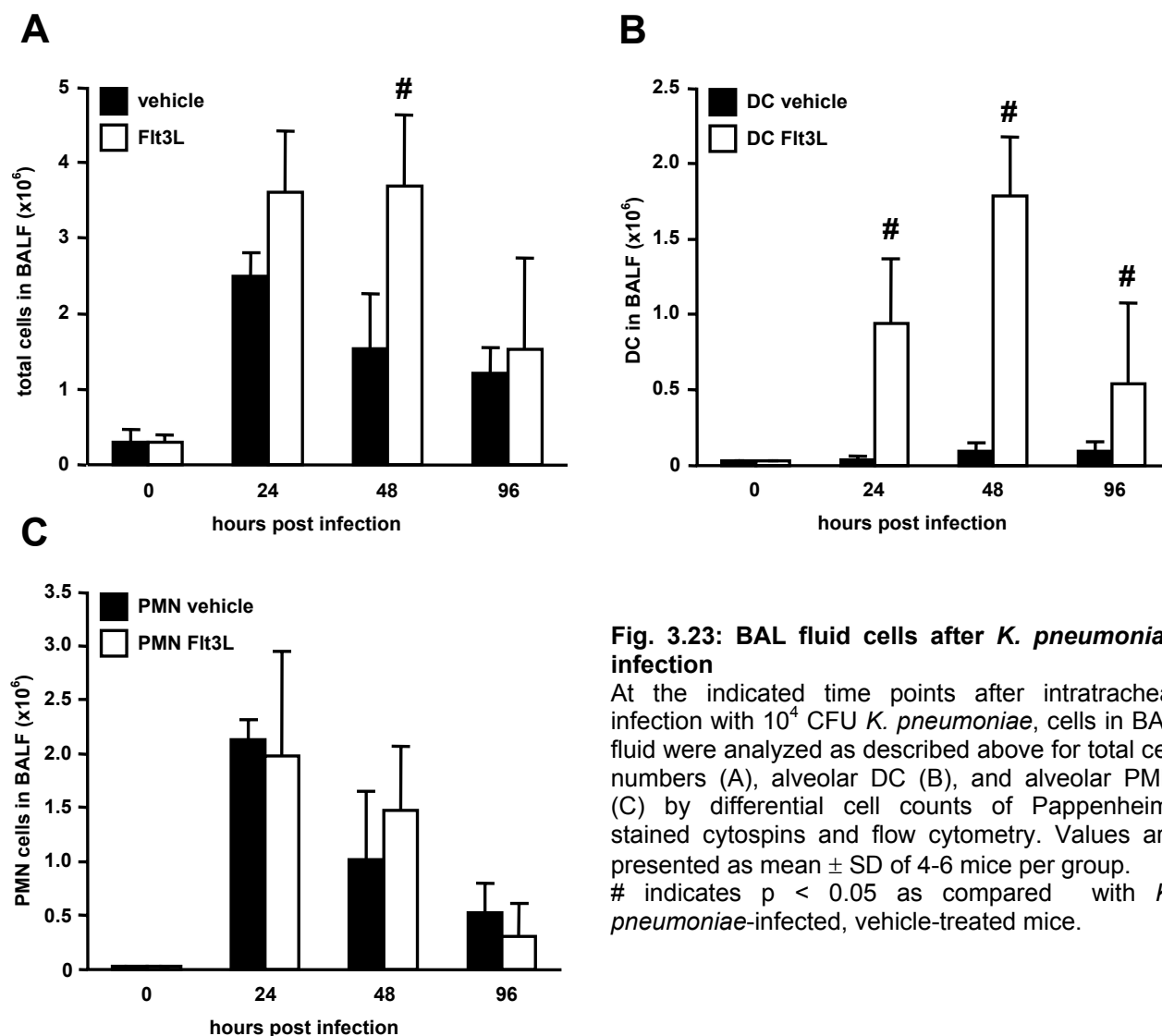


Fig. 3.23: BAL fluid cells after *K. pneumoniae* infection

At the indicated time points after intratracheal infection with 10^4 CFU *K. pneumoniae*, cells in BAL fluid were analyzed as described above for total cell numbers (A), alveolar DC (B), and alveolar PMN (C) by differential cell counts of Pappenheim-stained cytopins and flow cytometry. Values are presented as mean \pm SD of 4-6 mice per group. # indicates $p < 0.05$ as compared with *K. pneumoniae*-infected, vehicle-treated mice.

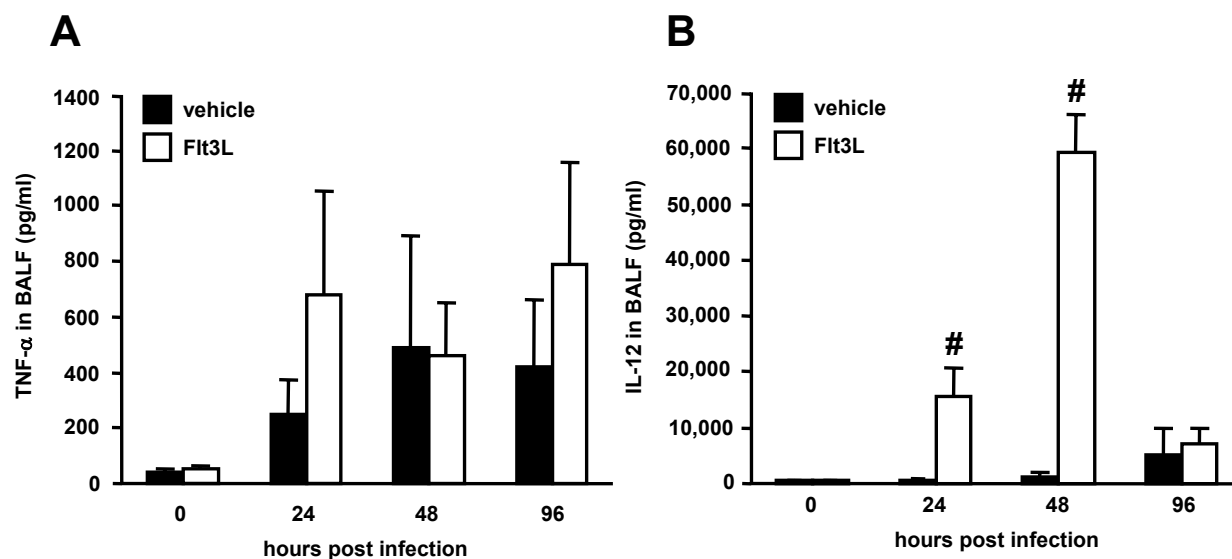


Fig. 3.24: Proinflammatory cytokines in BAL fluid after *K. pneumoniae* infection

Mice were treated as described above. Levels of TNF- α (A) and IL-12 (B) were measured with ELISA. Values are presented as mean \pm SD of 4-6 mice per group. # indicates $p < 0.05$ as compared with *K. pneumoniae*-infected, vehicle-treated mice.

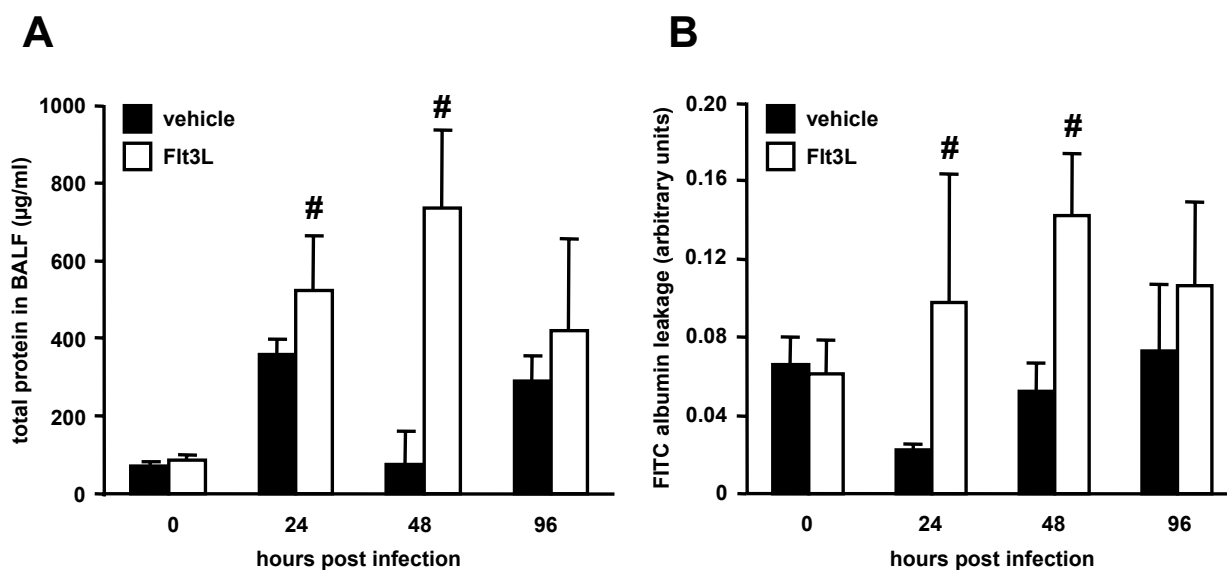


Fig. 3.25: Total protein in BAL fluid and FITC albumin leakage after *K. pneumoniae* infection

Lung leakage was assessed as described above for the mice after intratracheal LPS instillation. Total protein in BAL fluid (A) and FITC albumin leakage (B) were determined as described. Values are presented as mean \pm SD of 4-6 mice per group. # indicates $p < 0.05$ as compared with *K. pneumoniae*-infected, vehicle-treated mice.

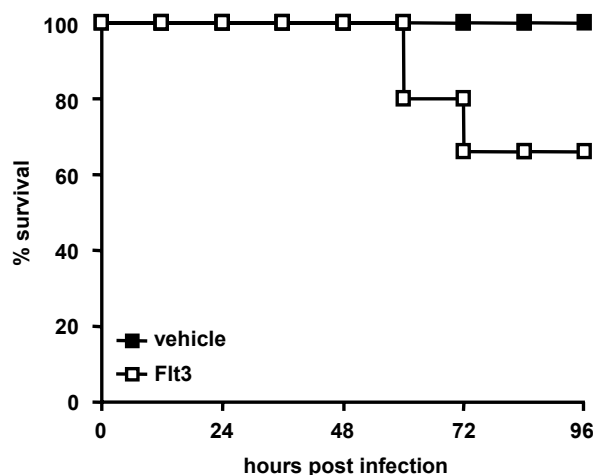


Fig. 3.26: Survival after intratracheal infection with *K. pneumoniae*

Mice were pretreated with Flt3L or vehicle as described. On day 9, mice were infected intratracheally, and survival was monitored for 96 h after infection (n = 6 mice per group).

3.7 LPS-induced peritonitis in Flt3L pretreated mice

To analyze whether the observed amplification of lung inflammatory responses in Flt3L-pretreated mice is a lung-specific phenomenon or might also develop in other organ systems, both Flt3L- and vehicle-treated mice were challenged with an intraperitoneal injection of 20 μ g ultrapure LPS. Peritoneal lavage for the analysis of differential cell counts and flow cytometric identification of peritoneal DC was performed 24h later. As shown in Fig. 3.27, Flt3L pre-treatment led to a strong and significant increase in peritoneal DC by a factor of ~15 and a slight but significant increase in neutrophil counts. In both Flt3L- and vehicle-treated mice, intraperitoneal LPS injection induced a significant increase in neutrophil numbers. However, in marked contrast to the observations made in the lung, Flt3L pre-treatment did not provoke increased numbers of DC or PMN accumulating in the peritoneal cavity upon intraperitoneal LPS application.

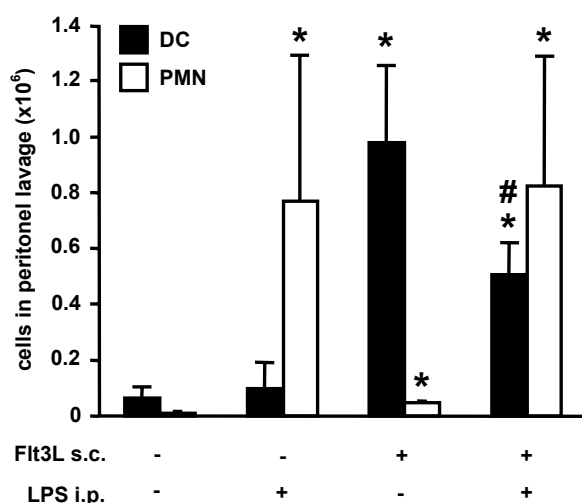


Fig. 3.27: Cells in peritoneal lavage after Flt3L and/or LPS injection

Mice were pretreated with Flt3L or vehicle for nine consecutive days, as indicated. On day 9, mice received an intraperitoneal injection of 20 μ g ultrapure LPS, and were analyzed 24h later. Cells in peritoneal lavage fluid were analyzed using Pappenheim-stained cytopins and flow cytometry. Values are presented as mean \pm SD of n=4 animals per group. * signifies p < 0.05 compared to vehicle-treated mice; # signifies p < 0.05 compared to LPS only treated mice. i.p., intraperitoneal.

3.8 Expression of proinflammatory cytokines by lung DC

3.8.1 *In vivo* expression of proinflammatory cytokines in lung DC after LPS instillation

To assess whether lung DC following *in vivo* exposure to bacterial toxins respond with proinflammatory cytokine release, mice received an intratracheal application of either LPS (1 $\mu\text{g}/\text{mouse}$) or sterile saline. Six hours later, flow-sorted lung DC were analyzed for TNF- α and macrophage inflammatory protein-2 (MIP-2) mRNA transcripts using RT-PCR. Lung DC strongly upregulated TNF- α and MIP-2 mRNA levels as compared to untreated mice, demonstrating their active participation in mediator production upon intra-alveolar LPS deposition. As a positive control, the induction of TNF- α and MIP-2 expression in resident alveolar M ϕ was also assessed; these cells are known to be major producers of these cytokines after intratracheal LPS instillation [125]. As shown in Fig. 3.28, both lung DC and M ϕ upregulated TNF- α mRNA. Lung DC upregulated also mRNA for MIP-2, while MIP-2 mRNA transcripts in lung M ϕ were already present in M ϕ from control mice. This is probably due to an activation of these highly sensitive cells by the flow sorting procedure.

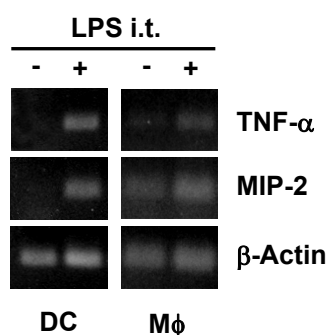


Fig. 3.28: Expression of TNF- α and MIP-2 mRNA in lung DC and lung M ϕ after intratracheal LPS instillation

Mice were instilled with either 1 μg LPS or sterile saline, as indicated. 6 h later, mice were killed, and DC and M ϕ were sorted from lung homogenates. After mRNA isolation, expression of TNF- α and MIP-2 were assessed with RT-PCR. β -Actin served as loading control. Gels are representative of 3 independent experiments.

3.8.2 Effect of Flt3L on LPS-induced cytokine gene expression in lung DC

In addition to the inducibility of proinflammatory cytokines in lung DC and lung M ϕ *in vivo*, we also questioned whether Flt3L application in mice affects the ability of lung DC to respond to LPS treatment with increased cytokine TNF- α , MIP-2, and IL-12 p35 mRNA levels. Flow-sorted lung DC from vehicle-treated or Flt3L pretreated mice were stimulated with 100 ng/ml LPS for 6h *in vitro*, followed by quantitative RT-PCR (qRT-PCR) analysis of TNF- α , MIP-2, and IL-12 p35 mRNA levels. As shown in Fig. 3.29, no significant differences in TNF- α and MIP-2 mRNA levels were noted in LPS-stimulated lung DC of vehicle-treated versus Flt3L pretreated mice, while the expression of IL-12 p35 was significantly upregulated in lung DC from Flt3L pretreated mice. This finding suggests that Flt3L application *in vivo* differentially affects the inflammatory response of lung DC to LPS treatment with an increased capability to produce the proinflammatory cytokine IL-12, while the increase in TNF- α in BAL fluid of Flt3L-pretreated mice after LPS instillation is most probable due to the Flt3L-elicited increase in total numbers of lung parenchymal and alveolar accumulating DC.

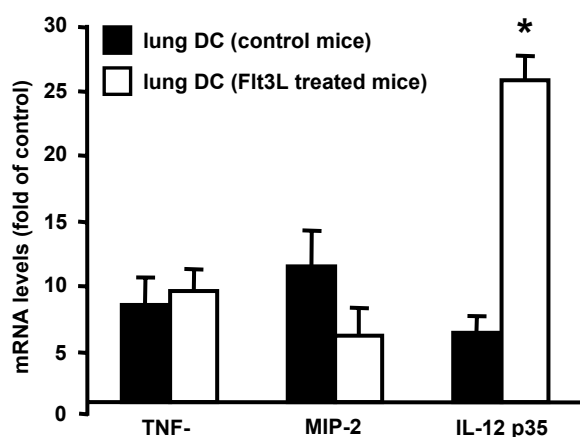


Fig. 3.29: Induction of proinflammatory cytokine expression in DC from Flt3 and vehicle-treated mice

Lung DC from Flt3L and vehicle-treated mice were flow sorted and stimulated *in vitro* for 6 h with LPS or medium alone. mRNA transcript levels of the indicated cytokines were analyzed using qRT-PCR. Data are displayed as fold-change of mRNA levels in LPS-stimulated DC as compared with unstimulated DC. Values are presented as mean \pm SD of 3 independent experiments. * indicates $p < 0.05$ as compared with vehicle-treated mice.

4 Discussion

In the present study, the hypothesis was tested that lung dendritic cells, beside their well-known role as antigen-presenting cells, might also sample and respond acutely to inhaled bacterial toxins and thus contribute to the regulation of acute lung inflammatory responses to inhaled bacterial pathogens. Since there is no reliable system available to deplete DC selectively from mouse lungs without interfering with the lung macrophage pool or other immune cells (see *also* 1.2), a model of lung DC enrichment and selective inhibition of DC enrichment had to be employed. Of note, Flt3L does not only enrich DC, but also other cells of the immune system, with the most important for innate immune responses being PMN [66, 68]. Therefore, a strategy of selective blockade and/or depletion of Flt3L elicited lung DC and lung PMN had to be established and employed.

The analysis of adhesion molecules mediating the enrichment of lung DC in response to systemic Flt3L treatment demonstrated that blockade of the β_2 integrin CD11a but not the β_1 integrin CD49d inhibited the Flt3L elicited lung DC accumulation without interfering with the lung neutrophil recruitment. Induction of transient neutropenia by application of anti-GR-1 mAb depleted both circulating neutrophils and Flt3L elicited lung neutrophils without interfering with the Flt3L elicited lung DC pool size. Importantly, Flt3L pretreated mice responded with both significantly higher lung and alveolar DC and neutrophil numbers upon intratracheal LPS challenge than either Flt3L or LPS alone treated mice, and this effect was accompanied by a highly elevated BAL fluid proinflammatory mediator release and a significantly increased lung permeability. Of note, antibody-mediated blockade of lung DC accumulation but not transient neutropenia decreased the LPS-induced lung permeability and mediator release to baseline levels, demonstrating a yet unrecognized role of lung DC in regulating lung barrier integrity. Such DC-dependently amplified lung inflammatory response to LPS was also observed in mice challenged intratracheally with *Klebsiella pneumoniae*. In addition, Flt3L pretreated mice infected with *K. pneumoniae* showed an increased mortality compared to vehicle-treated and *K. pneumoniae*-infected mice. These data demonstrate that

in the lung, DC may act as critical regulators of the lung inflammatory response to inhaled bacterial pathogens.

4.1 Identification and characterization of lung DC

In mice, the major surface antigen expressed by DC which is used for identification is the α_x integrin chain (CD11c). However, this marker is not restricted to DC, but other cell types also express this marker in different amounts, such as subsets of NK cells [126] and some microglia cells [127, 128]. Most importantly for the lung, also alveolar macrophages express high levels of CD11c [21, 56, 117, 129]. At present, no DC-specific marker has been described in the mouse system. For example, the murine homologues of the human DC-specific marker, DC-SIGN, are also expressed in different amounts in multiple other cells [130-132]. Thus, the flow cytometric characterization of mouse dendritic cells requires a combination of different markers. Recently, Vermaelen and Pauwels have described a method to discriminate lung DC and M ϕ on the basis of CD11c expression and autofluorescence, with DC displaying a low and M ϕ a high autofluorescence [56, 117]. Other authors have reported different protocols for lung DC isolation, mostly including a density gradient centrifugation step and/or a plastic adhesion to remove lung M ϕ [68, 133, 134]. These steps are not only laborious and yield relatively low numbers of lung DC, but they also affect lung DC maturation status and surface marker expression patterns. Instead, DC isolated directly using a fast positive selection strategy most probably reflect the typical lung DC best [134].

Therefore, the protocol based on magnetic bead isolation of CD11c^{positive} cells from lung homogenates, followed by flow cytometric detection of CD11c expression and autofluorescence, was adopted for the current study. In line with the results shown by Vermaelen and Pauwels, this approach yielded consistent numbers of lung DC and M ϕ that could be both analyzed for surface antigen expression and flow-sorted for mRNA isolation and *in vitro* stimulation experiments. Five-colour flow cytometric analysis confirmed the typical antigen expression profiles of the two cell populations (see 3.1.1). Most importantly, lung DC co-expressed high levels of MHC II and low levels of CD86, thus

representing immature DC. Flow-sorted low and high autofluorescent, CD11c^{positive} cells displayed the typical morphology of immature DC and lung M ϕ , respectively (see 3.1.2). Moreover, the high lymphocyte stimulatory capacity of lung DC as compared to lung M ϕ and lung PMN could be confirmed in an allogenic mixed lymphocyte reaction (see 3.1.3). Hence, the approach was confirmed to provide a reliable and stable isolation and analysis of lung DC. In other organs, DC were identified in flow cytometry by their CD11c^{positive} MHC II^{high} phenotype, an approach that has been established by many researchers over the past decades.

4.2 Treatment with Flt3L

Treatment with Flt3L to increase DC numbers in various organs, including the lung, is a well characterized model and has been described by a large body of literature. In almost all of these studies, recombinant human Flt3L has been used, which has been shown to work effectively also in mice [28, 66-68, 75, 76, 79, 134]. This is probably due to the high homology of human and mouse forms of Flt3L, which is 72% [70]. One study using an adenoviral vector to overexpress murine Flt3L in mice *in vivo* showed comparable effects on DC expansion, but demonstrated some differences in tumor control when compared to a treatment with human Flt3L [135]. However, since recombinant human Flt3L is the best characterized substance and already has some proposed therapeutic intervention applications [70], human Flt3L was chosen for the current study. The reported administration routes for systemic treatment are either subcutaneous or intraperitoneal. Both routes seem to work equally well. In the current study, in order to minimize the risk of peritoneal infection, the subcutaneous route was chosen.

Most authors have used a systemic application for Flt3L treatment. However, in rats a single intratracheal dose of Flt3L has been shown to increase functional lung and BAL DC numbers [69]. In preliminary experiments, it was attempted to reproduce these findings in mice. In contrast to the findings in rats, no significant increase of DC numbers in lung homogenate or BAL could be detected after the intratracheal instillation of 50 μ g Flt3L. Except a ~2fold increase in DC numbers in the mediastinal lymph nodes, no systemic effect was

noted (results are not shown in detail). Therefore, the systemic application model was chosen.

Up to present, no time course for Flt3L elicited lung DC accumulation has been reported in the literature. Most authors, and all studies that have investigated Flt3L effects in the lung, have reported a treatment for nine consecutive days; single studies have used a treatment time of 5 days [78], 6 days in neonatal mice [77], and both 9 and 11 days [67]. Hence, in order to define a time point with optimal DC accumulation in the lung with a minimal treatment time, a time course was undertaken. It turned out that a treatment for 9 consecutive days indeed revealed the best and most reliable increase in lung DC numbers (see Fig. 3.6); therefore, for the following experiments a treatment time of 9 days was chosen.

As reported by others before, systemic treatment with Flt3L did not only increase the numbers of mainly myeloid DC, but also significantly the number of PMN, a central cell in early immune responses and innate immunity, in the blood and in lung homogenate [66, 68]. Thus, to decipher the role of DC in acute lung inflammation, a strategy had to be developed to distinguish the effect of Flt3L treatment (which increases both DC and PMN numbers) and the effect of Flt3L elicited lung DC. For PMN, a simple, effective and specific depletion strategy by injection of anti-GR-1 mAb has been described that does not affect the GR-1^{positive} subset of monocytes in the peripheral blood [116]. Since a selective depletion system for lung DC is not available, a selective inhibition of lung DC recruitment after Flt3L treatment was addressed using monoclonal antibodies.

4.3 Adhesion molecules and recruitment of lung DC

As a first step to an intervention strategy with mAbs that target cellular adhesion molecule interaction, circulating PBMo, DC and PMN as well as lung DC and lung M ϕ were phenotyped by flow cytometry for their expression of various adhesion molecules (see Fig. 3.12). The panel was chosen according to previously published results showing that integrins and selectins play the most important role in recruitment of monocytes and PMN to various organs (reviewed in [88, 120]). The expression profiles (see Fig. 3.12) on PMN,

monocytes, the putative precursor cells for DC, and both circulating and lung DC are in line with recent results published by other authors [120, 136]. In the present study, the expression of L-selectin (CD62L) by monocytes and DC was only partial, but could not be attributed to an established subset. The expression of adhesion molecules was assessed in both vehicle- and Flt3L treated mice and did not show any changes in response to Flt3L.

Based on the phenotyping, a panel of function-blocking monoclonal antibodies was tested for inhibition of Flt3L elicited recruitment of DC and PMN in lung homogenate. Although there is a large body of literature investigating monocyte and PMN recruitment, only little is known about the adhesion molecules mediating DC recruitment to the lung [120]. The analysis showed that the Flt3L elicited recruitment of lung DC critically depended on β_2 integrins. Since the common β_2 integrin chain (CD18) is of crucial importance for almost all leukocyte recruitment processes in mammalian bodies [88], the blocking effect of anti-CD18 mAb confirms the report by Schneeberger et al. that gene deletion of CD18 in mice significantly lowers numbers of lung DC [137] and can be considered as a positive control for an effective application of the blocking antibodies. The β_2 integrin chain/CD18 forms heterodimers with α integrins *in vivo*; both main dimerization partners for CD18, α_L integrin (CD11a) and α_M integrin (CD11b), are also critically involved in recruitment of lung DC. This is in line with previous reports about monocyte recruitment under steady-state and inflammatory conditions [120, 121]. A blockade of the third β_2 integrin dimerization partner, α_X integrin (CD11c), was not undertaken, since gene deletion studies have not provided evidence for any overt difference in DC numbers and function in these animals [138]. In an *in vitro* model with human monocyte-derived DC, blocking of CD11a and CD11b, but not of CD11c inhibited adhesion of the DC to vascular endothelial cells [139]. Furthermore, at least on circulating PBMo, CD11c is only expressed on a minor subpopulation (see Fig. 3.12 and [120]).

Surprisingly, neither the blockade of α_4 integrin (CD49d), which forms together with the β_1 integrin chain VLA-4, the most important β_1 integrin complex for monocyte recruitment, nor blockade of its main interaction partner on

endothelial and epithelial cells, VCAM-1 (CD106), had any impact on DC recruitment. This is in marked contrast to what has been reported for monocyte recruitment, where the interaction between VLA-4 and VCAM-1 is of crucial importance in both steady-state and inflammatory recruitment to the lung and to the alveolar space *in vivo* [121] and for the monocyte migration over alveolar epithelial cells infected with Influenza virus [140].

When analysing PMN recruitment to the lung after Flt3L treatment, previously published results by Maus et al. could be confirmed that the inflammatory recruitment of PMN to the lung depended mainly on CD11b and was not significantly affected by the blockade of CD11a and VLA-4 [121]. This seems to be a lung specific phenomenon, since reports by other groups using targeted gene deletion of the CD11a and CD11b genes have demonstrated an important role for CD11a in PMN recruitment in models of air pouch skin inflammation and thioglycollate-induced peritonitis [141, 142]. Whether these differences are due to differences in the recruitment pathways in different organs or can be explained by a compensatory upregulation of other α integrins in gene-deleted mice remains an open question.

The α/β integrins on leukocytes can bind to several molecules on endothelial and epithelial cells, including members of the IgG superfamily, like the intercellular adhesion molecules (ICAMs) and vascular cell adhesion molecules (VCAMs), and to members of the junction adhesion molecule (JAM) family. *In vitro*, for many interactions of integrins with their counterreceptors an importance for leukocyte transmigration has been demonstrated [120, 143, 144]. However, since most of the integrins on leukocytes have more than one interaction partner on the endothelial and epithelial side [143], a blockade or targeted gene deletion of members of the IgG superfamily often has no clear *in vivo* effect. In accordance with these observations, in the current study, the blockade of ICAM-1 (CD54) and VCAM-1 (CD106) had no significant effect on Flt3L elicited lung DC recruitment. This confirms findings by others where numbers of lung DC were not affected in ICAM-1 knock-out mice [137]. Also, blockade of JAM-C, which interacts mainly with CD11b [122], partially, but not significantly altered DC recruitment.

A third important family of adhesion molecules are the selectins, consisting of three members, E-, L- and P-selectin. Since L-selectin (CD62L) is only expressed by a small subset of circulating monocytes and DC, it was not considered as a possible target. The ligand for endothelial P-selectin, PSGL-1 (CD162), is homogenously expressed on PBMo and DC. However, a recent report demonstrated no significant role of PSGL-1 for recruitment of circulating immature DC to inflamed skin [145]. Furthermore, in a model of allergic inflammation after intratracheal instillation of sheep erythrocytes, no recruitment defect for DC was reported in mice with a double targeted deletion of E- and P-selectin [54]. Thus, a blockade of selectins as an intervention strategy was not pursued.

Given these results, blockade of CD11a was chosen for selective inhibition of Flt3L elicited DC recruitment in the following experiments investigating the acute inflammatory potential of lung DC. In addition, a recent publication demonstrated an important role of CD11a but not CD11b for the transmigration of both CD11b^{pos} CD8 α ^{neg} myeloid DC and CD11b^{neg} CD8 α ^{pos} lymphoid DC over resting and TNF- α stimulated endothelial cells *in vitro* [146], collectively demonstrating an important role of CD11a in the inflammatory myeloid DC recruitment process.

In the next step, the recruitment of DC and PMN after intratracheal LPS challenge in Flt3L- and vehicle-treated mice was analysed. LPS challenge in vehicle-treated mice led to a slight, but significant increase in DC numbers in lung homogenate, consistent with previous reports [51, 147]. PMN numbers increased moderately in an amount comparable to Flt3L treatment alone. In Flt3L pre-treated mice, LPS challenge led to a massive additional recruitment of both DC and PMN to the lung parenchyma. This LPS-induced DC recruitment also depended on CD11a and was not affected by CD49d blockade. Notably, anti-CD11a treatment in Flt3L plus LPS treated mice did not affect the lung parenchymal neutrophil recruitment, but rather reduced the transepithelial migration of elicited neutrophils, indicating that these two steps of alveolar recruitment of circulating PMN depend on different mechanisms.

Taken together, these results confirm and expand previous reports by demonstrating that the Flt3L-elicited lung DC accumulation both in the absence

and presence of co-applied LPS is mediated by the β_2 integrin CD11a but not the β_1 integrin CD49d. Of note, both numbers of lung parenchymal and alveolar accumulating DC and neutrophils were synergistically increased in Flt3L pretreated mice co-challenged with LPS.

4.4 Aggravated lung inflammation to LPS in Flt3L pretreated mice

The analysis of the inflammatory phenotype after intratracheal LPS challenge showed in vehicle-treated mice a pronounced alveolar recruitment of PMN, combined with only a slight increase of alveolar DC in the absence of lymphocytes; a minor increase in alveolar leakage; and a modest release of TNF- α and IL-12. These findings are consistent with previously published results by others [118, 123-125]. In marked contrast, intratracheal LPS challenge of Flt3L pre-treated mice, in addition to the massive recruitment of DC and PMN to lung homogenate, led to a severely aggravated inflammatory phenotype as compared to vehicle-treated mice. In the BAL, the total numbers of leukocytes, the PMN, alveolar DC and lymphocytes were massively elevated. TNF- α levels were modestly and, most strikingly, IL-12 levels excessively increased. Furthermore, these mice displayed a severely aggravated leakage. By concomitant anti-CD11a mAb application, all of these findings could be reverted to the levels seen in vehicle-treated mice after LPS challenge. In contrast, blockade of VLA-4/CD49d had no effect. Importantly, both cytokine liberation in the BAL fluid and leakage persisted after neutrophil depletion. Although neutrophils *per se* are well accepted to mediate lung permeability changes in various models of acute lung inflammation [94, 99], the currently presented data strongly support the concept that in addition to neutrophils, lung DC may also play a critical role in determining the lung barrier integrity in response to acute lung inflammation. This concept is supported by two central observations: First, transient neutropenia was highly effective in depleting both lung parenchymal and alveolar accumulating neutrophils, while both proinflammatory mediator release and lung permeability in response to Flt3L plus LPS challenge were not affected. This indicated a minor role of lung and

alveolar neutrophils in induction of lung permeability in the presented model. In contrast, anti-CD11a treatment of the mice to block lung parenchymal and alveolar DC accumulation in response to Flt3L plus LPS was highly effective in reducing BAL fluid TNF- α and IL-12 levels and lung permeability changes, while numbers of interstitial PMN in lungs were not and numbers of alveolar recruited PMN were only partially affected. Furthermore, both the TNF- α and IL-12 release and the lung permeability changes in mice without Flt3L pretreatment did not differ significantly between neutropenic and control mice. Collectively, the presented findings define a novel, hitherto unrecognized role of lung DC in regulating the lung barrier integrity in response to bacterial toxins and Gram-negative pneumonia. As such, the presented data provide a possible explanation for the clinical observation that critically ill, neutropenic patients are known to develop ARDS, a clinical complication associated with a severe loss of lung barrier integrity [89, 100, 101] (see also 1.4). An experimental hint for an neutrophil-independent leakage after LPS stimulation has been provided by Tasaka et al., who showed that priming with Bacillus Calmette Guerin (BCG) severely enhanced the leakage after LPS challenge in guinea pigs also in neutrophil-depleted animals [148].

An important observation was that this severe aggravation of the pulmonary inflammatory phenotype after LPS challenge is not present in a model of LPS-induced peritonitis. Although Flt3L pre-treatment elicited an increase in DC numbers in the peritoneal cavity, the inflammatory phenotype after intraperitoneal LPS in respect to total cell numbers, neutrophil numbers and DC count did not differ between Flt3L-pretreated and vehicle treated mice (see Fig. 3.27). This indicates a fundamental difference between the pulmonary and peritoneal reaction pattern to LPS challenge and suggests also a different role of Flt3L-elicited DC in these two compartments.

As outlined in the Introduction section (see 1.4), the secretion of cytokines after an inflammatory stimulus is crucial for the development of lung inflammation. It had to be defined in the current model whether the modest increase in TNF- α levels and the dramatic increase in IL-12 levels in BAL fluid in Flt3L pre-treated mice resulted in the mere increase in DC numbers, or whether Flt3L elicited DC display a higher capacity of producing proinflammatory cytokines.

When analysing the production of TNF- α and MIP-2 mRNA in lung DC and lung M ϕ *in vivo* after intratracheal challenge with LPS, it could be shown that both population actively take part in the production of these classical pro-inflammatory cytokines. However, when flow-sorted lung DC from Flt3L and vehicle-treated mice were stimulated *in vitro* with LPS, there was no support that Flt3L directly modulates this LPS responsiveness of lung DC to produce TNF- α and MIP-2. Sorted lung DC from both groups of mice had similarly increased TNF- α and MIP-2 mRNA levels (see Fig. 3.29).

In marked contrast, the capability of lung DC to produce IL-12 p35 was significantly higher in DC from Flt3L-pretreated as compared to vehicle-treated mice. This increased capability of Flt3L elicited DC to produce higher amounts of IL-12 has been described by others before; the enhanced production leads to an increased skewing of T cells in a Th1 direction [149, 150]. This can be further enhanced by co-treatment of mice with Flt3L and anti-IL-10 antibodies [151]. However, the exact mechanisms underlying this observation remain to be elucidated.

Studies comparing human and mouse DC that have been isolated from Flt3L- versus vehicle-treated individuals have shown differences in the biologic behaviour of these cells, e.g., in respect of maturation stage and profile and amount of cytokine production after stimulation [134, 152]. However, the complete relevance of these findings has to be further clarified in future investigations. Also, the exact role of different cytokines on *in vivo* DC generation, subset composition, cytokine production, and T cell stimulation capacity remains controversial [74, 153].

However, the synergistic effect of Flt3L plus LPS treatment on the lung DC pool and the concomitant lung barrier dysfunction was noted within a 24h post LPS application period. The recruitment of DC to the airways after an inflammatory stimulus has been shown to take place within hours after stimulation [51, 52] [53]. Because Flt3L pre-treatment of mice is known to increase numbers of circulating monocytes and circulating DC acting as myeloid DC precursor cells, it appears likely that Flt3L elicited lung parenchymal DC upon LPS challenge additionally promote a rapid mobilization of circulating myeloid DC precursor

cells into both the lung parenchymal and alveolar air space that ultimately contribute to an aggravated lung inflammatory response.

4.5 *Klebsiella pneumoniae* infection in Flt3L pretreated mice

Although recognition of LPS by TLR4 is one of the critical steps in initiating an effective immune response in Gram-negative pneumonia [154, 155], LPS instillation alone does not reflect fully the complex situation in bacterial pneumonia. Therefore, an intratracheal infection model with *K. pneumoniae* was used to evaluate the role of Flt3L pretreatment in acute pneumonia. By this, the finding that Flt3L pre-treatment aggravates the lung inflammation in response to intratracheal LPS challenge could be confirmed. Furthermore, and in contrast to the findings after LPS instillation, the mice that were pretreated with Flt3L before infection showed an increased mortality, whereas all vehicle-treated mice were able to control the infection and survived the challenge (see Fig. 3.26). Like in the LPS challenge model, mice that had been pretreated with Flt3L displayed a severely aggravated alveolitis with increased leakage.

These findings were confirmed by a very recent report in a model of Gram-positive pneumonia with *Streptococcus pneumoniae* infection [156]. The increase in mortality in models of acute bacterial pneumonia after Flt3L pretreatment is in marked contrast to most reports by other authors addressing the mortality after Flt3L treatment in other infection models. Toliver-Kinsky et al. described a better survival of Flt3L treated mice in a model of *Pseudomonas aeruginosa* superinfection of burn wounds. A central role for Flt3L elicited DC in this model was demonstrated by the fact that adoptive transfer of splenic DC from Flt3L pretreated, but not from vehicle-treated, mice improved survival after burn and *P. aeruginosa* infection [78]. According to earlier published results, this effect may be due to a restoration of the secretion of IL-12 and interferon- γ in burned mice after Flt3L treatment [150]. Another possible explanation may be that Flt3L can reverse endotoxin tolerance-related immune paralysis, a disease state that can develop after sepsis, major trauma, or burns [80]. Flt3L pretreatment also improved survival in infection models with *Listeria monocytogenes* [76, 77]; however, other researchers have reported an increased *L. monocytogenes* burden in Flt3L pretreated mice [81]. In other

models, Flt3L treatment had no or even adverse effects: The outcome of *Pneumocystis carinii* pneumonia in rats was not affected by Flt3L treatment [157]; and bacterial burden and mortality was significantly higher in Flt3L treated than in vehicle-treated mice after infection with *Mycobacterium tuberculosis* [81].

In summary, the findings of this study point to the necessity to explore potential organ-specific effects, in this case of the lung, before applying a systemic immunomodulatory treatment. This is also underlined by the finding that, in marked contrast to the situation in the lung, Flt3L pretreated mice did not show an enhanced inflammatory response after intraperitoneal LPS challenge.

4.6 Conclusion and future perspectives

In the current study it was undertaken to evaluate the role of lung DC in a model of acute lung inflammation. Cumulatively, the data show that the β_2 integrin dependent Flt3L elicited accumulation of DC in the lung parenchymal compartment triggers an acute lung injury upon both *E. coli* endotoxin and infection with *K. pneumoniae*. This acute lung injury is characterized by an increased neutrophilic alveolitis, proinflammatory mediator release, a high increase in lung permeability, and, in case of *K. pneumoniae* infection, also an increased mortality.

Recent studies have addressed the effect of Flt3L treatment as immunotherapeutic option to antagonize chronic or systemic infections, to reverse airway changes in asthma, or as an adjuvant treatment in radiation therapy of cancer [70, 75-77, 79, 158]. Bearing in mind the results of the current study, immunoregulatory or tolerogenic strategies modulating the numbers and/or functions of DC pools to optimize immune responses of the lung to inhaled inflammatory or infectious antigens need to reflect the considerable proinflammatory potential associated with the lung DC pool.

Some aspects of the observed aggravation of lung inflammation after Flt3L pre-treatment and of the proposed central role for DC in initiating and skewing an acute lung inflammation appear to be interesting for more detailed investigations in following projects. Questions to be asked could be:

- (i) What are the exact mechanisms by which DC control the lung barrier integrity? How can these mechanisms be addressed in terms of an intervention strategy?
- (ii) Can these findings be reproduced in a model of specific depletion of lung DC without the (rather artificial) prior enrichment by Flt3L application? For answering this question, in a first step a model of efficient depletion of lung DC would have to be established, e.g. by using bone-marrow chimera of wild-type and CD11c-diphtheria toxin receptor transgenic mice [61].
- (iii) Could DC be targeted by pharmacologic agents to modify their role in acute bacterial pneumonia?
- (iv) Does the initiation of an acute lung inflammation require a direct sensing of PAMPs and/or bacteria by DC, or are DC activated in a secondary step by other sentinel cells (then presumably alveolar macrophages and/or alveolar epithelial cells)?
- (v) How are DC integrated in the close anatomical network in the alveolar space? Which are the factors that allow communication between alveolar macrophages, epithelial, endothelial and stroma cells? What role do DC play under steady-state conditions in this network?
- (vi) What is the role of this network in the later course of the inflammation, i.e. in the resolution and repair phase of an acute pulmonary infection?

The main mechanisms of Flt3L-elicited DC migration and of the acute inflammatory potential of lung DC, as well as the questions arising from these findings, have been visualized and summarized in Fig. 4.1.

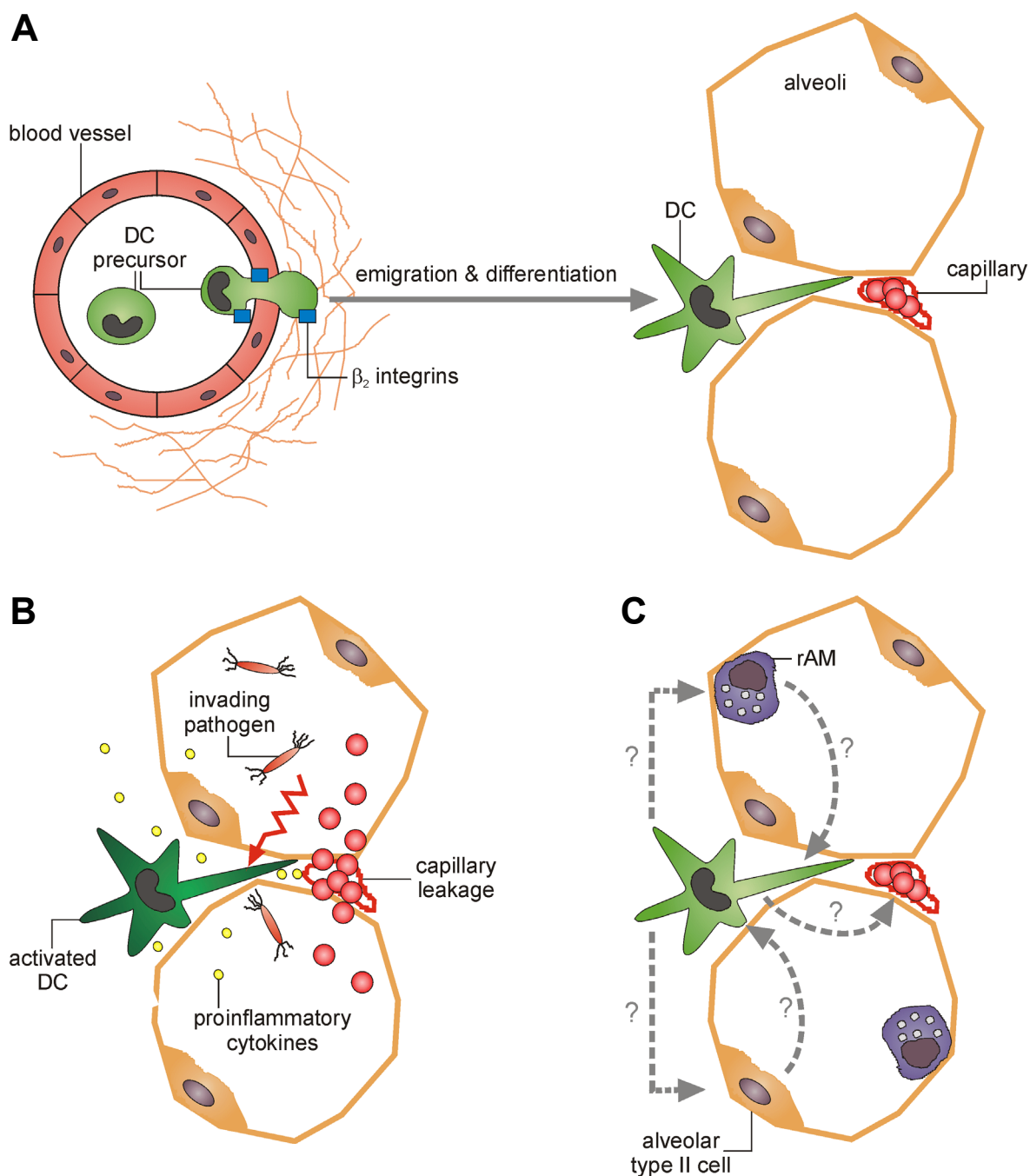


Fig. 4.1: Schematic outline of the major findings and the possible future perspectives presented in this thesis

(A) DC precursors emigrate from the blood into the lung tissue mainly by using β_2 integrins and differentiate within the lung into immature DC. They reside in close proximity to the alveolar space and the small capillaries. (B) Immediately after the alveolar space has been invaded by pathogens, DC come into contact with them. By this, DC are rapidly activated to produce high amounts of proinflammatory cytokines, such as $\text{TNF-}\alpha$, MIP-2, and IL-12. Moreover, they initiate a dysfunction of the capillary walls, resulting in an increased leakage of blood constituents into the alveolar space. (C) As outlined in the text, there are open questions remaining, e.g., (i) how are DC integrated into the close network of other leukocyte populations in the lung, namely resident alveolar macrophages, under acute inflammatory conditions? (ii) Is there a cross-talk between lung DC and alveolar epithelial type II cells, which present a major source of cytokines during acute inflammation? (iii) What are the exact mechanisms of the induction of the alveolo-capillary leakage?

5 Summary

5.1 Summary

Dendritic cells (DCs) are important regulators of the immune system and are critically involved in the immunosurveillance of the lung. They reside in close proximity to both the large airways and the alveoli and constantly take up and process antigen. While many aspects of lung DC biology in adaptive immune responses have been addressed, their role in acute bacterial pneumonia is less well understood. Their unique equipment with receptors and effector molecules of the innate immune system, however, and their capacity to produce large amounts of both proinflammatory and immunoregulatory cytokines within the first hours after antigen contact raises the question of the contribution of lung DC to the initiation and course of the early phase of bacterial pneumonia. Another question that has been only partially addressed is the contribution of the different adhesion molecules for DC recruitment to the lung under non-inflammatory and inflammatory conditions.

To address these questions, mice were treated systemically with Fms-like tyrosine kinase-3 ligand (Flt3L), the most important *in vivo* growth factor for DC proliferation and differentiation. The contribution of adhesion molecules were analyzed by coapplication of function-blocking monoclonal antibodies against various adhesion molecules. Flt3L treatment of mice elicited a strong lung DC accumulation that was mainly dependent on β_2 integrins, blockade of which led to a >80% reduction of DC numbers in lung homogenates. In contrast, blockade of both β_1 integrin CD29/CD49d and VCAM-1 did not affect Flt3L elicited lung DC accumulation.

Intratracheal challenge with lipopolysaccharide resulted in a much more severe inflammatory response in the lung of Flt3L pretreated than of vehicle-treated mice, as demonstrated by increased leukocyte numbers in lung tissue and bronchoalveolar lavage; moderately increased TNF- α and dramatically increased IL-12 levels; and, most importantly, a severe aggravation of the lung leakage. This aggravated inflammation could be inhibited by anti-CD11a-mediated inhibition of Flt3L elicited lung DC accumulation, but persisted after depletion of neutrophils, indicating a novel, hitherto unrecognized role of lung

DC in the regulation of the lung barrier integrity. Importantly, these findings could be confirmed in *Klebsiella pneumoniae* infection model, where Flt3L pretreated mice did not only exhibit a severely aggravated inflammation, but also an increased mortality compared to vehicle-treated mice.

Taken together, the results of this study shed a new light on the role of lung DC in the initiation and the early phase of acute bacterial pneumonia, and expand and partially redefine the pathophysiologic concept of acute lung inflammation.

5.2 Zusammenfassung

Dendritische Zellen (DC) sind wichtige Regulatoren des Immunsystems und sind zentral in die Abwehrfunktion der Lunge integriert. Sie sind in enger Nachbarschaft zu den großen Atemwegen und den Alveolen lokalisiert und phagozytieren und prozessieren kontinuierlich Antigene. Viele Aspekte der DC-Biologie in der Lunge und ihrer Rolle in der adaptiven Immunantwort sind eingehend untersucht worden; ihre Rolle in akuten Entzündungsreaktionen wie der akuten bakteriellen Pneumonie ist hingegen bisher kaum bekannt. DC sind mit einer einzigartigen Vielzahl von Rezeptoren des angeborenen Immunsystems bestückt und sind außerdem in der Lage, innerhalb der ersten Stunden nach Antigenkontakt große Mengen proinflammatorischer und immunregulatorischer Zytokine zu produzieren. Dieses wirft die Frage auf, inwieweit DC an Initiierung und Verlauf der frühen Phase einer bakteriellen Pneumonie beteiligt sind. Nur teilweise bekannt ist ferner der Beitrag verschiedener Adhäsionsmoleküle zur Rekrutierung von DC in die Lunge unter Ruhe- und Entzündungsbedingungen.

Zur Beantwortung dieser Fragen wurden Mäuse systemisch mit Fms-like tyrosine kinase-3-Ligand (Flt3L), dem wichtigsten *in vivo*-Wachstumsfaktor für die DC-Differenzierung, behandelt. Der Beitrag verschiedener Adhäsionsmoleküle zur DC-Rekrutierung wurde durch Gabe von funktionsblockierenden monoklonalen Antikörpern untersucht. Die Gabe von Flt3L führte zu einer starken Anreicherung von DC in der Lunge; diese Rekrutierung war abhängig von β_2 -Integrinen, während die Blockade des β_1 -Integrins CD29/CD49d und seines Interaktionspartners VCAM-1 keinen blockierenden Effekt hatte.

Die intratracheale Gabe von Lipopolysaccharid führte in Flt3L-vorbehandelten Mäusen zu einem dramatisch verstärkten Entzündungsphänotyp im Vergleich zu den Kontrollen, ablesbar an einer deutlich höheren Zahl von Leukozyten im Lungengewebe und in der bronchoalveolären Lavage, einem moderaten TNF- α - und dramatischen IL-12-Anstieg und einer schweren Schädigung der alveolokapillären Schrankenfunktion. Diese aggravierte Entzündung konnte durch eine Blockade der DC-Anreicherung in der Lunge durch anti-CD11a-Antikörper auf das Niveau der kontroll-behandelten Mäuse reduziert werden,

persistierte aber nach einer Depletion der neutrophilen Granulozyten. Dieses zeigt eine neue, bisher unbekannte Bedeutung von DC für die Regulation der Schrankenfunktion in der Lunge. Diese Befunde konnten in einem Infektionsmodell mit *Klebsiella pneumoniae* bestätigt werden. Auch in diesem Modell zeigte sich eine starke Verstärkung der Entzündungsantwort in Flt3L-vorbehandelten Tieren, zudem wiesen diese Tiere eine deutlich erhöhte Mortalität gegenüber den Kontrolltieren auf.

In der Zusammenschau zeigen die Ergebnisse der vorliegenden Untersuchung eine neue, bisher unbekannte Funktion von DC der Lunge in der Initiierung und der frühen Phase bakterieller Pneumonien. Darüberhinaus erweitern und modifizieren diese hier präsentierten Ergebnisse das bisher bekannte pathophysiologische Bild dieser wichtigen Erkrankung.

6 References

1. Unanue, E. R. 1984. Antigen-presenting function of the macrophage. *Annu Rev Immunol* 2:395.
2. Steinman, R. M. 1991. The dendritic cell system and its role in immunogenicity. *Annu Rev Immunol* 9:271.
3. Banchereau, J., F. Briere, C. Caux, J. Davoust, S. Lebecque, Y. J. Liu, B. Pulendran, and K. Palucka. 2000. Immunobiology of dendritic cells. *Annu Rev Immunol* 18:767.
4. Lipscomb, M. F., and B. J. Masten. 2002. Dendritic cells: immune regulators in health and disease. *Physiol Rev* 82:97.
5. Cavanagh, L. L., and U. H. Von Andrian. 2002. Travellers in many guises: the origins and destinations of dendritic cells. *Immunol Cell Biol* 80:448.
6. Steinman, R. M. 2007. Dendritic cells: versatile controllers of the immune system. *Nat Med* 13:1155.
7. Unanue, E. R. 2007. Ito cells, stellate cells, and myofibroblasts: new actors in antigen presentation. *Immunity* 26:9.
8. Winau, F., G. Hegasy, R. Weiskirchen, S. Weber, C. Cassan, P. A. Sieling, R. L. Modlin, R. S. Liblau, A. M. Gressner, and S. H. Kaufmann. 2007. Ito cells are liver-resident antigen-presenting cells for activating T cell responses. *Immunity* 26:117.
9. Kabel, P. J., M. de Haan-Meulman, H. A. Voorbij, M. Kleingeld, E. F. Knol, and H. A. Drexhage. 1989. Accessory cells with a morphology and marker pattern of dendritic cells can be obtained from elutriator-purified blood monocyte fractions. An enhancing effect of metrizamide in this differentiation. *Immunobiology* 179:395.
10. Peters, J. H., S. Ruhl, and D. Friedrichs. 1987. Veiled accessory cells deduced from monocytes. *Immunobiology* 176:154.
11. Romani, N., S. Gruner, D. Brang, E. Kampgen, A. Lenz, B. Trockenbacher, G. Konwalinka, P. O. Fritsch, R. M. Steinman, and G. Schuler. 1994. Proliferating dendritic cell progenitors in human blood. *J Exp Med* 180:83.
12. Sallusto, F., and A. Lanzavecchia. 1994. Efficient presentation of soluble antigen by cultured human dendritic cells is maintained by

- granulocyte/macrophage colony-stimulating factor plus interleukin 4 and downregulated by tumor necrosis factor alpha. *J Exp Med* 179:1109.
13. Randolph, G. J., S. Beaulieu, S. Lebecque, R. M. Steinman, and W. A. Muller. 1998. Differentiation of monocytes into dendritic cells in a model of transendothelial trafficking. *Science* 282:480.
 14. Randolph, G. J., K. Inaba, D. F. Robbani, R. M. Steinman, and W. A. Muller. 1999. Differentiation of phagocytic monocytes into lymph node dendritic cells in vivo. *Immunity* 11:753.
 15. Geissmann, F., S. Jung, and D. R. Littman. 2003. Blood monocytes consist of two principal subsets with distinct migratory properties. *Immunity* 19:71.
 16. Serbina, N. V., T. P. Salazar-Mather, C. A. Biron, W. A. Kuziel, and E. G. Pamer. 2003. TNF/iNOS-producing dendritic cells mediate innate immune defense against bacterial infection. *Immunity* 19:59.
 17. Fogg, D. K., C. Sibon, C. Miled, S. Jung, P. Aucouturier, D. R. Littman, A. Cumano, and F. Geissmann. 2006. A clonogenic bone marrow progenitor specific for macrophages and dendritic cells. *Science* 311:83.
 18. Varol, C., L. Landsman, D. K. Fogg, L. Greenshtein, B. Gildor, R. Margalit, V. Kalchenko, F. Geissmann, and S. Jung. 2007. Monocytes give rise to mucosal, but not splenic, conventional dendritic cells. *J Exp Med* 204:171.
 19. Kennedy, D. W., and J. L. Abkowitz. 1998. Mature monocytic cells enter tissues and engraft. *Proc Natl Acad Sci U S A* 95:14944.
 20. Landsman, L., C. Varol, and S. Jung. 2007. Distinct differentiation potential of blood monocyte subsets in the lung. *J Immunol* 178:2000.
 21. Landsman, L., and S. Jung. 2007. Lung Macrophages Serve as Obligatory Intermediate between Blood Monocytes and Alveolar Macrophages. *J Immunol* 179:3488.
 22. Morelli, A. E., and A. W. Thomson. 2007. Tolerogenic dendritic cells and the quest for transplant tolerance. *Nat Rev Immunol* 7:610.
 23. Kim, S., K. B. Elkon, and X. Ma. 2004. Transcriptional suppression of interleukin-12 gene expression following phagocytosis of apoptotic cells. *Immunity* 21:643.
 24. Henson, P. M. 2004. Fingering IL-12 with apoptotic cells. *Immunity* 21:604.

25. Erwig, L. P., and P. M. Henson. 2007. Immunological consequences of apoptotic cell phagocytosis. *Am J Pathol* 171:2.
26. Okunishi, K., M. Dohi, K. Nakagome, R. Tanaka, S. Mizuno, K. Matsumoto, J. Miyazaki, T. Nakamura, and K. Yamamoto. 2005. A novel role of hepatocyte growth factor as an immune regulator through suppressing dendritic cell function. *J Immunol* 175:4745.
27. Hackstein, H., T. Taner, A. J. Logar, and A. W. Thomson. 2002. Rapamycin inhibits macropinocytosis and mannose receptor-mediated endocytosis by bone marrow-derived dendritic cells. *Blood* 100:1084.
28. Hackstein, H., T. Taner, A. F. Zahorchak, A. E. Morelli, A. J. Logar, A. Gessner, and A. W. Thomson. 2003. Rapamycin inhibits IL-4--induced dendritic cell maturation in vitro and dendritic cell mobilization and function in vivo. *Blood* 101:4457.
29. Hackstein, H., and A. W. Thomson. 2004. Dendritic cells: emerging pharmacological targets of immunosuppressive drugs. *Nat Rev Immunol* 4:24.
30. Hackstein, H., F. C. Renner, A. Bohnert, A. Nockher, T. Frommer, G. Bein, and R. Weimer. 2005. Dendritic cell deficiency in the blood of kidney transplant patients on long-term immunosuppression: results of a prospective matched-cohort study. *Am J Transplant* 5:2945.
31. Taner, T., H. Hackstein, Z. Wang, A. E. Morelli, and A. W. Thomson. 2005. Rapamycin-treated, alloantigen-pulsed host dendritic cells induce ag-specific T cell regulation and prolong graft survival. *Am J Transplant* 5:228.
32. Reis e Sousa, C. 2006. Dendritic cells in a mature age. *Nat Rev Immunol* 6:476.
33. Shortman, K., and Y. J. Liu. 2002. Mouse and human dendritic cell subtypes. *Nat Rev Immunol* 2:151.
34. Ardavin, C. 2003. Origin, precursors and differentiation of mouse dendritic cells. *Nat Rev Immunol* 3:582.
35. Villadangos, J. A., and P. Schnorrer. 2007. Intrinsic and cooperative antigen-presenting functions of dendritic-cell subsets in vivo. *Nat Rev Immunol* 7:543.
36. Dudziak, D., A. O. Kamphorst, G. F. Heidkamp, V. R. Buchholz, C. Trumppheller, S. Yamazaki, C. Cheong, K. Liu, H. W. Lee, C. G. Park, R. M. Steinman, and M. C. Nussenzweig. 2007. Differential antigen processing by dendritic cell subsets in vivo. *Science* 315:107.

37. Janeway, C. A., Jr., and R. Medzhitov. 2002. Innate immune recognition. *Annu Rev Immunol* 20:197.
38. Iwasaki, A., and R. Medzhitov. 2004. Toll-like receptor control of the adaptive immune responses. *Nat Immunol* 5:987.
39. Reis e Sousa, C. 2004. Activation of dendritic cells: translating innate into adaptive immunity. *Curr Opin Immunol* 16:21.
40. Hotchkiss, R. S., K. W. Tinsley, P. E. Swanson, M. H. Grayson, D. F. Osborne, T. H. Wagner, J. P. Cobb, C. Coopersmith, and I. E. Karl. 2002. Depletion of dendritic cells, but not macrophages, in patients with sepsis. *J Immunol* 168:2493.
41. Scumpia, P. O., P. F. McAuliffe, K. A. O'Malley, R. Ungaro, T. Uchida, T. Matsumoto, D. G. Remick, M. J. Clare-Salzler, L. L. Moldawer, and P. A. Efron. 2005. CD11c+ dendritic cells are required for survival in murine polymicrobial sepsis. *J Immunol* 175:3282.
42. Benjamim, C. F., S. K. Lundy, N. W. Lukacs, C. M. Hogaboam, and S. L. Kunkel. 2005. Reversal of long-term sepsis-induced immunosuppression by dendritic cells. *Blood* 105:3588.
43. Oberholzer, A., C. Oberholzer, K. S. Bahjat, R. Ungaro, C. L. Tannahill, M. Murday, F. R. Bahjat, Z. Abouhamze, V. Tsai, D. LaFace, B. Hutchins, L. L. Moldawer, and M. J. Clare-Salzler. 2002. Increased survival in sepsis by in vivo adenovirus-induced expression of IL-10 in dendritic cells. *J Immunol* 168:3412.
44. Huang, X., F. Venet, C. S. Chung, J. Lomas-Neira, and A. Ayala. 2007. Changes in dendritic cell function in the immune response to sepsis. Cell- & tissue-based therapy. *Expert Opin Biol Ther* 7:929.
45. Holt, P. G., S. Haining, D. J. Nelson, and J. D. Sedgwick. 1994. Origin and steady-state turnover of class II MHC-bearing dendritic cells in the epithelium of the conducting airways. *J Immunol* 153:256.
46. Vermaelen, K., and R. Pauwels. 2005. Pulmonary dendritic cells. *Am J Respir Crit Care Med* 172:530.
47. Lambrecht, B. N., J. B. Prins, and H. C. Hoogsteden. 2001. Lung dendritic cells and host immunity to infection. *Eur Respir J* 18:692.

48. Hammad, H., and B. N. Lambrecht. 2006. Recent progress in the biology of airway dendritic cells and implications for understanding the regulation of asthmatic inflammation. *J Allergy Clin Immunol* 118:331.
49. Niess, J. H., S. Brand, X. Gu, L. Landsman, S. Jung, B. A. McCormick, J. M. Vyas, M. Boes, H. L. Ploegh, J. G. Fox, D. R. Littman, and H. C. Reinecker. 2005. CX3CR1-mediated dendritic cell access to the intestinal lumen and bacterial clearance. *Science* 307:254.
50. Chieppa, M., M. Rescigno, A. Y. Huang, and R. N. Germain. 2006. Dynamic imaging of dendritic cell extension into the small bowel lumen in response to epithelial cell TLR engagement. *J Exp Med* 203:2841.
51. McWilliam, A. S., S. Napoli, A. M. Marsh, F. L. Pemper, D. J. Nelson, C. L. Pimm, P. A. Stumbles, T. N. Wells, and P. G. Holt. 1996. Dendritic cells are recruited into the airway epithelium during the inflammatory response to a broad spectrum of stimuli. *J Exp Med* 184:2429.
52. Jahnsen, F. L., E. D. Moloney, T. Hogan, J. W. Upham, C. M. Burke, and P. G. Holt. 2001. Rapid dendritic cell recruitment to the bronchial mucosa of patients with atopic asthma in response to local allergen challenge. *Thorax* 56:823.
53. Jahnsen, F. L., D. H. Strickland, J. A. Thomas, I. T. Tobagus, S. Napoli, G. R. Zosky, D. J. Turner, P. D. Sly, P. A. Stumbles, and P. G. Holt. 2006. Accelerated antigen sampling and transport by airway mucosal dendritic cells following inhalation of a bacterial stimulus. *J Immunol* 177:5861.
54. Osterholzer, J. J., T. Ames, T. Polak, J. Sonstein, B. B. Moore, S. W. Chensue, G. B. Toews, and J. L. Curtis. 2005. CCR2 and CCR6, but not endothelial selectins, mediate the accumulation of immature dendritic cells within the lungs of mice in response to particulate antigen. *J Immunol* 175:874.
55. Vermaelen, K., and R. Pauwels. 2003. Accelerated airway dendritic cell maturation, trafficking, and elimination in a mouse model of asthma. *Am J Respir Cell Mol Biol* 29:405.
56. Vermaelen, K. Y., I. Carro-Muino, B. N. Lambrecht, and R. A. Pauwels. 2001. Specific migratory dendritic cells rapidly transport antigen from the airways to the thoracic lymph nodes. *J Exp Med* 193:51.

57. Marino, S., S. Pawar, C. L. Fuller, T. A. Reinhart, J. L. Flynn, and D. E. Kirschner. 2004. Dendritic cell trafficking and antigen presentation in the human immune response to *Mycobacterium tuberculosis*. *J Immunol* 173:494.
58. Bozza, S., R. Gaziano, A. Spreca, A. Bacci, C. Montagnoli, P. di Francesco, and L. Romani. 2002. Dendritic cells transport conidia and hyphae of *Aspergillus fumigatus* from the airways to the draining lymph nodes and initiate disparate Th responses to the fungus. *J Immunol* 168:1362.
59. Lambrecht, B. N., B. Salomon, D. Klatzmann, and R. A. Pauwels. 1998. Dendritic cells are required for the development of chronic eosinophilic airway inflammation in response to inhaled antigen in sensitized mice. *J Immunol* 160:4090.
60. van Rijt, L. S., S. Jung, A. Kleinjan, N. Vos, M. Willart, C. Duez, H. C. Hoogsteden, and B. N. Lambrecht. 2005. In vivo depletion of lung CD11c+ dendritic cells during allergen challenge abrogates the characteristic features of asthma. *J Exp Med* 201:981.
61. Jung, S., D. Unutmaz, P. Wong, G. Sano, K. De los Santos, T. Sparwasser, S. Wu, S. Vuthoori, K. Ko, F. Zavala, E. G. Pamer, D. R. Littman, and R. A. Lang. 2002. In vivo depletion of CD11c(+) dendritic cells abrogates priming of CD8(+) T cells by exogenous cell-associated antigens. *Immunity* 17:211.
62. McKenna, H. J., K. L. Stocking, R. E. Miller, K. Brasel, T. De Smedt, E. Maraskovsky, C. R. Maliszewski, D. H. Lynch, J. Smith, B. Pulendran, E. R. Roux, M. Teepe, S. D. Lyman, and J. J. Peschon. 2000. Mice lacking flt3 ligand have deficient hematopoiesis affecting hematopoietic progenitor cells, dendritic cells, and natural killer cells. *Blood* 95:3489.
63. Lyman, S. D., L. James, T. Vanden Bos, P. de Vries, K. Brasel, B. Gliniak, L. T. Hollingsworth, K. S. Picha, H. J. McKenna, R. R. Splett, and et al. 1993. Molecular cloning of a ligand for the flt3/flk-2 tyrosine kinase receptor: a proliferative factor for primitive hematopoietic cells. *Cell* 75:1157.
64. Lyman, S. D., L. James, L. Johnson, K. Brasel, P. de Vries, S. S. Escobar, H. Downey, R. R. Splett, M. P. Beckmann, and H. J. McKenna. 1994. Cloning of the human homologue of the murine flt3 ligand: a growth factor for early hematopoietic progenitor cells. *Blood* 83:2795.

65. Hannum, C., J. Culpepper, D. Campbell, T. McClanahan, S. Zurawski, J. F. Bazan, R. Kastelein, S. Hudak, J. Wagner, J. Mattson, and et al. 1994. Ligand for FLT3/FLK2 receptor tyrosine kinase regulates growth of haematopoietic stem cells and is encoded by variant RNAs. *Nature* 368:643.
66. Brasel, K., H. J. McKenna, P. J. Morrissey, K. Charrier, A. E. Morris, C. C. Lee, D. E. Williams, and S. D. Lyman. 1996. Hematologic effects of flt3 ligand in vivo in mice. *Blood* 88:2004.
67. Maraskovsky, E., K. Brasel, M. Teepe, E. R. Roux, S. D. Lyman, K. Shortman, and H. J. McKenna. 1996. Dramatic increase in the numbers of functionally mature dendritic cells in Flt3 ligand-treated mice: multiple dendritic cell subpopulations identified. *J Exp Med* 184:1953.
68. Masten, B. J., G. K. Olson, D. F. Kusewitt, and M. F. Lipscomb. 2004. Flt3 ligand preferentially increases the number of functionally active myeloid dendritic cells in the lungs of mice. *J Immunol* 172:4077.
69. Pabst, R., A. Luhrmann, I. Steinmetz, and T. Tschernig. 2003. A single intratracheal dose of the growth factor Fms-like tyrosine kinase receptor-3 ligand induces a rapid differential increase of dendritic cells and lymphocyte subsets in lung tissue and bronchoalveolar lavage, resulting in an increased local antibody production. *J Immunol* 171:325.
70. Antonysamy, M. A., and A. W. Thomson. 2000. Flt3 ligand (FL) and its influence on immune reactivity. *Cytokine* 12:87.
71. Inaba, K., M. Inaba, N. Romani, H. Aya, M. Deguchi, S. Ikehara, S. Muramatsu, and R. M. Steinman. 1992. Generation of large numbers of dendritic cells from mouse bone marrow cultures supplemented with granulocyte/macrophage colony-stimulating factor. *J Exp Med* 176:1693.
72. McKenna, H. J. 2001. Role of hematopoietic growth factors/flt3 ligand in expansion and regulation of dendritic cells. *Curr Opin Hematol* 8:149.
73. Maraskovsky, E., E. Daro, E. Roux, M. Teepe, C. R. Maliszewski, J. Hoek, D. Caron, M. E. Lebsack, and H. J. McKenna. 2000. In vivo generation of human dendritic cell subsets by Flt3 ligand. *Blood* 96:878.
74. Pulendran, B., J. Banchereau, S. Burkeholder, E. Kraus, E. Guinet, C. Chalouni, D. Caron, C. Maliszewski, J. Davoust, J. Fay, and K. Palucka. 2000.

- Flt3-ligand and granulocyte colony-stimulating factor mobilize distinct human dendritic cell subsets in vivo. *J Immunol* 165:566.
75. Edwan, J. H., G. Perry, J. E. Talmadge, and D. K. Agrawal. 2004. Flt-3 ligand reverses late allergic response and airway hyper-responsiveness in a mouse model of allergic inflammation. *J Immunol* 172:5016.
76. Gregory, S. H., A. J. Sagnimeni, N. B. Zurowski, and A. W. Thomson. 2001. Flt3 ligand pretreatment promotes protective immunity to *Listeria monocytogenes*. *Cytokine* 13:202.
77. Vollstedt, S., M. Franchini, H. P. Hefti, B. Odermatt, M. O'Keeffe, G. Alber, B. Glanzmann, M. Riesen, M. Ackermann, and M. Suter. 2003. Flt3 ligand-treated neonatal mice have increased innate immunity against intracellular pathogens and efficiently control virus infections. *J Exp Med* 197:575.
78. Toliver-Kinsky, T. E., W. Cui, E. D. Murphey, C. Lin, and E. R. Sherwood. 2005. Enhancement of dendritic cell production by fms-like tyrosine kinase-3 ligand increases the resistance of mice to a burn wound infection. *J Immunol* 174:404.
79. Chakravarty, P. K., A. Alfieri, E. K. Thomas, V. Beri, K. E. Tanaka, B. Vikram, and C. Guha. 1999. Flt3-ligand administration after radiation therapy prolongs survival in a murine model of metastatic lung cancer. *Cancer Res* 59:6028.
80. Wysocka, M., L. J. Montaner, and C. L. Karp. 2005. Flt3 ligand treatment reverses endotoxin tolerance-related immunoparalysis. *J Immunol* 174:7398.
81. Alaniz, R. C., S. Sandall, E. K. Thomas, and C. B. Wilson. 2004. Increased dendritic cell numbers impair protective immunity to intracellular bacteria despite augmenting antigen-specific CD8+ T lymphocyte responses. *J Immunol* 172:3725.
82. File, T. M. 2003. Community-acquired pneumonia. *Lancet* 362:1991.
83. Lode, H. M. 2007. Managing community-acquired pneumonia: a European perspective. *Respir Med* 101:1864.
84. Wenisch, C., and C. M. Bonelli. 2006. Community acquired pneumonia (CAP). *Wien Klin Wochenschr* 118:153.
85. Armstrong, G. L., L. A. Conn, and R. W. Pinner. 1999. Trends in infectious disease mortality in the United States during the 20th century. *Jama* 281:61.
86. Mizgerd, J. P. 2006. Lung infection--a public health priority. *PLoS Med* 3:e76.

87. Mizgerd, J. P. 2008. Acute lower respiratory tract infection. *N Engl J Med* 358:716.
88. Hogg, J. C., and C. M. Doerschuk. 1995. Leukocyte traffic in the lung. *Annu Rev Physiol* 57:97.
89. Rosseau, S., P. Hammerl, U. Maus, H. D. Walmrath, H. Schutte, F. Grimminger, W. Seeger, and J. Lohmeyer. 2000. Phenotypic characterization of alveolar monocyte recruitment in acute respiratory distress syndrome. *Am J Physiol Lung Cell Mol Physiol* 279:L25.
90. Ashbaugh, D. G., D. B. Bigelow, T. L. Petty, and B. E. Levine. 1967. Acute respiratory distress in adults. *Lancet* 2:319.
91. Petty, T. L., and D. G. Ashbaugh. 1971. The adult respiratory distress syndrome. Clinical features, factors influencing prognosis and principles of management. *Chest* 60:233.
92. Ware, L. B., and M. A. Matthay. 2000. The acute respiratory distress syndrome. *N Engl J Med* 342:1334.
93. Wheeler, A. P., and G. R. Bernard. 2007. Acute lung injury and the acute respiratory distress syndrome: a clinical review. *Lancet* 369:1553.
94. Puneet, P., S. Moochhala, and M. Bhatia. 2005. Chemokines in acute respiratory distress syndrome. *Am J Physiol Lung Cell Mol Physiol* 288:L3.
95. Kobayashi, T., K. Tashiro, X. Cui, T. Konzaki, Y. Xu, C. Kabata, and K. Yamamoto. 2001. Experimental models of acute respiratory distress syndrome: clinical relevance and response to surfactant therapy. *Biol Neonate* 80 Suppl 1:26.
96. Gunther, A., C. Siebert, R. Schmidt, S. Ziegler, F. Grimminger, M. Yabut, B. Temmesfeld, D. Walmrath, H. Morr, and W. Seeger. 1996. Surfactant alterations in severe pneumonia, acute respiratory distress syndrome, and cardiogenic lung edema. *Am J Respir Crit Care Med* 153:176.
97. Spragg, R. G., J. F. Lewis, H. D. Walmrath, J. Johannigman, G. Bellingan, P. F. Laterre, M. C. Witte, G. A. Richards, G. Rippin, F. Rathgeb, D. Hafner, F. J. Taut, and W. Seeger. 2004. Effect of recombinant surfactant protein C-based surfactant on the acute respiratory distress syndrome. *N Engl J Med* 351:884.
98. Walmrath, D., F. Grimminger, D. Pappert, C. Knothe, U. Obertacke, A. Benzing, A. Gunther, T. Schmehl, H. Leuchte, and W. Seeger. 2002. Bronchoscopic

- administration of bovine natural surfactant in ARDS and septic shock: impact on gas exchange and haemodynamics. *Eur Respir J* 19:805.
99. Abraham, E. 2003. Neutrophils and acute lung injury. *Crit Care Med* 31:S195.
 100. Lafe, M. D., R. H. Simon, A. Flint, and J. B. Keller. 1986. Adult respiratory distress syndrome in neutropenic patients. *Am J Med* 80:1022.
 101. Sivan, Y., C. Mor, S. al-Jundi, and C. J. Newth. 1990. Adult respiratory distress syndrome in severely neutropenic children. *Pediatr Pulmonol* 8:104.
 102. Bersten, A., and W. J. Sibbald. 1989. Acute lung injury in septic shock. *Crit Care Clin* 5:49.
 103. Metz, C., and W. J. Sibbald. 1991. Anti-inflammatory therapy for acute lung injury. A review of animal and clinical studies. *Chest* 100:1110.
 104. Mizgerd, J. P., and S. J. Skerrett. 2007. Animal models of human pneumonia. *Am J Physiol Lung Cell Mol Physiol* doi:10.1152/ajplung.00330.2007.
 105. Nuermberger, E. 2005. Murine models of pneumococcal pneumonia and their applicability to the study of tissue-directed antimicrobials. *Pharmacotherapy* 25:134S.
 106. Knapp, S., M. J. Schultz, and T. van der Poll. 2005. Pneumonia models and innate immunity to respiratory bacterial pathogens. *Shock* 24 Suppl 1:12.
 107. Podschun, R., and U. Ullmann. 1998. Klebsiella spp. as nosocomial pathogens: epidemiology, taxonomy, typing methods, and pathogenicity factors. *Clin Microbiol Rev* 11:589.
 108. Kang, C. I., S. H. Kim, J. W. Bang, H. B. Kim, N. J. Kim, E. C. Kim, M. D. Oh, and K. W. Choe. 2006. Community-acquired versus nosocomial Klebsiella pneumoniae bacteremia: clinical features, treatment outcomes, and clinical implication of antimicrobial resistance. *J Korean Med Sci* 21:816.
 109. Huang, H. H., Y. Y. Zhang, Q. Y. Xiu, X. Zhou, S. G. Huang, Q. Lu, D. M. Wang, and F. Wang. 2006. Community-acquired pneumonia in Shanghai, China: microbial etiology and implications for empirical therapy in a prospective study of 389 patients. *Eur J Clin Microbiol Infect Dis* 25:369.
 110. Harris, A. D., E. N. Perencevich, J. K. Johnson, D. L. Paterson, J. G. Morris, S. M. Strauss, and J. A. Johnson. 2007. Patient-to-patient transmission is

- important in extended-spectrum beta-lactamase-producing *Klebsiella pneumoniae* acquisition. *Clin Infect Dis* 45:1347.
111. Rice, L. B. 2007. Emerging issues in the management of infections caused by multidrug-resistant gram-negative bacteria. *Cleve Clin J Med* 74 Suppl 4:S12.
 112. Sanchez-Madrid, F., P. Simon, S. Thompson, and T. A. Springer. 1983. Mapping of antigenic and functional epitopes on the alpha- and beta-subunits of two related mouse glycoproteins involved in cell interactions, LFA-1 and Mac-1. *J Exp Med* 158:586.
 113. Springer, T., G. Galfre, D. S. Secher, and C. Milstein. 1978. Monoclonal xenogeneic antibodies to murine cell surface antigens: identification of novel leukocyte differentiation antigens. *Eur J Immunol* 8:539.
 114. Metlay, J. P., M. D. Witmer-Pack, R. Agger, M. T. Crowley, D. Lawless, and R. M. Steinman. 1990. The distinct leukocyte integrins of mouse spleen dendritic cells as identified with new hamster monoclonal antibodies. *J Exp Med* 171:1753.
 115. Miyake, K., I. L. Weissman, J. S. Greenberger, and P. W. Kincade. 1991. Evidence for a role of the integrin VLA-4 in lympho-hemopoiesis. *J Exp Med* 173:599.
 116. Maus, U., K. von Grote, W. A. Kuziel, M. Mack, E. J. Miller, J. Cihak, M. Stangassinger, R. Maus, D. Schlondorff, W. Seeger, and J. Lohmeyer. 2002. The role of CC chemokine receptor 2 in alveolar monocyte and neutrophil immigration in intact mice. *Am J Respir Crit Care Med* 166:268.
 117. Vermaelen, K., and R. Pauwels. 2004. Accurate and simple discrimination of mouse pulmonary dendritic cell and macrophage populations by flow cytometry: methodology and new insights. *Cytometry A* 61:170.
 118. Maus, U., J. Huwe, R. Maus, W. Seeger, and J. Lohmeyer. 2001. Alveolar JE/MCP-1 and endotoxin synergize to provoke lung cytokine upregulation, sequential neutrophil and monocyte influx, and vascular leakage in mice. *Am J Respir Crit Care Med* 164:406.
 119. Livak, K. J., and T. D. Schmittgen. 2001. Analysis of relative gene expression data using real-time quantitative PCR and the 2(-Delta Delta C(T)) Method. *Methods* 25:402.

120. Imhof, B. A., and M. Aurrand-Lions. 2004. Adhesion mechanisms regulating the migration of monocytes. *Nat Rev Immunol* 4:432.
121. Maus, U., J. Huwe, L. Ermert, M. Ermert, W. Seeger, and J. Lohmeyer. 2002. Molecular pathways of monocyte emigration into the alveolar air space of intact mice. *Am J Respir Crit Care Med* 165:95.
122. Aurrand-Lions, M., C. Lamagna, J. P. Dangerfield, S. Wang, P. Herrera, S. Nourshargh, and B. A. Imhof. 2005. Junctional adhesion molecule-C regulates the early influx of leukocytes into tissues during inflammation. *J Immunol* 174:6406.
123. Maus, U., S. Herold, H. Muth, R. Maus, L. Ermert, M. Ermert, N. Weissmann, S. Rosseau, W. Seeger, F. Grimminger, and J. Lohmeyer. 2001. Monocytes recruited into the alveolar air space of mice show a monocytic phenotype but upregulate CD14. *Am J Physiol Lung Cell Mol Physiol* 280:L58.
124. Steinmuller, M., M. Srivastava, W. A. Kuziel, J. W. Christman, W. Seeger, T. Welte, J. Lohmeyer, and U. A. Maus. 2006. Endotoxin induced peritonitis elicits monocyte immigration into the lung: implications on alveolar space inflammatory responsiveness. *Respir Res* 7:30.
125. Maus, U. A., M. A. Koay, T. Delbeck, M. Mack, M. Ermert, L. Ermert, T. S. Blackwell, J. W. Christman, D. Schlondorff, W. Seeger, and J. Lohmeyer. 2002. Role of resident alveolar macrophages in leukocyte traffic into the alveolar air space of intact mice. *Am J Physiol Lung Cell Mol Physiol* 282:L1245.
126. Laouar, Y., F. S. Sutterwala, L. Gorelik, and R. A. Flavell. 2005. Transforming growth factor-beta controls T helper type 1 cell development through regulation of natural killer cell interferon-gamma. *Nat Immunol* 6:600.
127. Reichmann, G., M. Schroeter, S. Jander, and H. G. Fischer. 2002. Dendritic cells and dendritic-like microglia in focal cortical ischemia of the mouse brain. *J Neuroimmunol* 129:125.
128. Remington, L. T., A. A. Babcock, S. P. Zehntner, and T. Owens. 2007. Microglial recruitment, activation, and proliferation in response to primary demyelination. *Am J Pathol* 170:1713.
129. Gonzalez-Juarrero, M., T. S. Shim, A. Kipnis, A. P. Junqueira-Kipnis, and I. M. Orme. 2003. Dynamics of macrophage cell populations during murine pulmonary tuberculosis. *J Immunol* 171:3128.

130. Geijtenbeek, T. B., R. Torensma, S. J. van Vliet, G. C. van Duijnhoven, G. J. Adema, Y. van Kooyk, and C. G. Figdor. 2000. Identification of DC-SIGN, a novel dendritic cell-specific ICAM-3 receptor that supports primary immune responses. *Cell* 100:575.
131. Parent, S. A., T. Zhang, G. Chrebet, J. A. Clemas, D. J. Figueroa, B. Ky, R. A. Blevins, C. P. Austin, and H. Rosen. 2002. Molecular characterization of the murine SIGNR1 gene encoding a C-type lectin homologous to human DC-SIGN and DC-SIGNR. *Gene* 293:33.
132. Park, C. G., K. Takahara, E. Umemoto, Y. Yashima, K. Matsubara, Y. Matsuda, B. E. Clausen, K. Inaba, and R. M. Steinman. 2001. Five mouse homologues of the human dendritic cell C-type lectin, DC-SIGN. *Int Immunol* 13:1283.
133. Masten, B. J., and M. F. Lipscomb. 1999. Comparison of lung dendritic cells and B cells in stimulating naive antigen-specific T cells. *J Immunol* 162:1310.
134. Swanson, K. A., Y. Zheng, K. M. Heidler, Z. D. Zhang, T. J. Webb, and D. S. Wilkes. 2004. Flt3-ligand, IL-4, GM-CSF, and adherence-mediated isolation of murine lung dendritic cells: assessment of isolation technique on phenotype and function. *J Immunol* 173:4875.
135. Miller, G., V. G. Pillarisetty, A. B. Shah, S. Lahrs, and R. P. DeMatteo. 2003. Murine Flt3 ligand expands distinct dendritic cells with both tolerogenic and immunogenic properties. *J Immunol* 170:3554.
136. Cavanagh, L. L., R. Bonasio, I. B. Mazo, C. Halin, G. Cheng, A. W. van der Velden, A. Cariappa, C. Chase, P. Russell, M. N. Starnbach, P. A. Koni, S. Pillai, W. Weninger, and U. H. von Andrian. 2005. Activation of bone marrow-resident memory T cells by circulating, antigen-bearing dendritic cells. *Nat Immunol* 6:1029.
137. Schneeberger, E. E., Q. Vu, B. W. LeBlanc, and C. M. Doerschuk. 2000. The accumulation of dendritic cells in the lung is impaired in CD18^{-/-} but not in ICAM-1^{-/-} mutant mice. *J Immunol* 164:2472.
138. Wu, H., J. R. Rodgers, X. Y. Perrard, J. L. Perrard, J. E. Prince, Y. Abe, B. K. Davis, G. Dietsch, C. W. Smith, and C. M. Ballantyne. 2004. Deficiency of CD11b or CD11d results in reduced staphylococcal enterotoxin-induced T cell response and T cell phenotypic changes. *J Immunol* 173:297.

139. D'Amico, G., G. Bianchi, S. Bernasconi, L. Bersani, L. Piemonti, S. Sozzani, A. Mantovani, and P. Allavena. 1998. Adhesion, transendothelial migration, and reverse transmigration of in vitro cultured dendritic cells. *Blood* 92:207.
140. Herold, S., W. von Wulffen, M. Steinmueller, S. Pleschka, W. A. Kuziel, M. Mack, M. Srivastava, W. Seeger, U. A. Maus, and J. Lohmeyer. 2006. Alveolar epithelial cells direct monocyte transepithelial migration upon influenza virus infection: impact of chemokines and adhesion molecules. *J Immunol* 177:1817.
141. Lu, H., C. W. Smith, J. Perrard, D. Bullard, L. Tang, S. B. Shappell, M. L. Entman, A. L. Beaudet, and C. M. Ballantyne. 1997. LFA-1 is sufficient in mediating neutrophil emigration in Mac-1-deficient mice. *J Clin Invest* 99:1340.
142. Ding, Z. M., J. E. Babensee, S. I. Simon, H. Lu, J. L. Perrard, D. C. Bullard, X. Y. Dai, S. K. Bromley, M. L. Dustin, M. L. Entman, C. W. Smith, and C. M. Ballantyne. 1999. Relative contribution of LFA-1 and Mac-1 to neutrophil adhesion and migration. *J Immunol* 163:5029.
143. Ulbrich, H., E. E. Eriksson, and L. Lindbom. 2003. Leukocyte and endothelial cell adhesion molecules as targets for therapeutic interventions in inflammatory disease. *Trends Pharmacol Sci* 24:640.
144. Muller, W. A. 2003. Leukocyte-endothelial-cell interactions in leukocyte transmigration and the inflammatory response. *Trends Immunol* 24:327.
145. Pendl, G. G., C. Robert, M. Steinert, R. Thanos, R. Eytner, E. Borges, M. K. Wild, J. B. Lowe, R. C. Fuhlbrigge, T. S. Kupper, D. Vestweber, and S. Grabbe. 2002. Immature mouse dendritic cells enter inflamed tissue, a process that requires E- and P-selectin, but not P-selectin glycoprotein ligand 1. *Blood* 99:946.
146. Colvin, B. L., A. H. Lau, A. M. Schell, and A. W. Thomson. 2004. Disparate ability of murine CD8alpha- and CD8alpha+ dendritic cell subsets to traverse endothelium is not determined by differential CD11b expression. *Immunology* 113:328.
147. Schon-Hegrad, M. A., J. Oliver, P. G. McMenamin, and P. G. Holt. 1991. Studies on the density, distribution, and surface phenotype of intraepithelial class II major histocompatibility complex antigen (Ia)-bearing dendritic cells (DC) in the conducting airways. *J Exp Med* 173:1345.

148. Tasaka, S., A. Ishizaka, T. Urano, K. Sayama, F. Sakamaki, H. Nakamura, T. Terashima, Y. Waki, K. Soejima, Y. Oyamada, and et al. 1995. BCG priming enhances endotoxin-induced acute lung injury independent of neutrophils. *Am J Respir Crit Care Med* 152:1041.
149. Vollstedt, S., M. O'Keeffe, B. Odermatt, R. Beat, B. Glanzmann, M. Riesen, K. Shortman, and M. Suter. 2004. Treatment of neonatal mice with Flt3 ligand leads to changes in dendritic cell subpopulations associated with enhanced IL-12 and IFN-alpha production. *Eur J Immunol* 34:1849.
150. Toliver-Kinsky, T. E., C. Y. Lin, D. N. Herndon, and E. R. Sherwood. 2003. Stimulation of hematopoiesis by the Fms-like tyrosine kinase 3 ligand restores bacterial induction of Th1 cytokines in thermally injured mice. *Infect Immun* 71:3058.
151. Das, L., J. DeVecchio, and F. P. Heinzl. 2005. Fms-like tyrosine kinase 3-based immunoprophylaxis against infection is improved by adjuvant treatment with anti-interleukin-10 antibody. *J Infect Dis* 192:693.
152. Jefford, M., M. Schnurr, T. Toy, K. A. Masterman, A. Shin, T. Beecroft, T. Y. Tai, K. Shortman, M. Shackleton, I. D. Davis, P. Parente, T. Luft, W. Chen, J. Cebon, and E. Maraskovsky. 2003. Functional comparison of DCs generated in vivo with Flt3 ligand or in vitro from blood monocytes: differential regulation of function by specific classes of physiologic stimuli. *Blood* 102:1753.
153. O'Keeffe, M., H. Hochrein, D. Vremec, J. Pooley, R. Evans, S. Woulfe, and K. Shortman. 2002. Effects of administration of progenipoietin 1, Flt-3 ligand, granulocyte colony-stimulating factor, and pegylated granulocyte-macrophage colony-stimulating factor on dendritic cell subsets in mice. *Blood* 99:2122.
154. Branger, J., S. Knapp, S. Weijer, J. C. Leemans, J. M. Pater, P. Speelman, S. Florquin, and T. van der Poll. 2004. Role of Toll-like receptor 4 in gram-positive and gram-negative pneumonia in mice. *Infect Immun* 72:788.
155. Schurr, J. R., E. Young, P. Byrne, C. Steele, J. E. Shellito, and J. K. Kolls. 2005. Central role of toll-like receptor 4 signaling and host defense in experimental pneumonia caused by Gram-negative bacteria. *Infect Immun* 73:532.
156. Winter, C., K. Taut, F. Langer, M. Mack, D. E. Briles, J. C. Paton, R. Maus, M. Srivastava, T. Welte, and U. A. Maus. 2007. FMS-Like Tyrosine Kinase 3

- Ligand Aggravates the Lung Inflammatory Response to *Streptococcus pneumoniae* Infection in Mice: Role of Dendritic Cells. *J Immunol* 179:3099.
157. Oz, H. S., W. T. Hughes, J. E. Rehg, and E. K. Thomas. 2000. Effect of CD40 ligand and other immunomodulators on *Pneumocystis carinii* infection in rat model. *Microb Pathog* 29:187.
158. Lynch, D. H., A. Andreasen, E. Maraskovsky, J. Whitmore, R. E. Miller, and J. C. Schuh. 1997. Flt3 ligand induces tumor regression and antitumor immune responses in vivo. *Nat Med* 3:625.

7 Appendix

7.1 Publications

Original publication from the PhD thesis

von Wulffen, W., M. Steinmueller, S. Herold, L. M. Marsh, P. Bulau, W. Seeger, T. Welte, J. Lohmeyer, and U. A. Maus. 2007. Lung Dendritic Cells Elicited by Fms-like Tyrosin 3-Kinase Ligand Amplify the Lung Inflammatory Response to Lipopolysaccharide. *Am J Respir Crit Care Med* 176:892.

Other original publications

Herold, S., **W. von Wulffen**, M. Steinmueller, S. Pleschka, W. A. Kuziel, M. Mack, M. Srivastava, W. Seeger, U. A. Maus, and J. Lohmeyer. 2006. Alveolar epithelial cells direct monocyte transepithelial migration upon influenza virus infection: impact of chemokines and adhesion molecules. *J Immunol* 177:1817.

Rival, C., V. A. Guazzone, **W. von Wulffen**, H. Hackstein, E. Schneider, L. Lustig, A. Meinhardt, and M. Fijak. 2007. Expression of Costimulatory Molecules, Chemokine Receptors and Proinflammatory Cytokines in Dendritic Cells from Normal and Chronically Inflamed Rat Testis. *Mol Hum Reprod* 13:853-861.

Hansmann L., S. Groeger, **W. von Wulffen**, G. Bein, and H. Hackstein. 2008. Human monocytes represent a competitive source of interferon- α in peripheral blood. *Clin Immunol* 127:252.

Abstracts and oral presentations from PhD thesis

von Wulffen, W., J. Lohmeyer, W. Seeger, and U.A. Maus. 2005. Flt3L elicited lung dendritic cells are recruited via β 2 integrin dependent pathways and amplify the lung inflammatory response to LPS. *Jahrestagung der Sektion der Zellbiologie der Deutschen Gesellschaft für Pneumologie, Bonn; Oct. 25, 2005*

von Wulffen, W., J. Lohmeyer, W. Seeger, and U. A. Maus. 2006. Flt3L elicited lung dendritic cells are recruited via β 2 integrin dependent pathways and amplify the lung inflammatory response to LPS. *International Conference of the American Thoracic Society, San Diego, CA, USA; May 19-24, 2006* Abstract No 2698.

7.2 Declaration

I declare that I have completed this dissertation single-handedly without the unauthorized help of a second party and only with the assistance acknowledged therein. I have appropriately acknowledged and referenced all text passages that are derived literally from or are based on the content of published or unpublished work of others, and all information that relates to verbal communications. I have abided by the principles of good scientific conduct laid down in the charter of the Justus Liebig University of Giessen in carrying out the investigations described in the dissertation.

Werner von Wulffen

7.3 Acknowledgments

There are many people I would like to thank and without whom the work presented in this thesis would not have been possible: Prof. Jürgen Lohmeyer and Prof. Werner Seeger for putting me on the topic of lung dendritic cells, for giving me the opportunity to work in this field, and for their constant support; PD Dr. Ulrich Maus for giving the finetuning to the project and substantial help in publishing the results; Dr. Oliver Eickelberg, Dr. Rory Morty and the 2006 class of the MBML for their excellent training in science and the vivid and helpful discussions; my lab colleagues, namely Mirko Steinmüller, Susanne Herold, Maciej Cabanski, Lidija Cakarova, Leigh Marsh and Zbigniew Zasłona, for an always fruitful discussion and for creating and maintaining the special atmosphere that makes working in the Lohmeyer Lab so nice and grateful; the technicians in the Lohmeyer Lab, namely Gudrun Biemer-Mansouri, Emma Braun, Petra Janssen, and Margret Lohmeyer, for their invaluable help in many respects; Dr. Kathrin Ahlbrecht for showing me how to prepare slides for immunohistochemistry; Dr. Patrick Bulau for help with the protein analysis in BAL fluid and for the MALDI-TOF analysis of the albumin band on the SDS-PAGE; Dr. Leigh Marsh for help with the real-time PCR analysis; Amgen Inc. for supplying the Flt3L; Altana Pharma AG, Konstanz, for providing me with a graduate scholarship; and the Deutsche Forschungsgemeinschaft (DFG) and CAPNETZ/BMBF for financial support of the project.

To my parents I am indebted for their support in more than one respect – last but not least for the financial part of it that made a graduate college scholarship and me having a newborn family an eligible match.

Finally, I would like to thank my wife Christiane for her constant support, encouragement and love.

7.4 Curriculum vitae

Werner von Wulffen

born January 4th, 1975 in Hannover

1994	Abitur (Gymnasium Großburgwedel)
1994 – 1995	civil service (Zivildienst)
1995 – 2002	Medical studies (Friedrich-Schiller-University Jena)
2000 – 2003	Dissertation (Dr. med. degree) at the Institute for Medical Microbiology, FSU Jena (Supervisor Prof. Dr. E. Straube)
	Title of the dissertation: „Der Einfluss der Protease Elastase auf das Adhärenz- und Internalisierungsverhalten uropathogener <i>Escherichia coli</i> “
	Doctoral defense July 2004 (overall rating: summa cum laude)
2002 – 2003	Internship (Arzt im Praktikum), Institute for Medical Microbiology, FSU Jena
2003	Internship (Arzt im Praktikum) continued, Department of Internal Medicine II, JLU Gießen
2003 – 2006	Graduate College „Molecular Biology and Medicine of the Lung (MBML)“
since 2004	Student in the PhD-Program, JLU Gießen
since 2006	Assistant physician (Assistenzarzt), Department of Internal Medicine II, JLU Gießen